White Dwarfs Accreting Planetary Material Determined from X-ray Observations

Tim Cunningham
NASA Hubble Fellow
Harvard University

NASA Hubble Fellowship Program

CENTER FOR ASTROPHYSICS
HARVARD & SMITHSONIAN

HARVARD UNIVERSITY

Image credit: Mark Garlick

Exoplanetary HRD

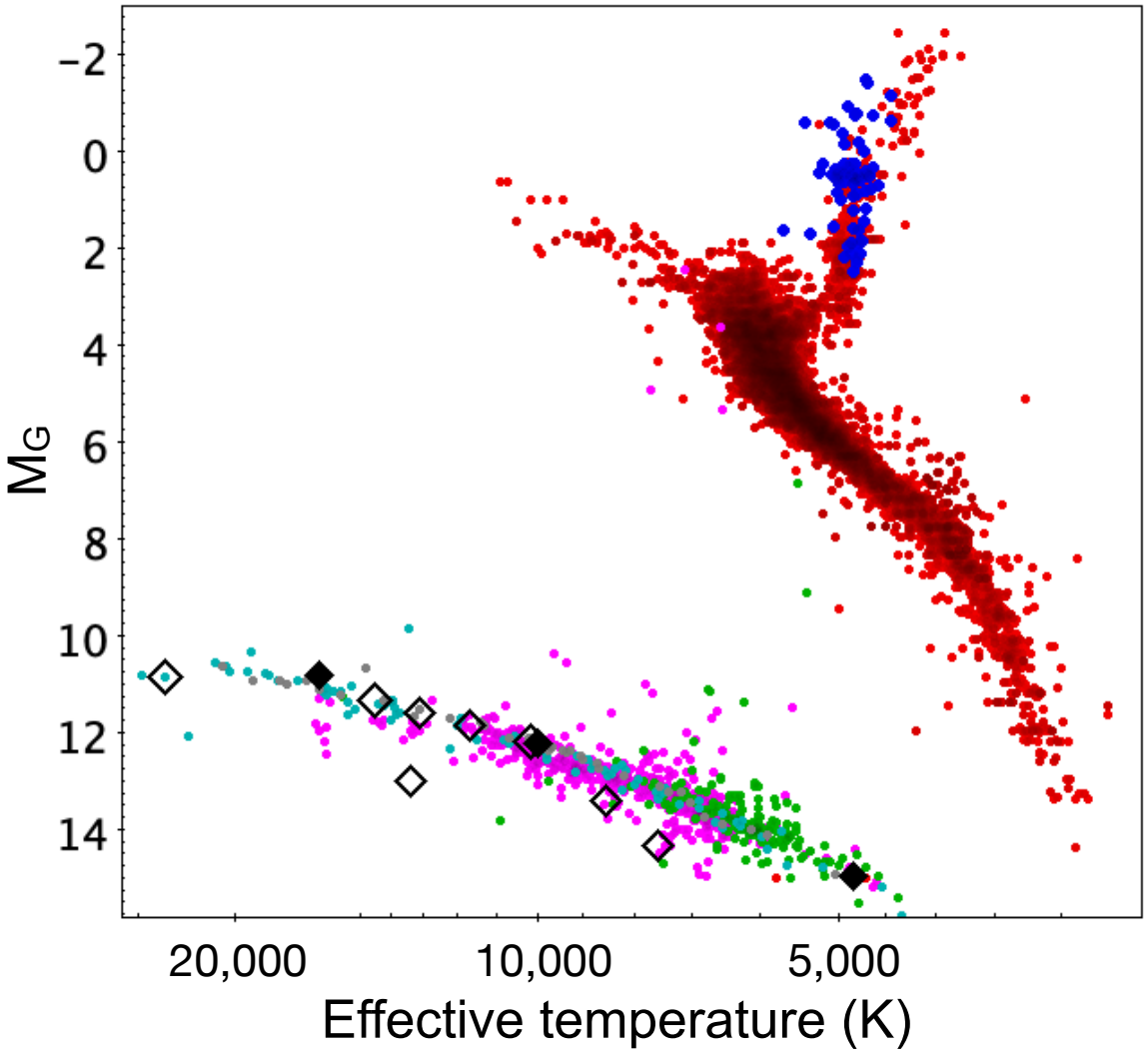

- NASA Exoplanet Archive
- Giant stars (S. Reffert)
- DZ (Coutu et al. 2019)
- DZ (Hollands et al. 2017)
- DAZ/DZ (Farihi 2016)
- DAZ (Koester & Wilken 2006)
- ◆ WD planets/candidates
- ◇ WD transiting debris

Exoplanetary HRD

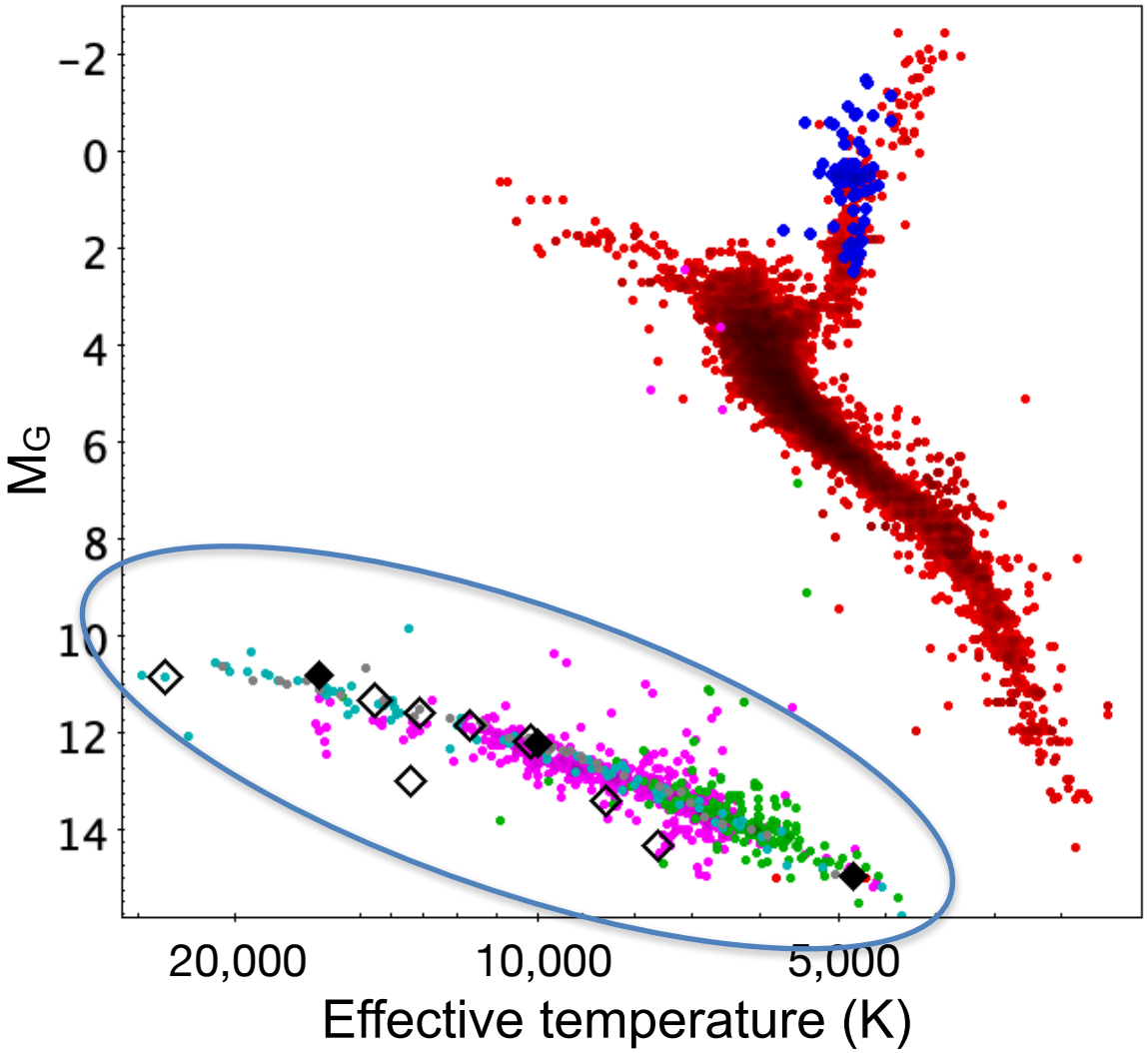

- NASA Exoplanet Archive
- Giant stars (S. Reffert)
- DZ (Coutu et al. 2019)
- DZ (Hollands et al. 2017)
- DAZ/DZ (Farihi 2016)
- DAZ (Koester & Wilken 2006)
- ◆ WD planets/candidates
- ◇ WD transiting debris

White dwarfs: general properties

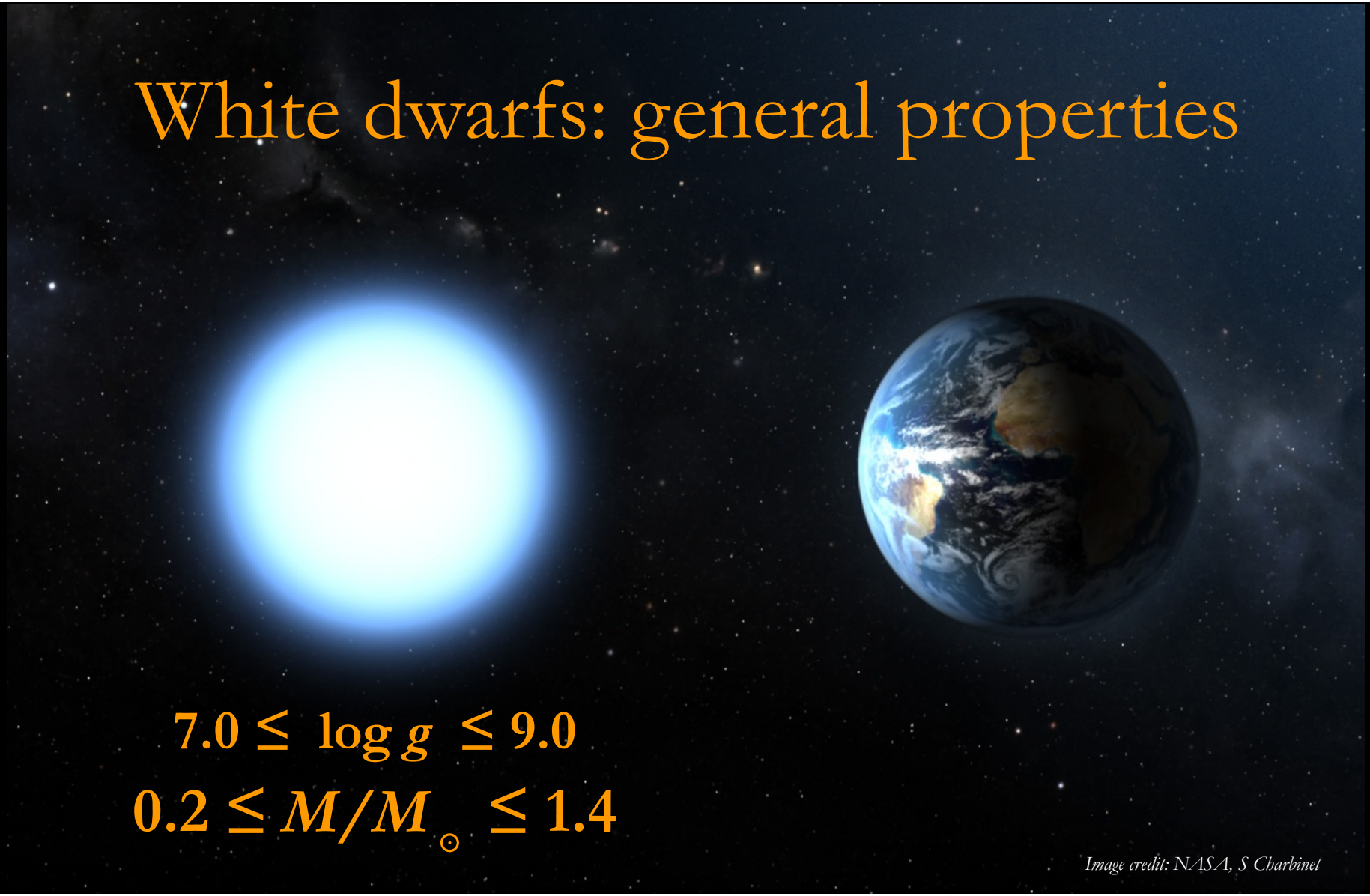

$7.0 \leq \log g \leq 9.0$

$0.2 \leq M/M_{\odot} \leq 1.4$

Image credit: NASA, S Charbinet

White dwarfs: general properties

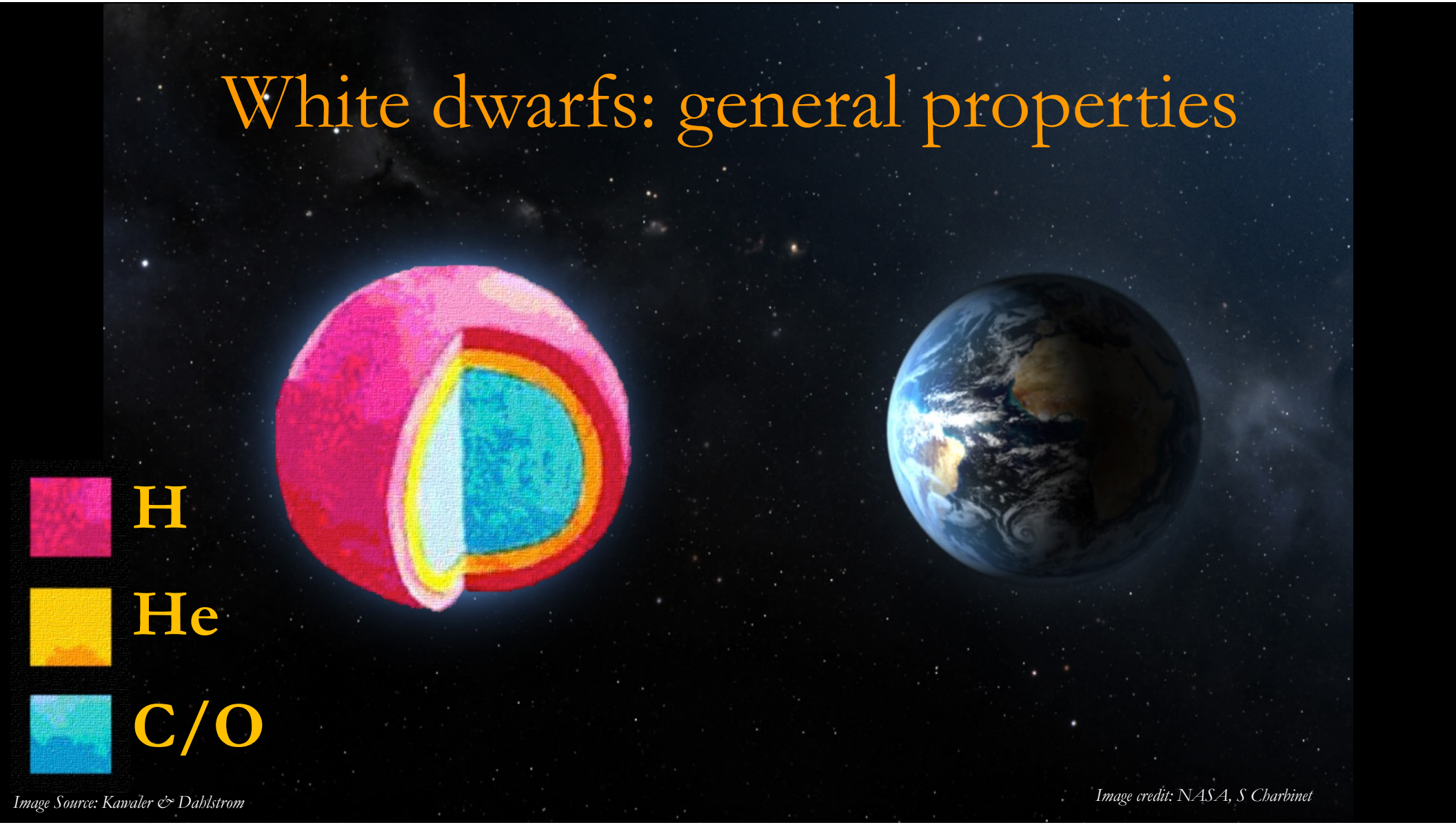

Image Source: Kawaler & Dahlstrom

Image credit: NASA, S Charbinet

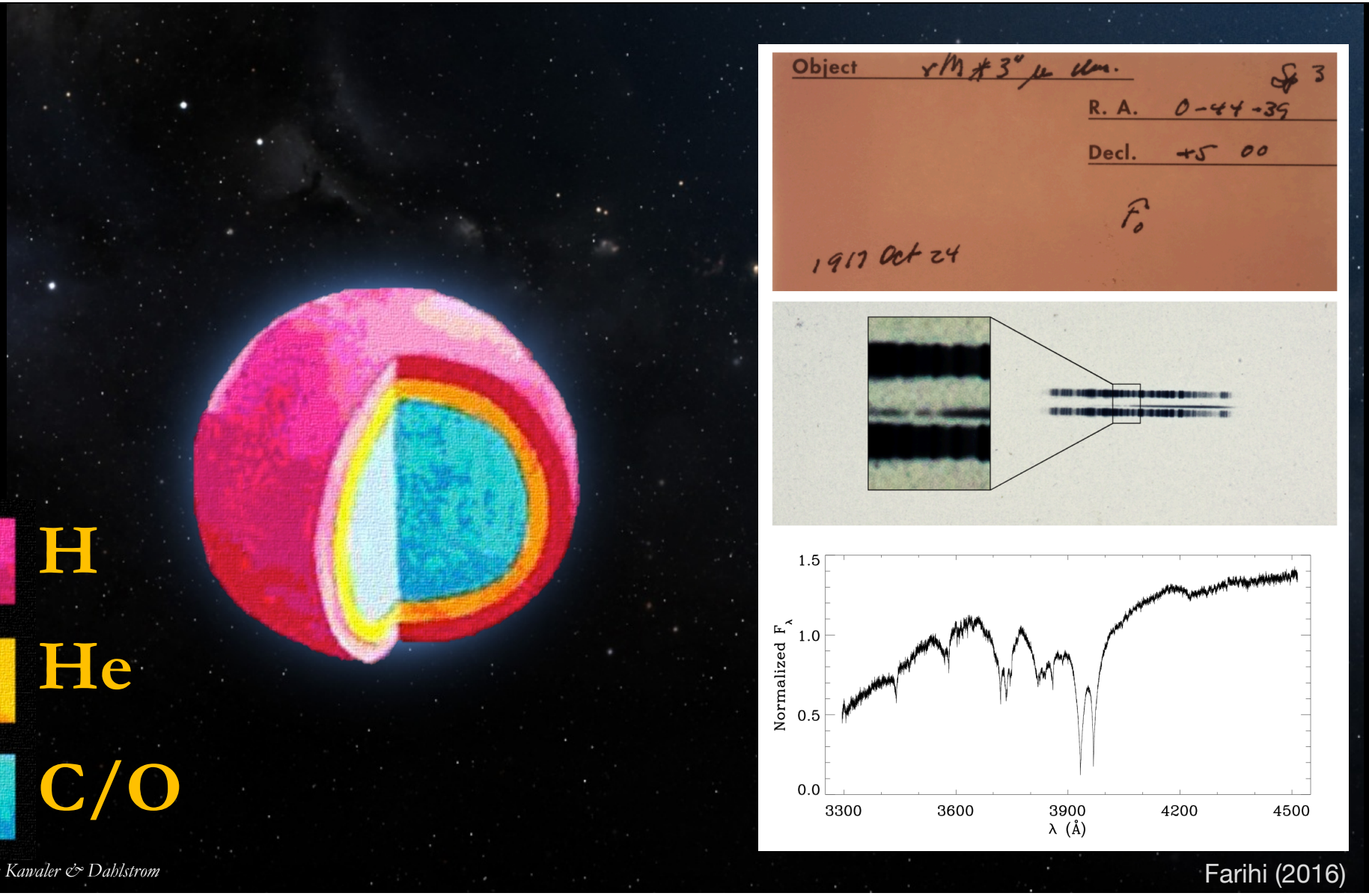

Image Source: Kawaler & Dahlstrom

Farihi (2016)

Discovery of 23 white dwarf photospheric metals

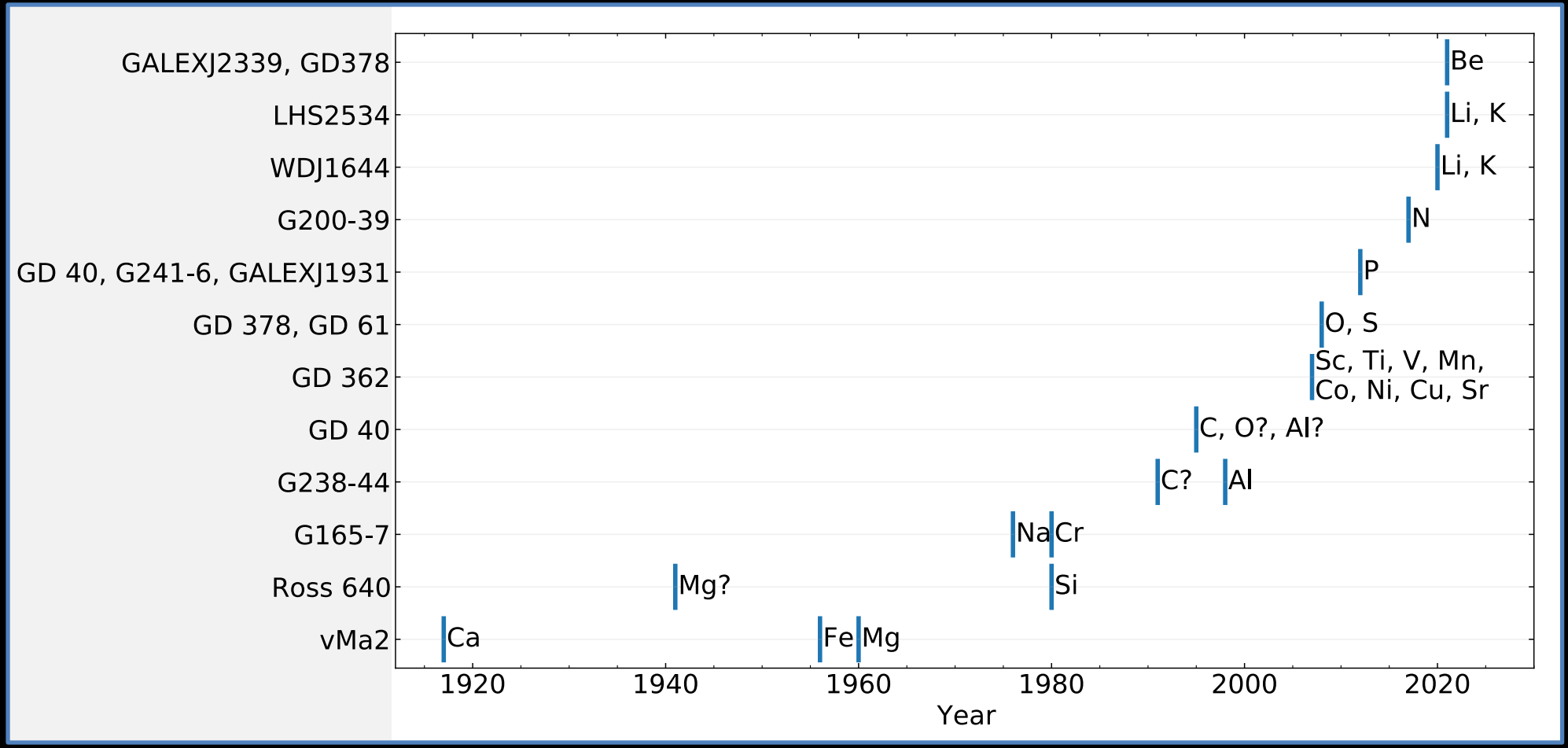

Data from Klein et al. 2021, Table 1

Discovery of 23 white dwarf photospheric metals

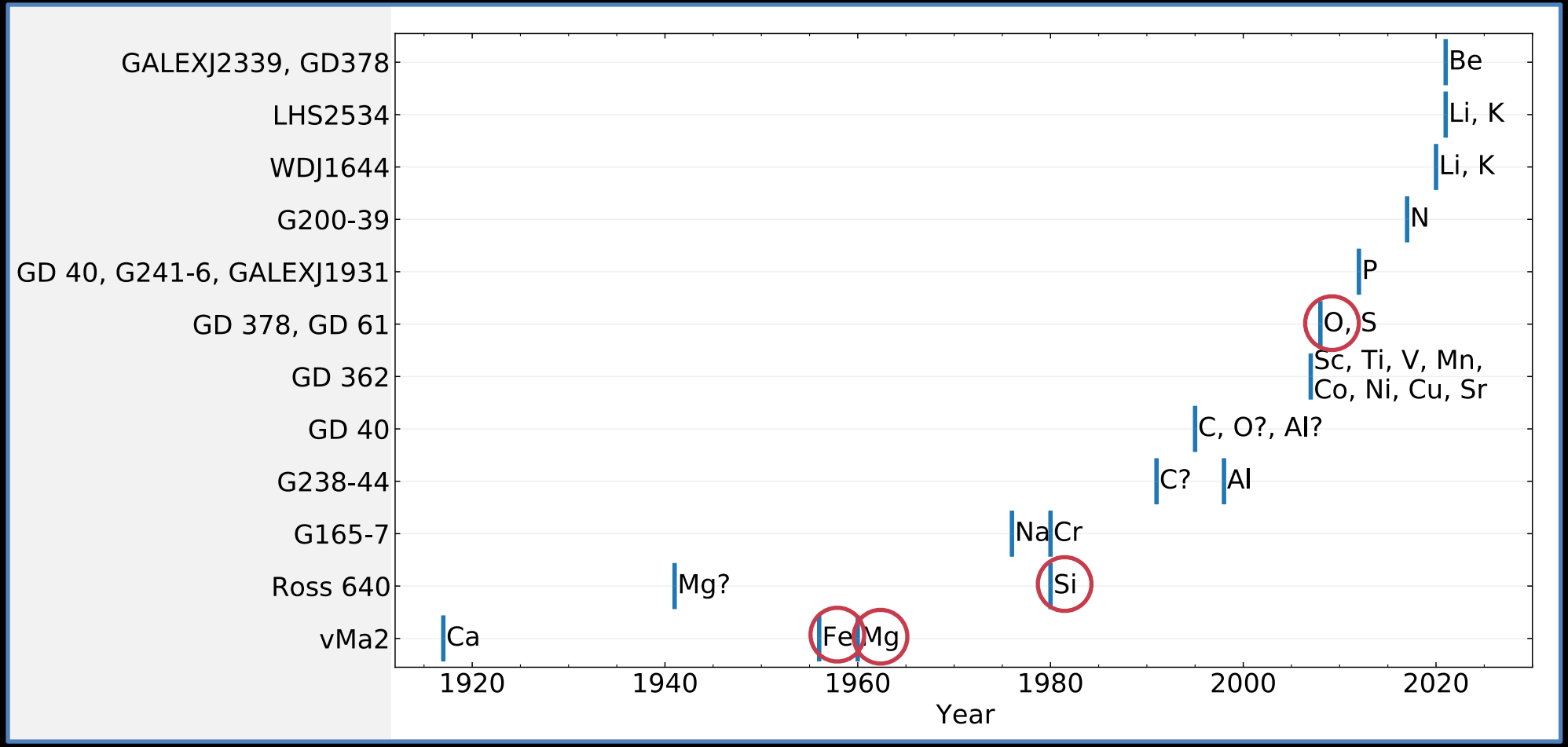

Data from Klein et al. 2021, Table 1

Discovery of 23 white dwarf photospheric metals

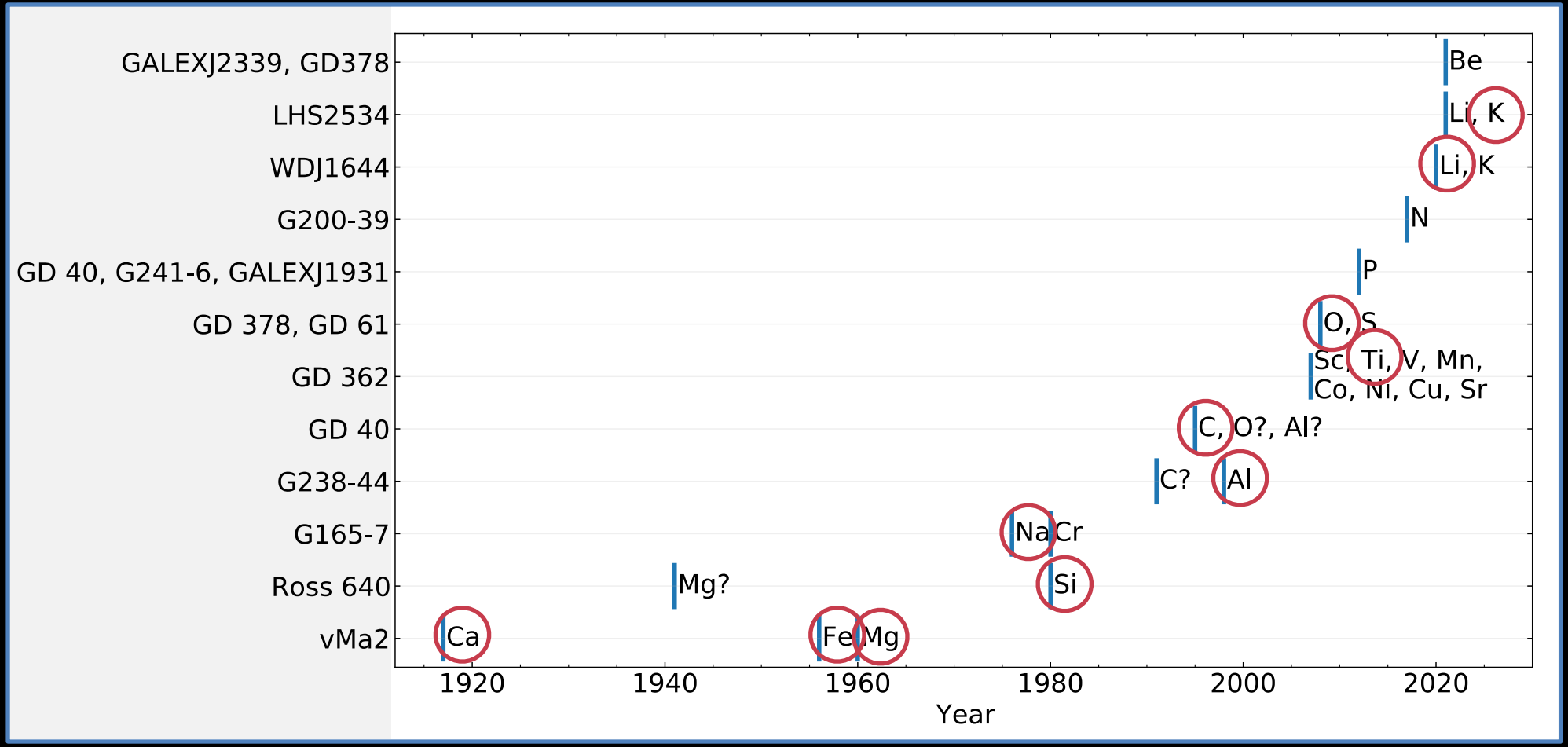

Data from Klein et al. 2021, Table 1

Discovery of 23 white dwarf photospheric metals

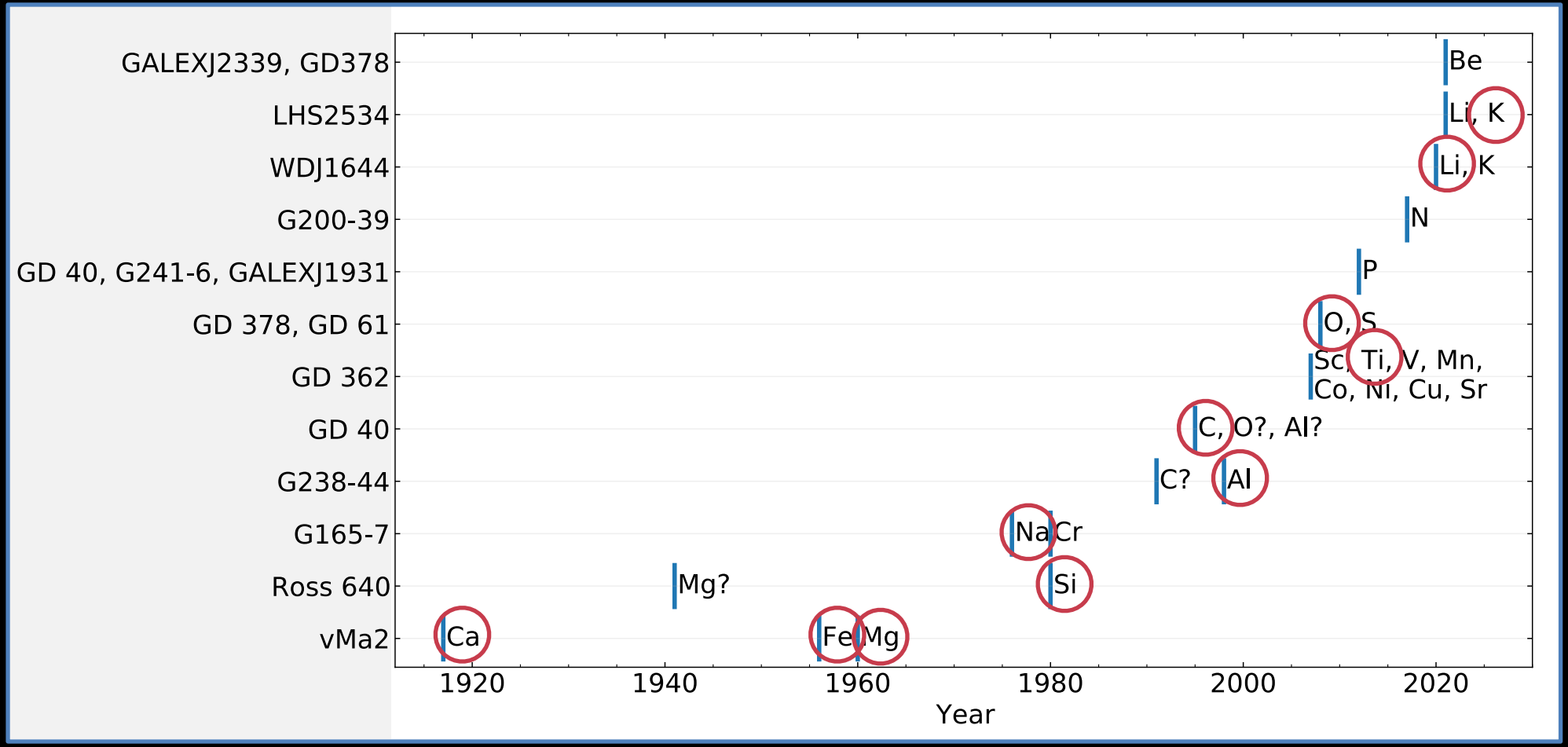

Data from Klein et al. 2021, Table 1


~360,000 white dwarf candidates
(Gentile Fusillo et al. 2021)
~40,000 spectroscopically confirmed
~25-50% w/ metal pollution...
(Koester et al. 2014)
...must be from accretion.
Image credit: NASA/JPL-Caltech

~360,000 white dwarf candidates (Gentile Fusillo et al. 2021)

~40,000 spectroscopically confirmed

~25-50% w/ metal pollution... (Koester et al. 2014)

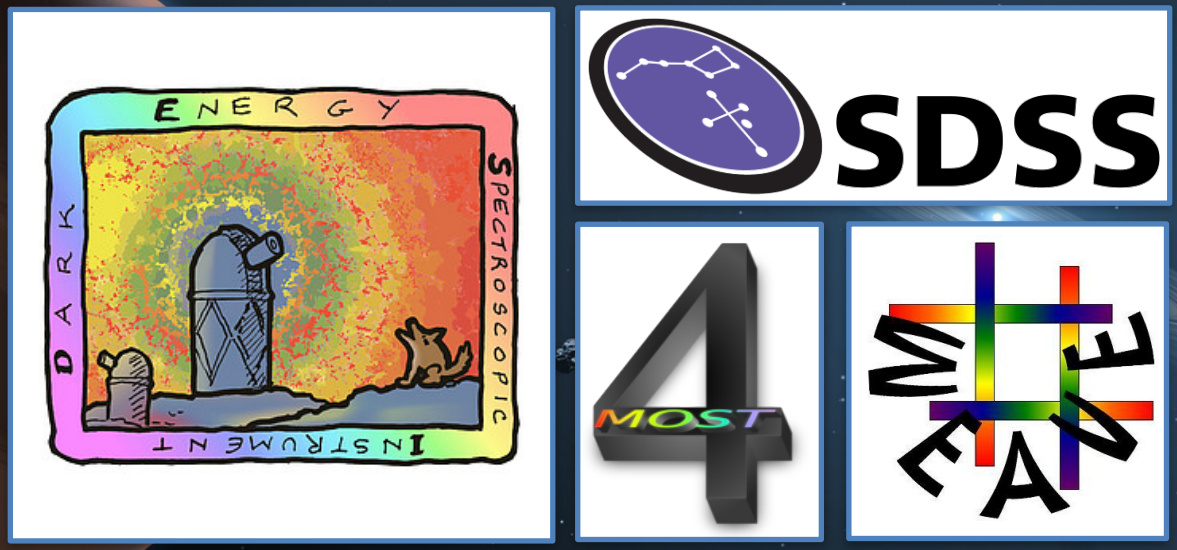

...must be from accretion.

Image credit: NASA/JPL-Caltech

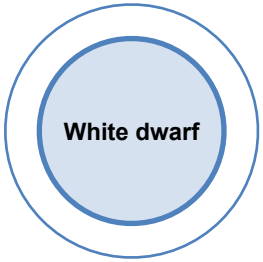
White dwarf

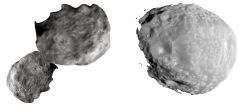

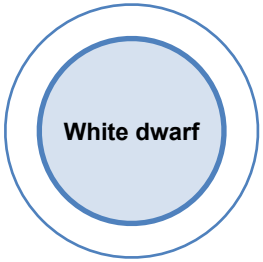
White dwarf

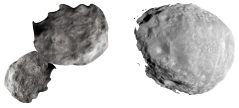

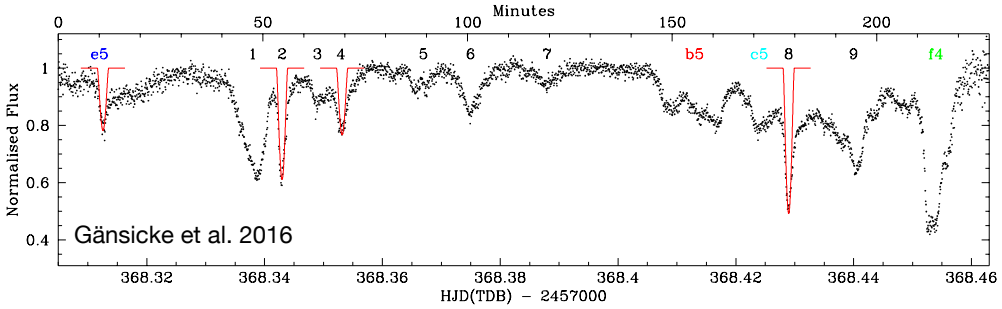

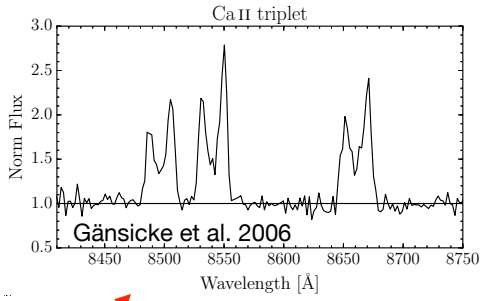

Transits

Gas

White dwarf

Dust

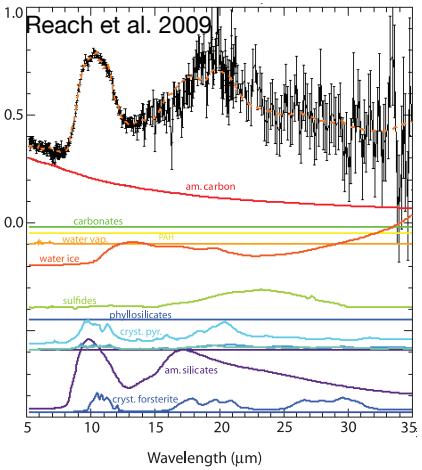

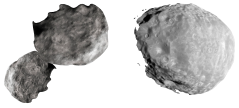

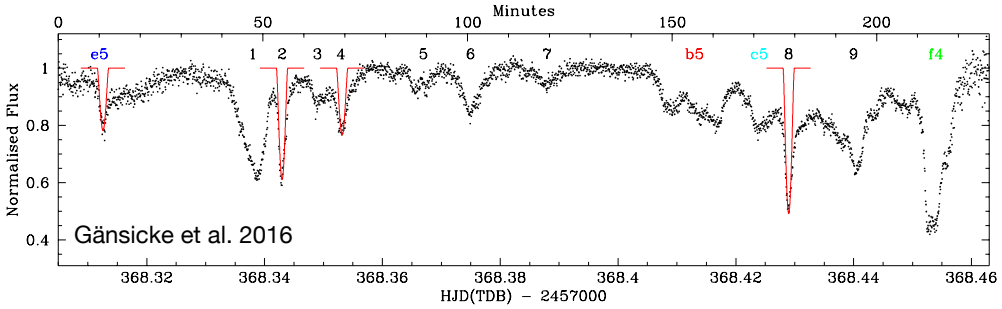

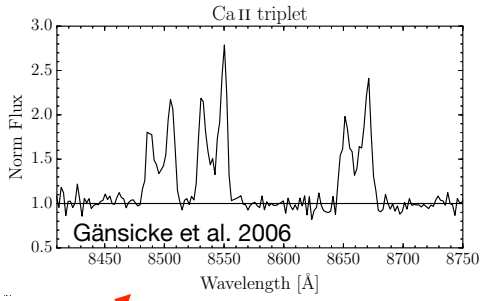

Transits

Gas

White dwarf

Atmospheric pollution

Dust

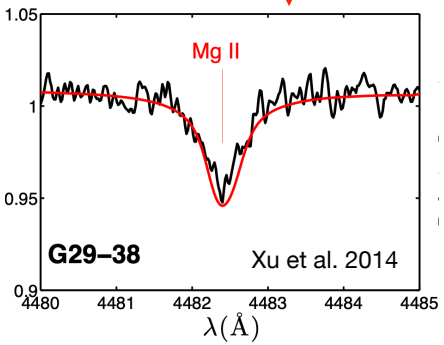

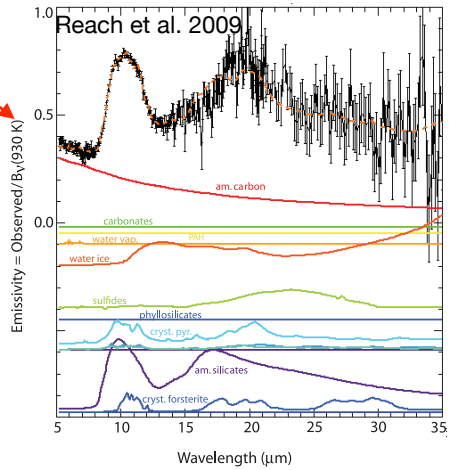

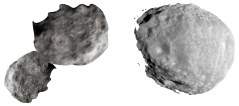

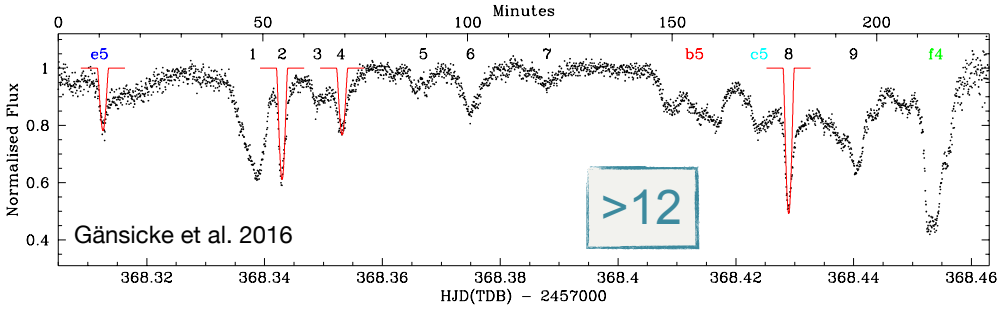

>12

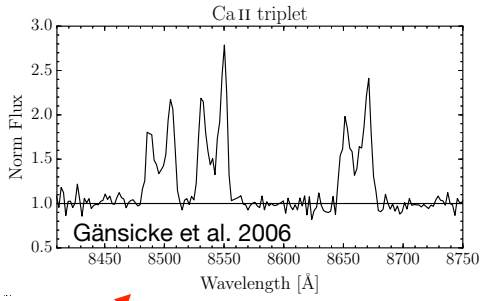

≈0.07%

Manser et al. 2020

Transits

Gas

White dwarf

Atmospheric pollution

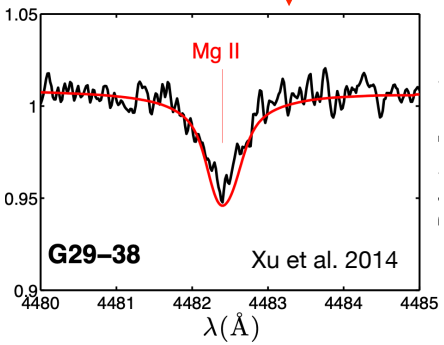

25—50%

Zuckerman et al. 2003
Zuckerman et al. 2010
Koester et. al. 2014

Dust

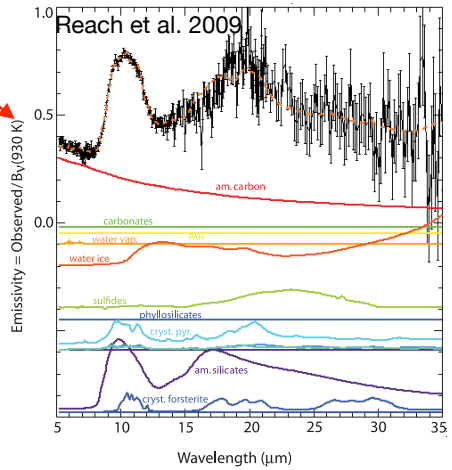

1—3%

Farihi et al. 2009
Rocchetto et al. 2015
Wilson et al. 2019

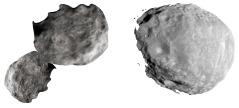

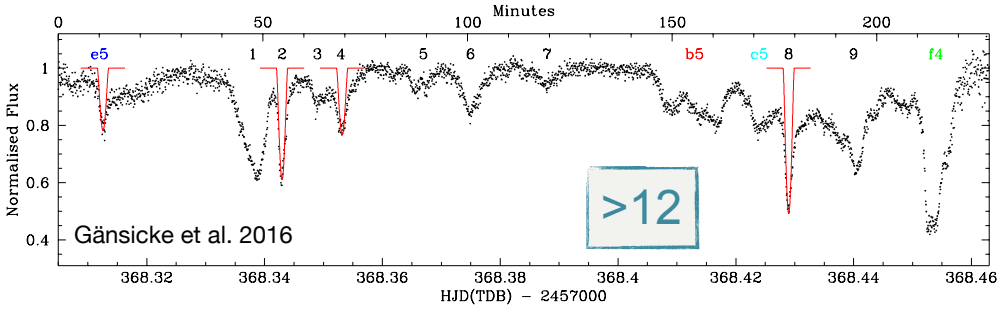

>12

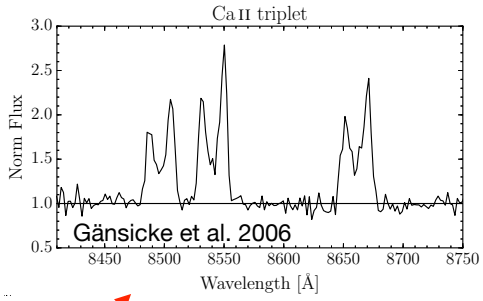

≈0.07%

Manser et al. 2020

Transits

Gas

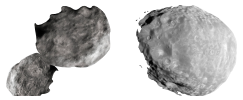

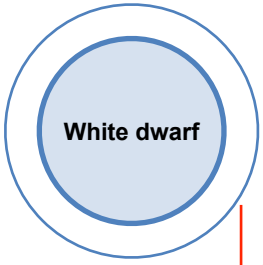

Atmospheric pollution

Dust

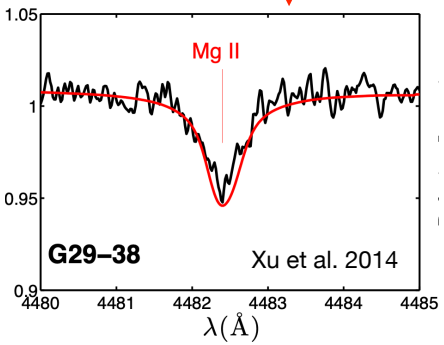

25—50%

Zuckerman et al. 2003
Zuckerman et al. 2010
Koester et. al. 2014

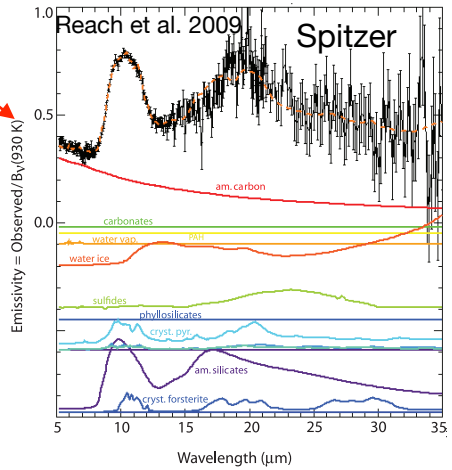

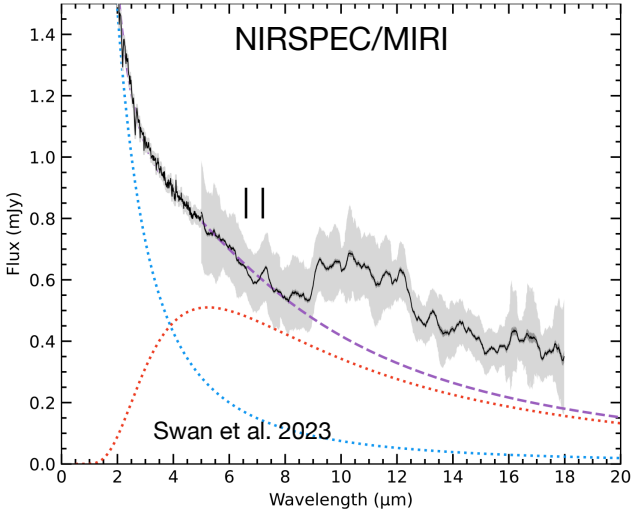

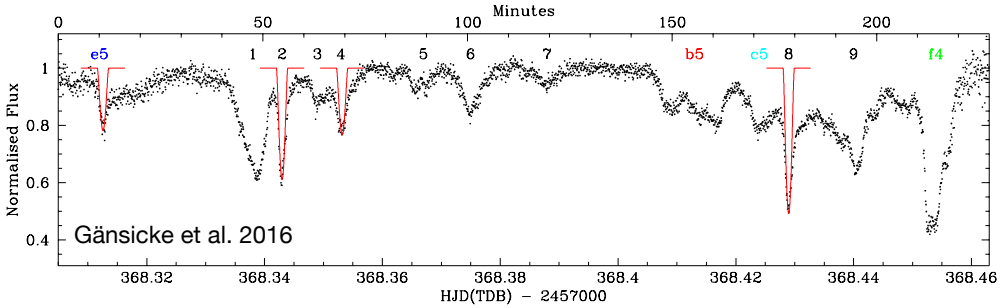

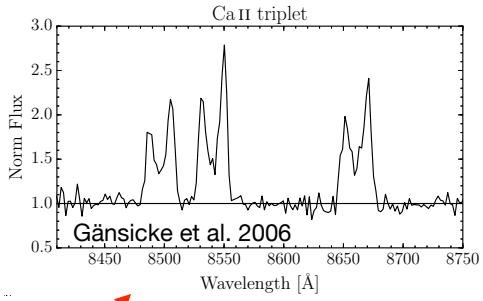

Transits

Gas

Indirect evidence of accretion

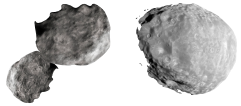

White dwarf

Atmospheric pollution

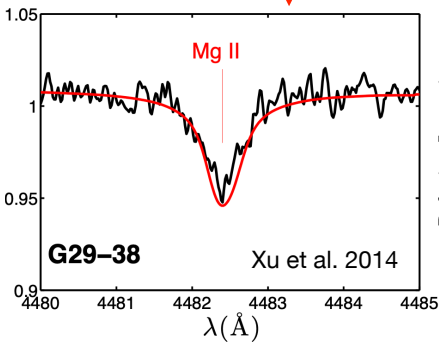

Dust

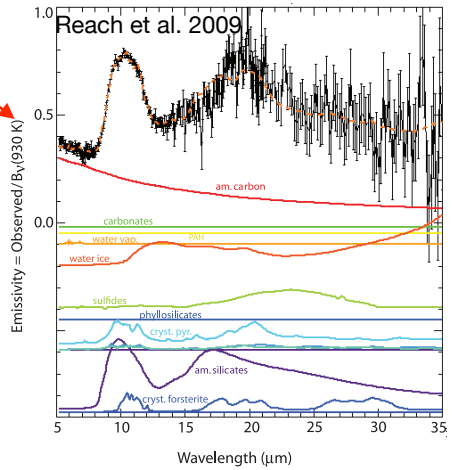

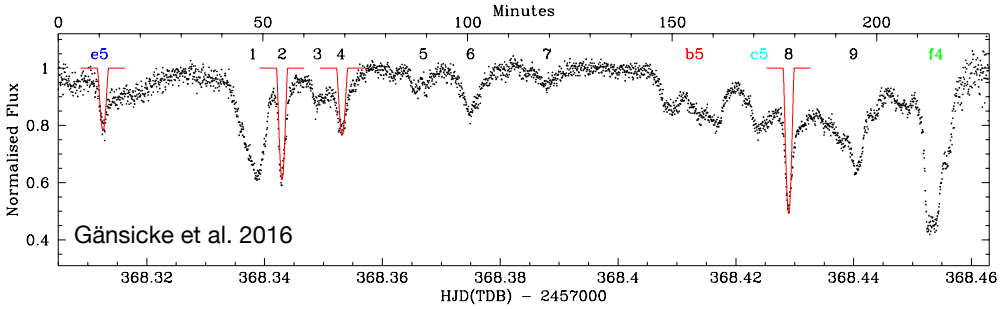

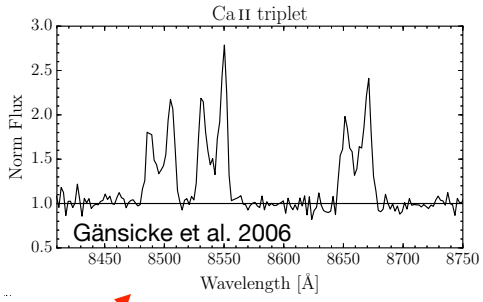

Transits

Gas

First direct evidence of accretion via X-rays

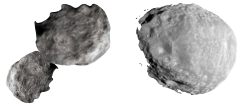

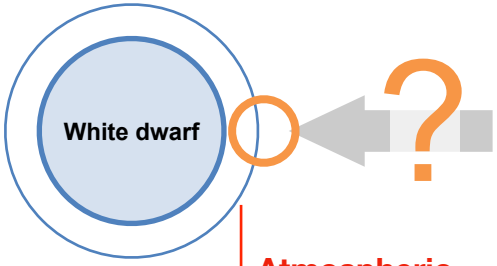

Atmospheric pollution

Dust

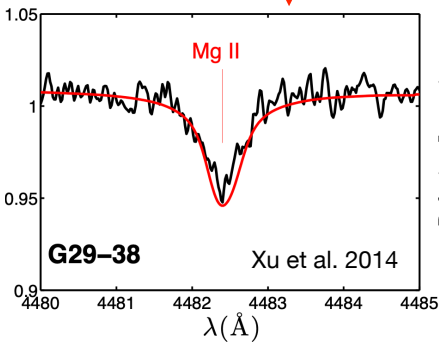

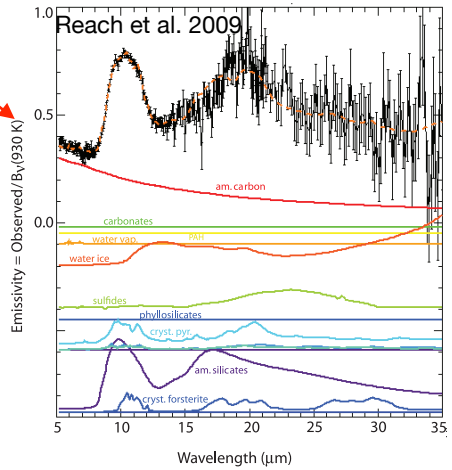

White dwarf metal pollution

Xu et al. (2014)

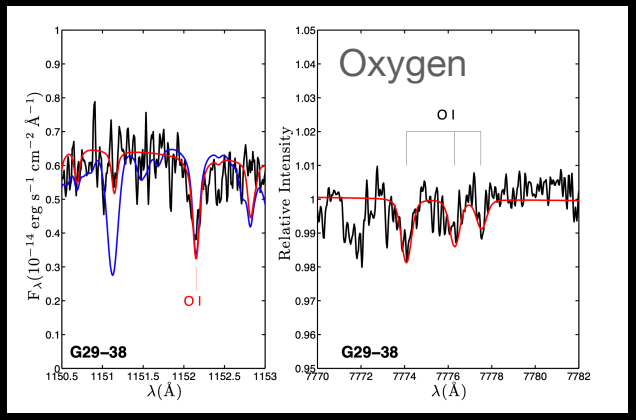

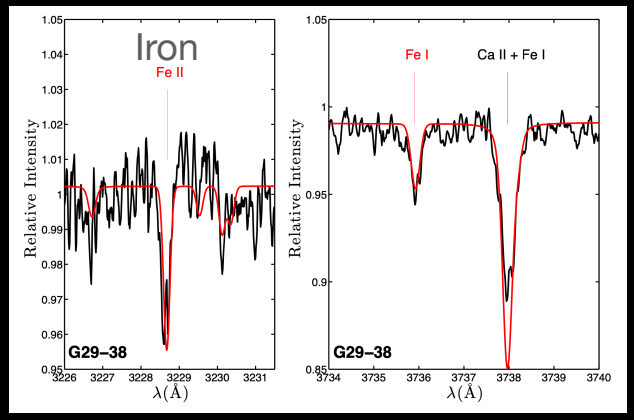

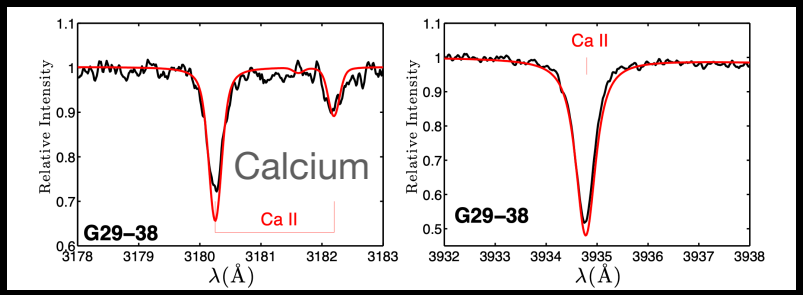

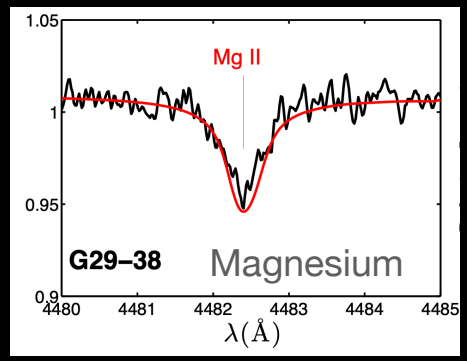

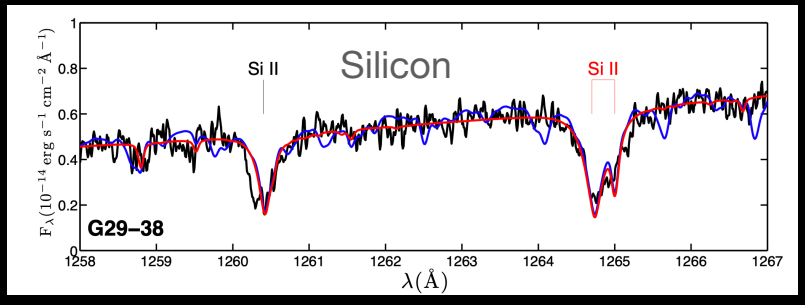

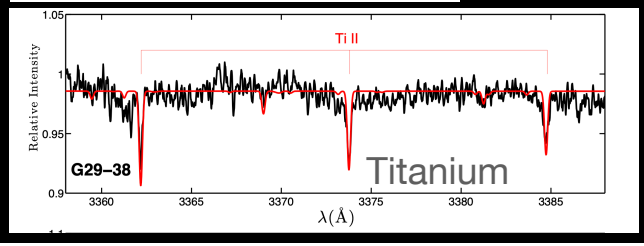

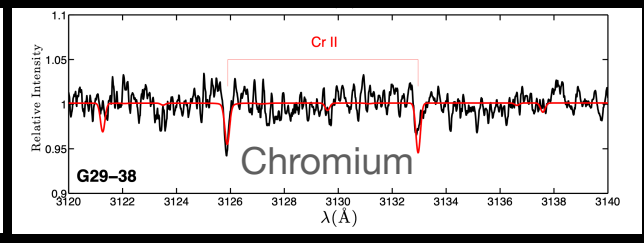

Z	[Z/H][a]
C	-6.90 ± 0.12
N	< -5.7
O	-5.00 ± 0.12
Na	< -6.7
Mg	-5.77 ± 0.13
Al	< -6.1
Si	-5.60 ± 0.17
S	< -7.0
Ca	-6.58 ± 0.12
Ti	-7.90 ± 0.16
Cr	-7.51 ± 0.12
Mn	< -7.2
Fe	-5.90 ± 0.10
Ni	< -7.3

White dwarf metal pollution

Xu et al. (2014)

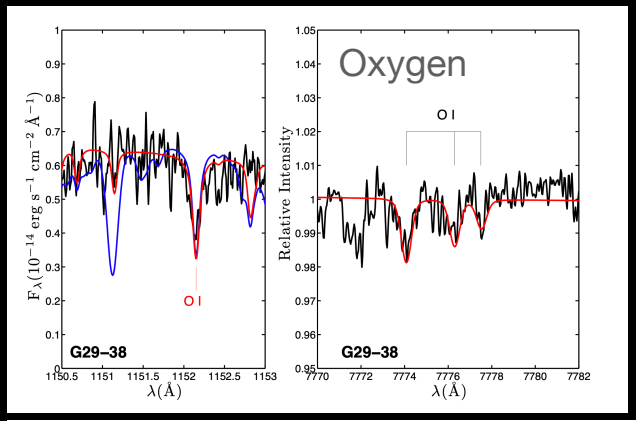

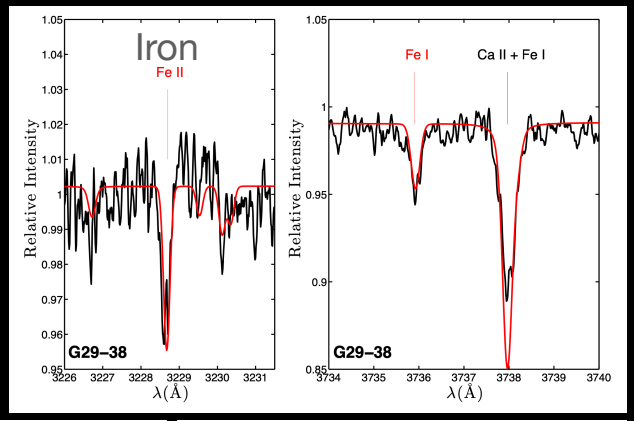

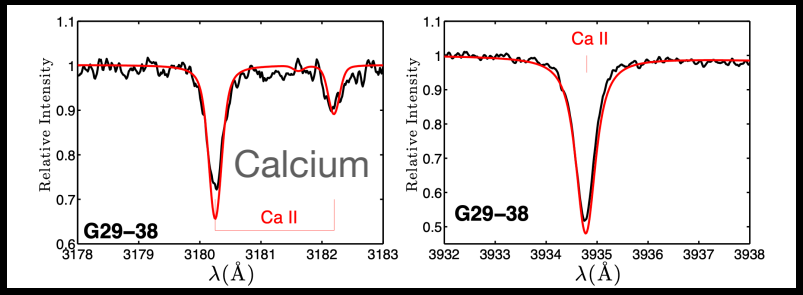

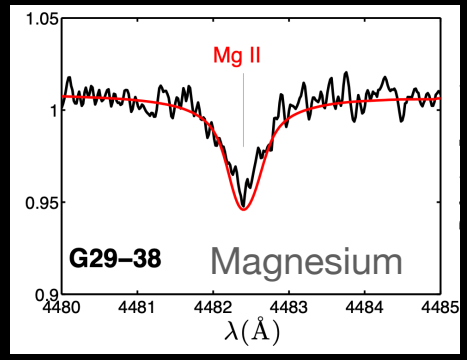

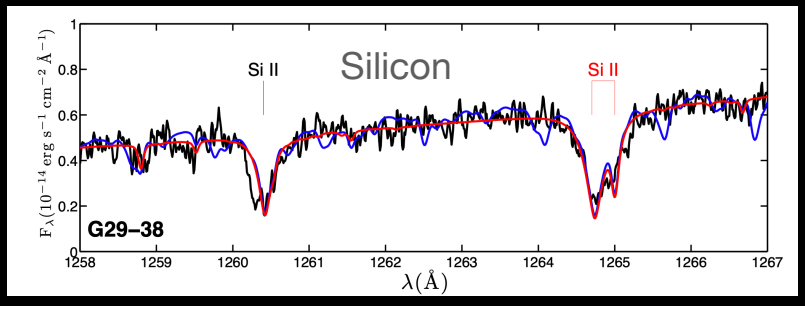

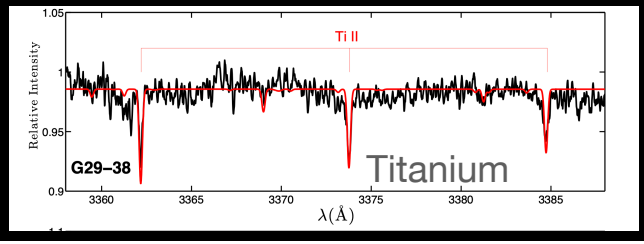

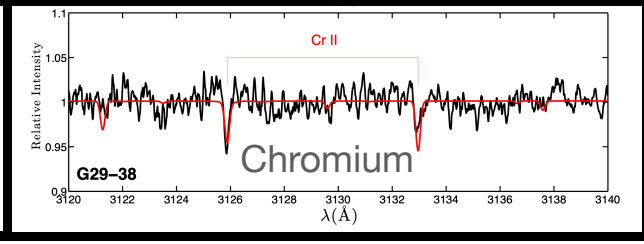

Z	[Z/H]^a	t_{set} (10^{-1} yr)
C	-6.90 ± 0.12	7.8
N	< -5.7	6.4
O	-5.00 ± 0.12	4.5
Na	< -6.7	2.1
Mg	-5.77 ± 0.13	2.5
Al	< -6.1	3.4
Si	-5.60 ± 0.17	4.6
S	< -7.0	4.1
Ca	-6.58 ± 0.12	2.0
Ti	-7.90 ± 0.16	2.7
Cr	-7.51 ± 0.12	2.4
Mn	< -7.2	2.2
Fe	-5.90 ± 0.10	2.1
Ni	< -7.3	1.9

White dwarf metal pollution

Xu et al. (2014)

$$\dot{M} = X_i \frac{M_{\rm cvz}}{\tau_{\rm diff,i}}$$

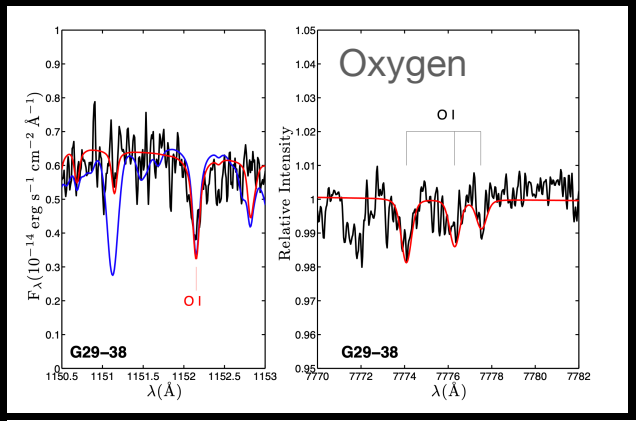

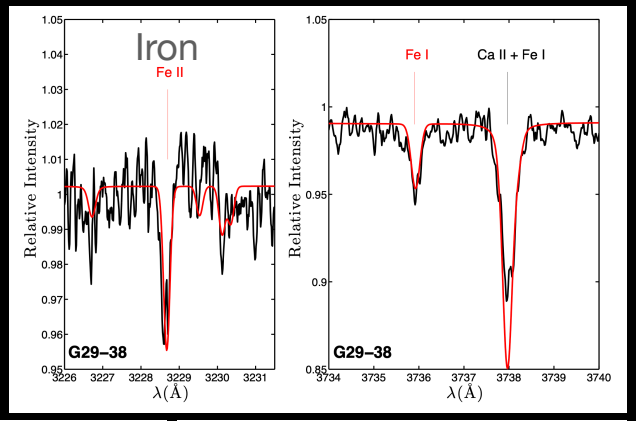

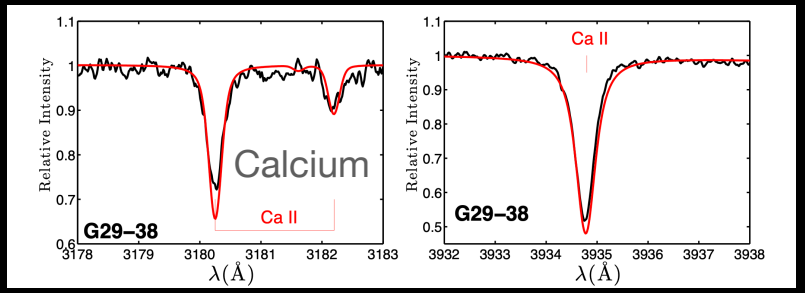

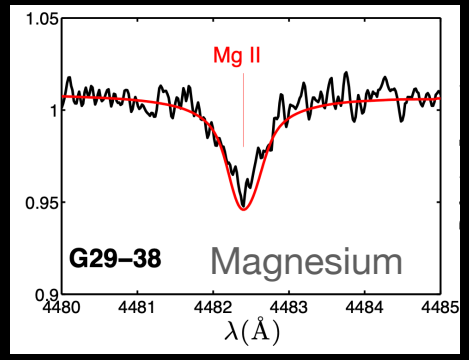

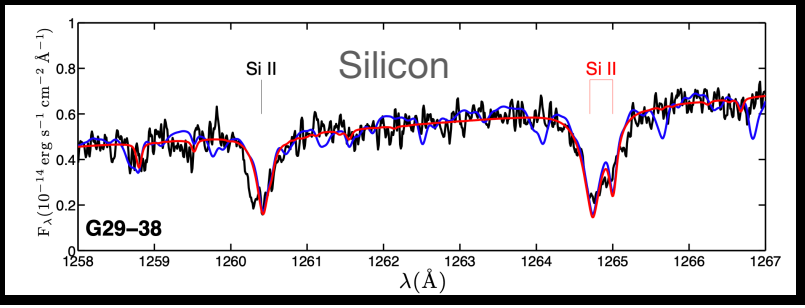

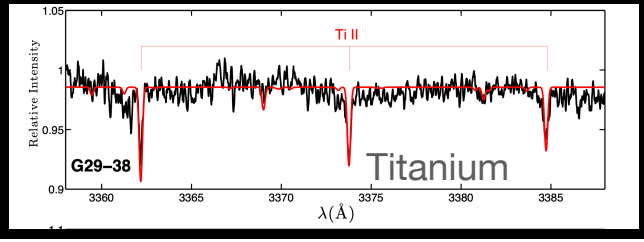

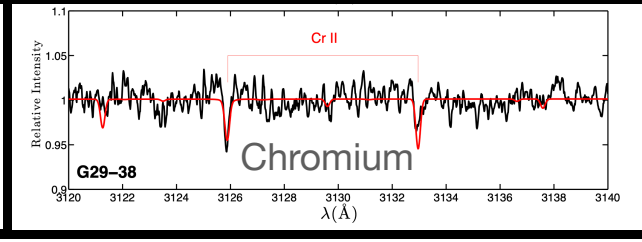

Z	[Z/H]^a	t_{set} (10^{-1} yr)	$\dot{M}(Z_i)^b$ (g s^{-1})
C	-6.90 ± 0.12	7.8	1.2×10^6
N	< -5.7	6.4	$< 2.6 \times 10^7$
O	-5.00 ± 0.12	4.5	2.2×10^8
Na	< -6.7	2.1	$< 1.3 \times 10^7$
Mg	-5.77 ± 0.13	2.5	9.8×10^7
Al	< -6.1	3.4	$< 3.8 \times 10^7$
Si	-5.60 ± 0.17	4.6	9.4×10^7
S	< -7.0	4.1	$< 4.8 \times 10^6$
Ca	-6.58 ± 0.12	2.0	3.1×10^7
Ti	-7.90 ± 0.16	2.7	1.4×10^6
Cr	-7.51 ± 0.12	2.4	4.0×10^6
Mn	< -7.2	2.2	$< 9.5 \times 10^6$
Fe	-5.90 ± 0.10	2.1	2.0×10^8
Ni	< -7.3	1.9	$< 9.6 \times 10^6$
Total^c			6.5×10^8

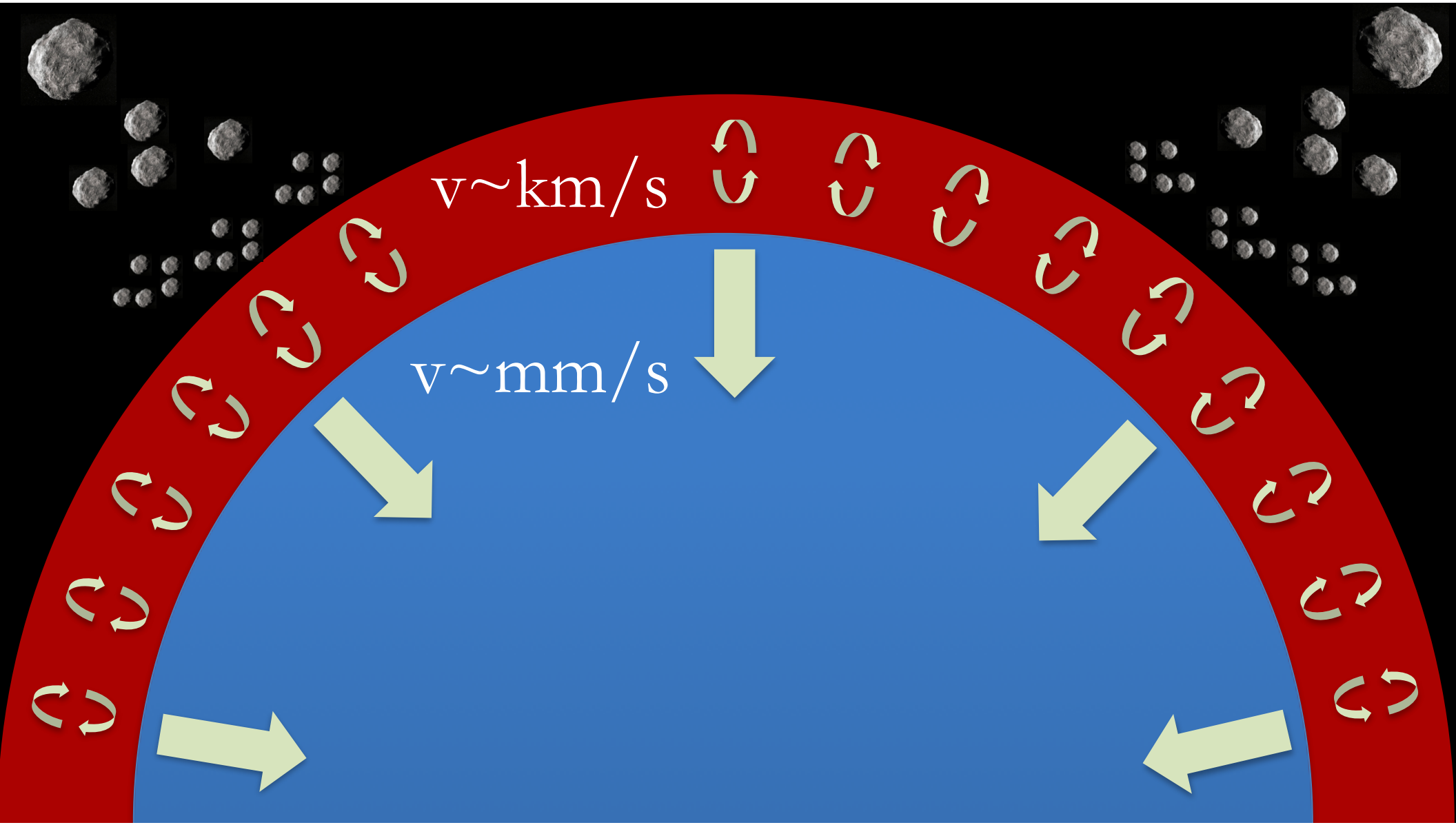
v~km/s
v~mm/s

1D Mixi

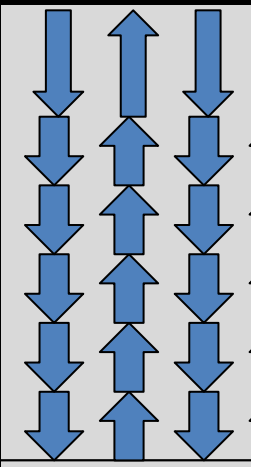

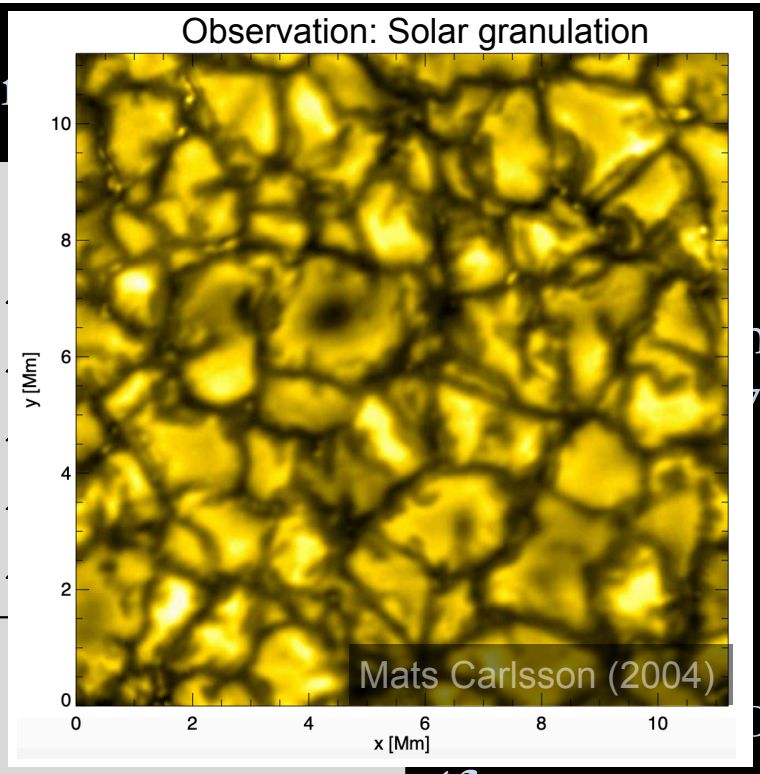

(free parameters)

vs.

first principles
(numerical parameters)

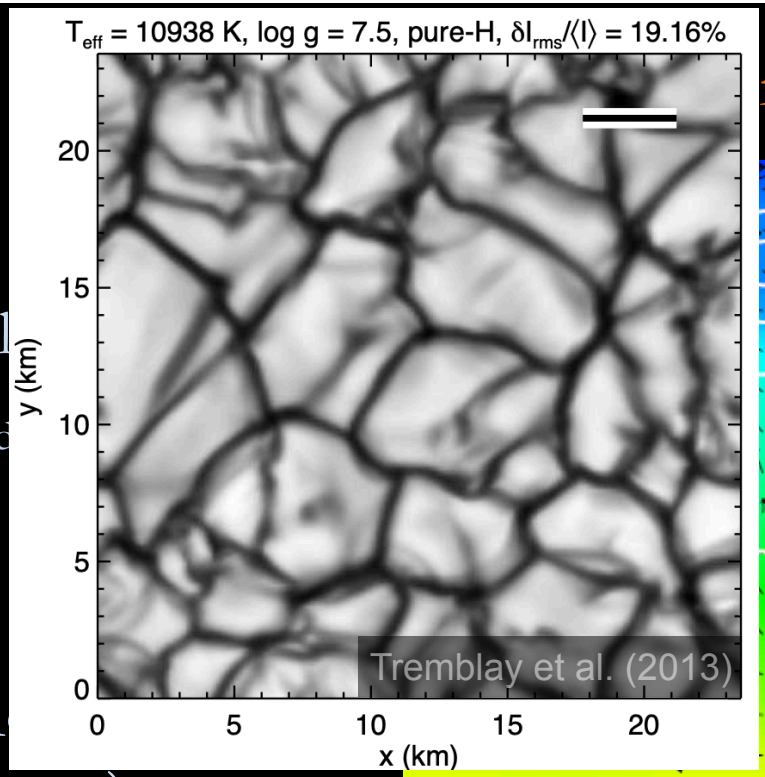

rodynamics

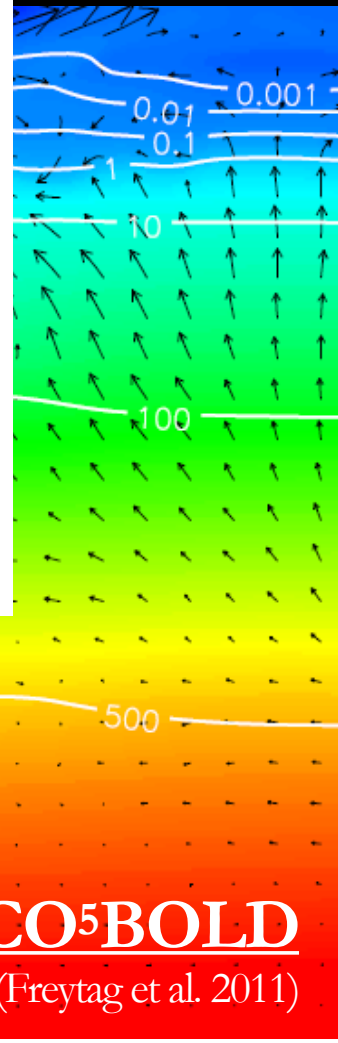

CO5BOLD
(Freytag et al. 2011)

WD convection: 3D radiation hydrodynamic simulations with CO5BOLD

(Freytag et al. 2012)

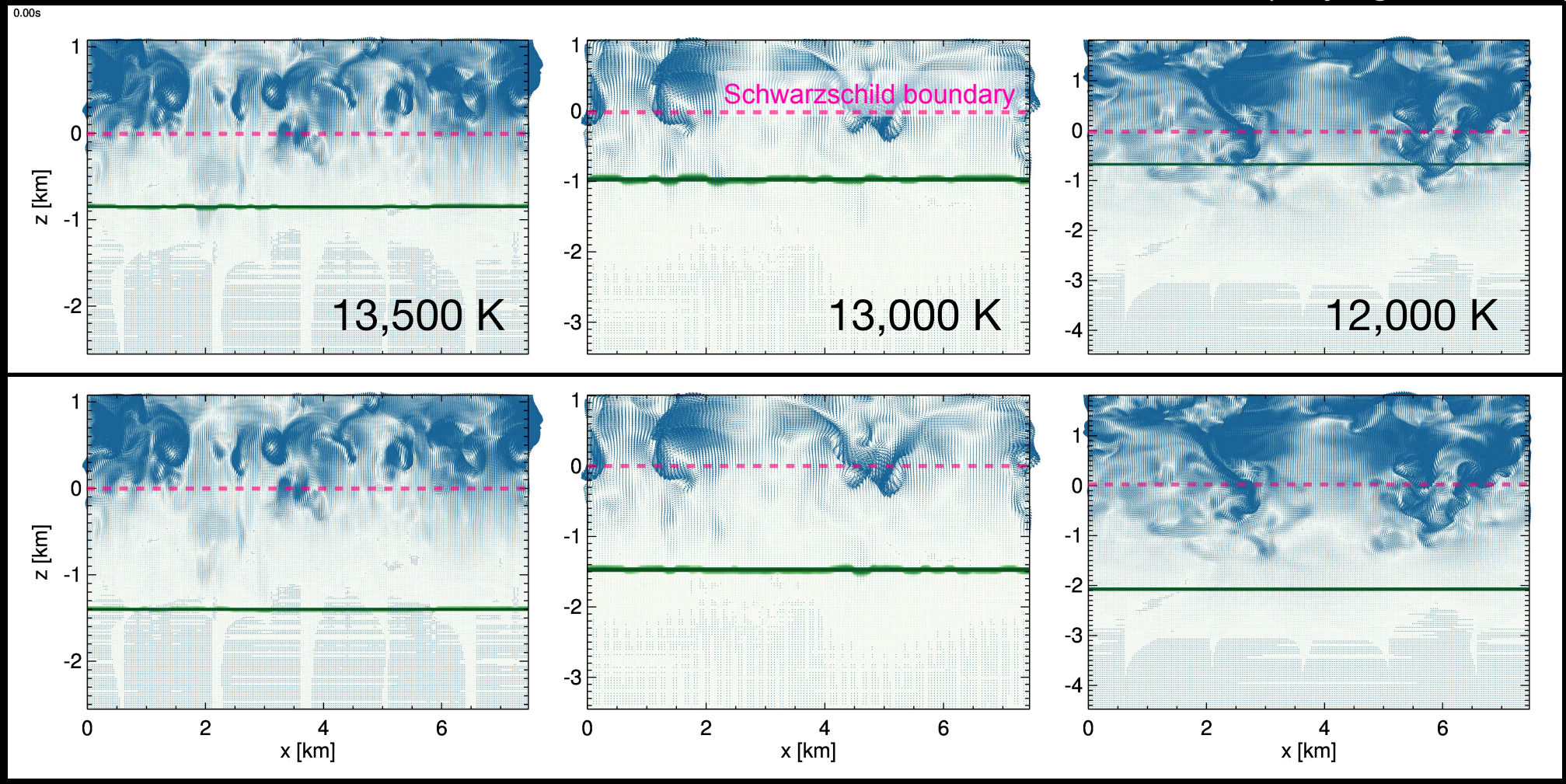

warwick.ac.uk/timcunningham/movies/

Cunningham et al. (2019)

Diffusion timescales and mixed mass - 3D convective overshoot

$$\dot{M} = X_i \frac{M_{\mathrm{cvz}}}{\tau_{\mathrm{diff,i}}}$$

Mixed mass

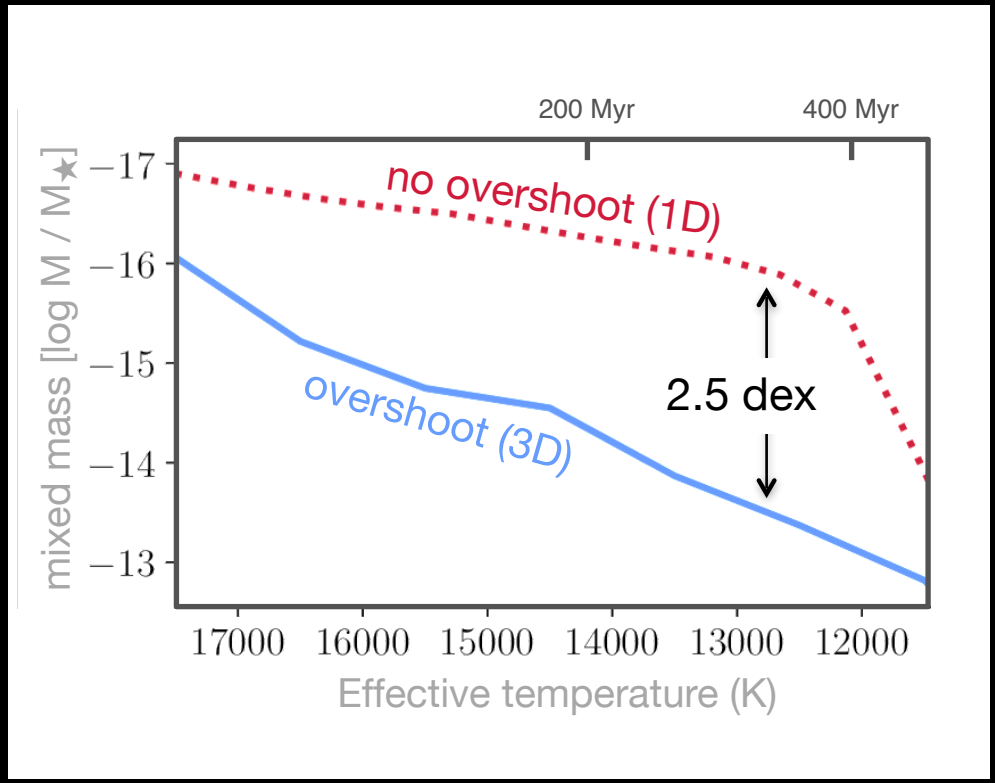

Diffusion timescales

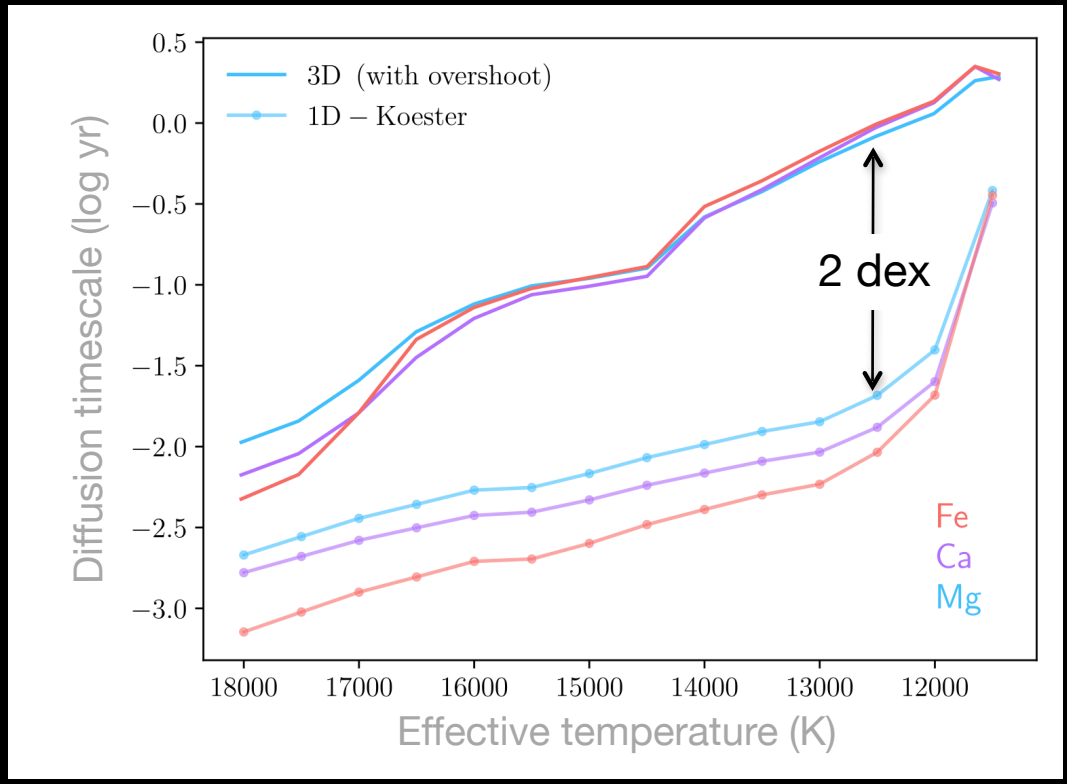

Cunningham et al. (2019)

Diffusion timescales and mixed mass - 3D convective overshoot

$$\dot{M} = X_i \frac{M_{\rm cvz}}{\tau_{\rm diff,i}}$$

Mixed mass

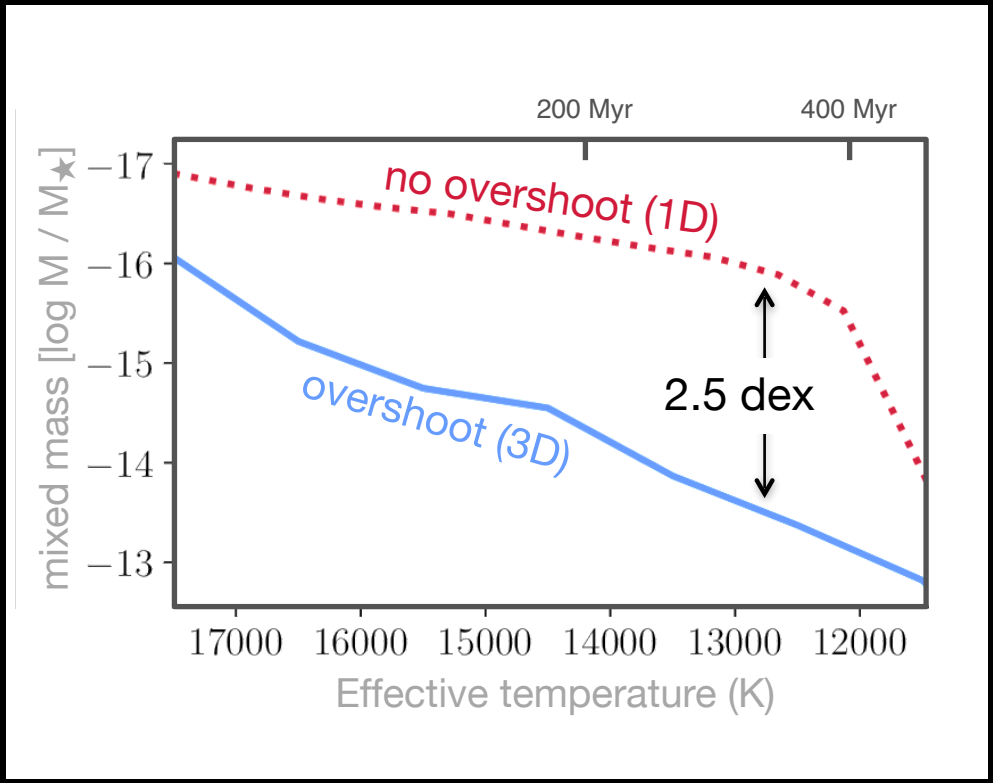

Diffusion timescales

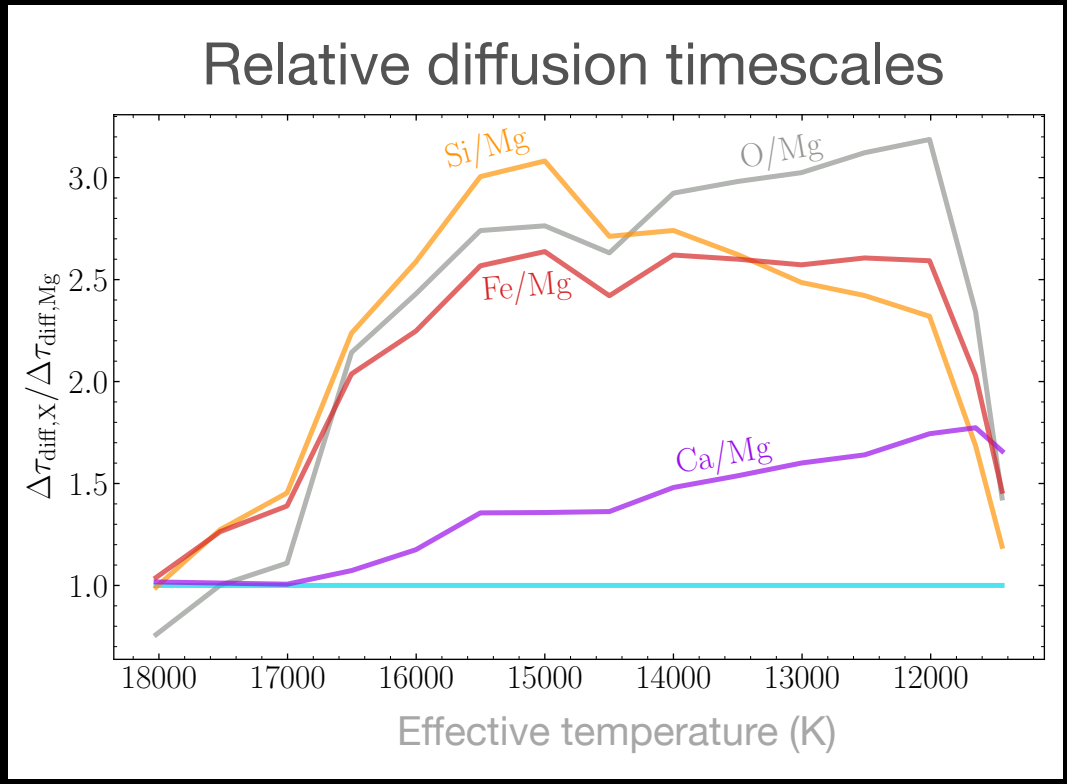

Cunningham et al. (2019)

Accretion rates depend on atmospheric models

Convective overshoot (3D)

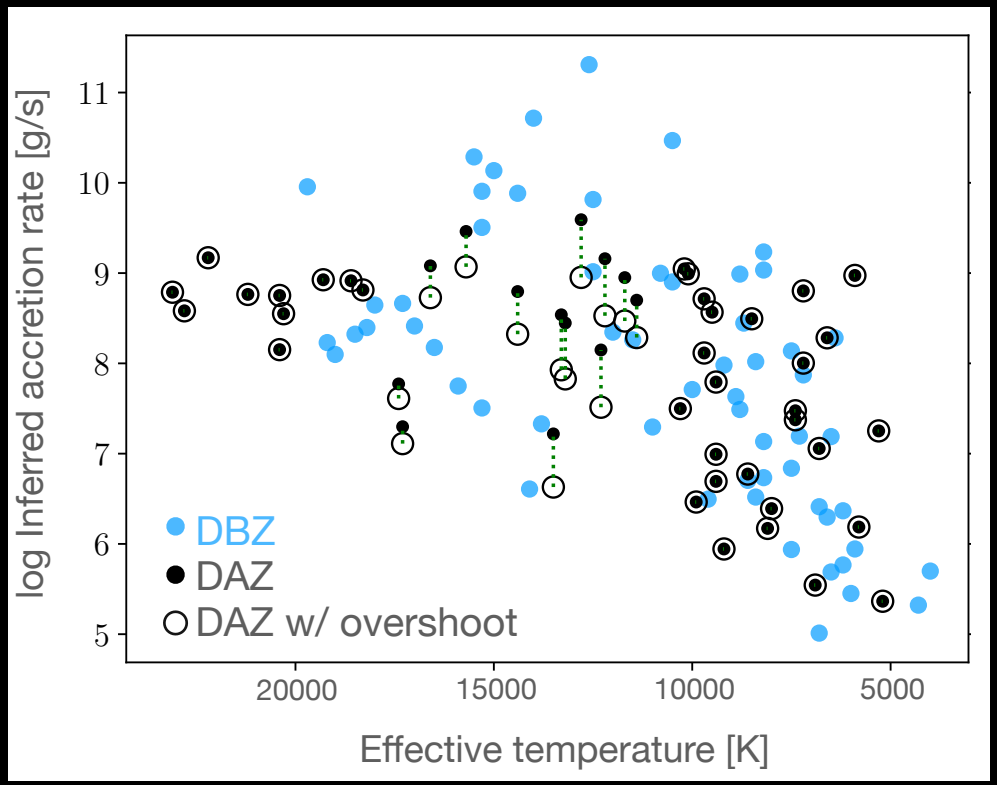

Cunningham et al. (2019)

up to 0.7 dex increase

Thermohaline mixing

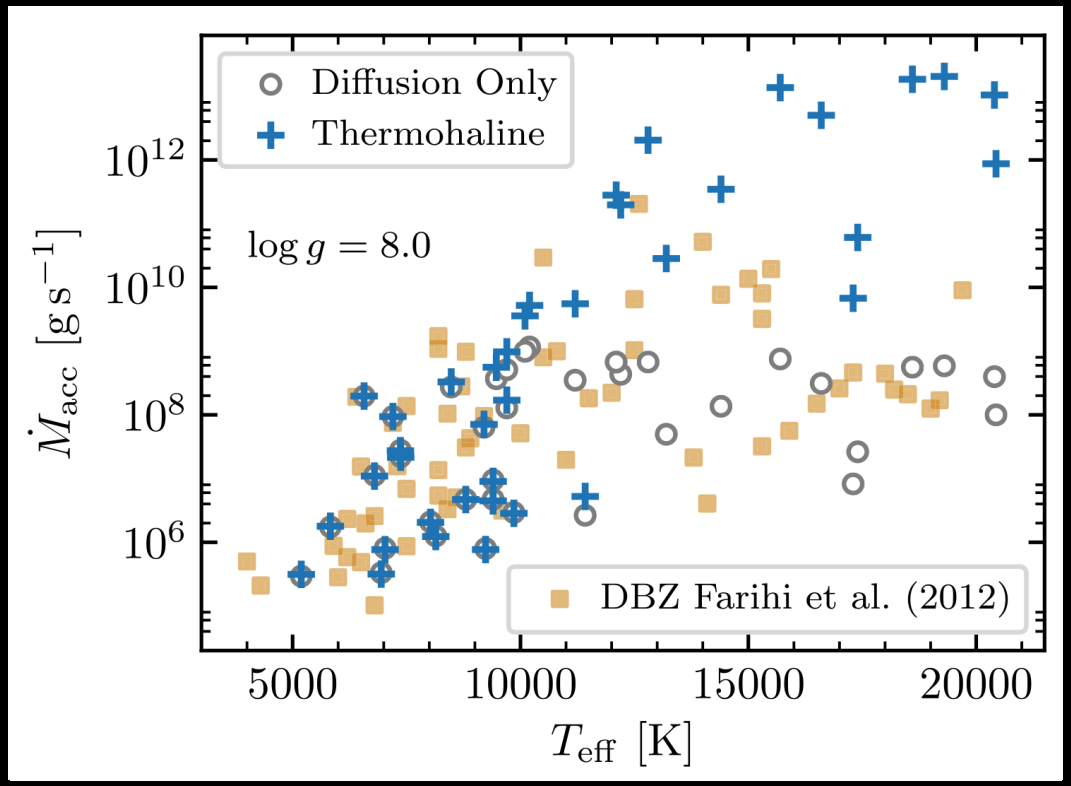

up to 3–4 dex increase

Bauer & Bildsten (2018; 2019)

G29–38: the prototypical metal-polluted WD

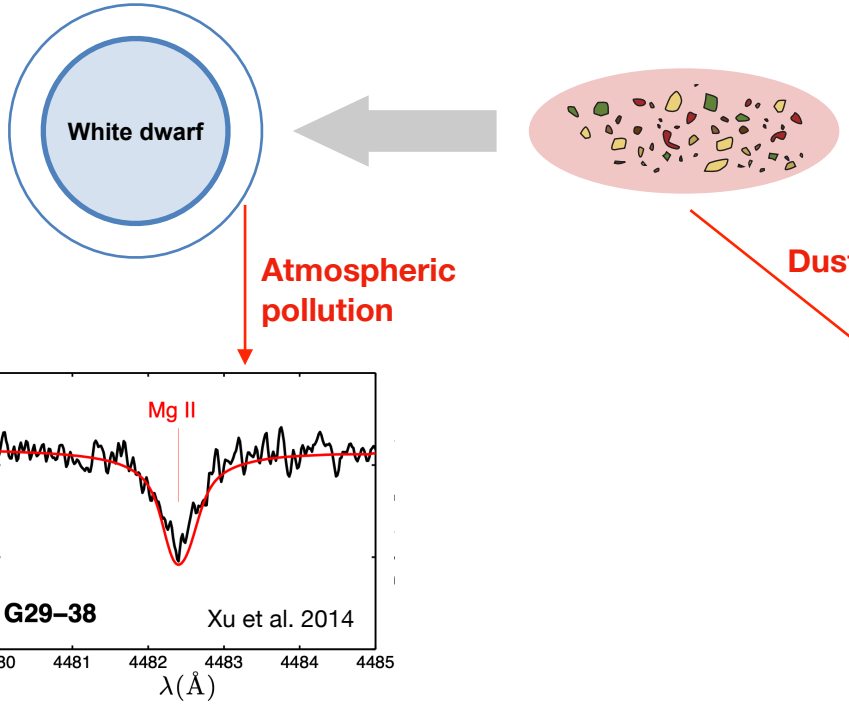

G29–38: the prototypical metal-polluted WD

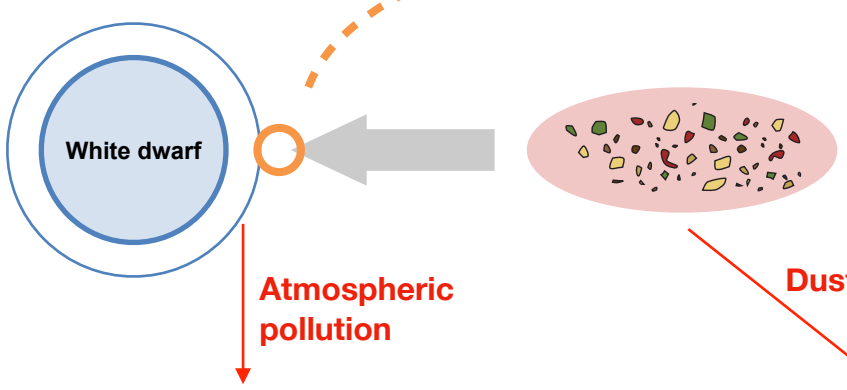

Atmospheric pollution

Dust

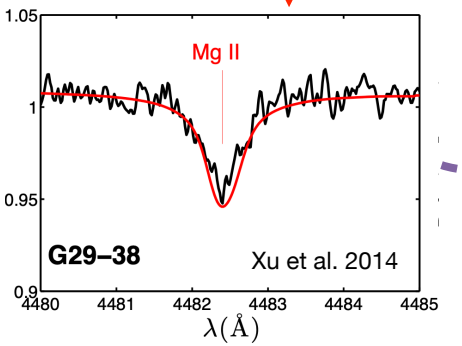

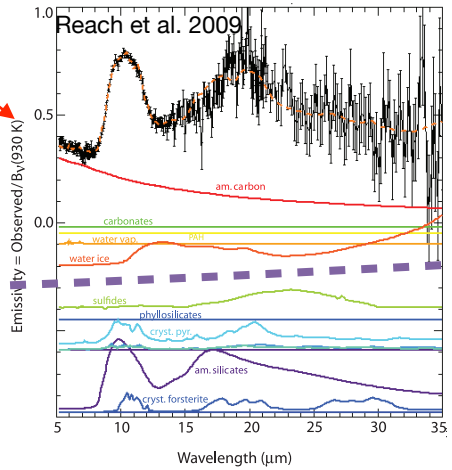

Accretion-induced luminosity:

$$L_{\rm X} = \frac{GM_\star \dot{M}}{2R_\star}$$

Mdot from X-ray luminosity:

$$\dot{M}_{\rm X} = 2L_{\rm X}\frac{R_\star}{GM_\star}$$

Mdot from photospheric abundances, X_i:

$$\dot{M} = X_i \frac{M_{\rm cvz}}{\tau_{\rm diff},\, i}$$

X-rays as direct evidence of ongoing accretion

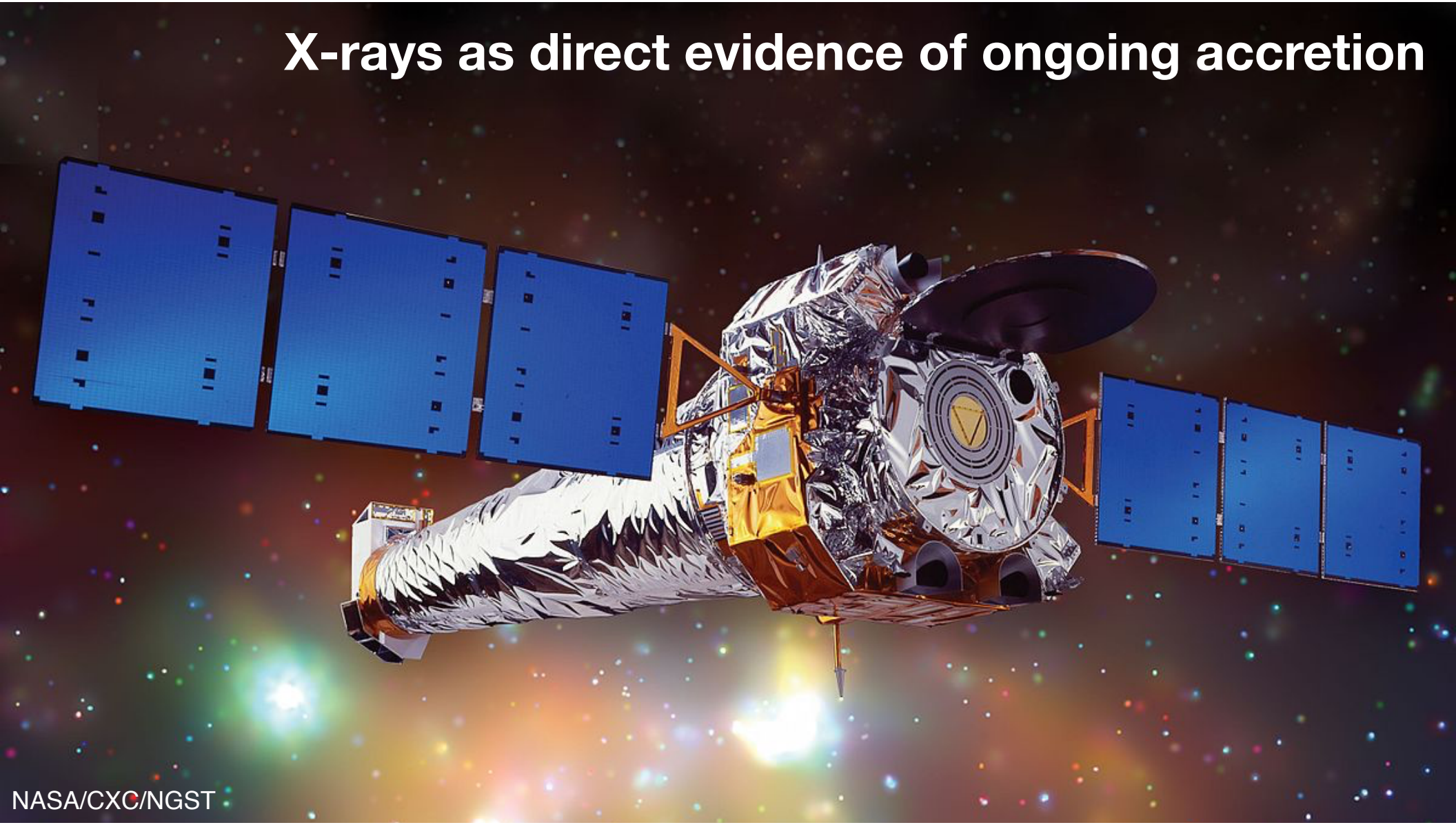

NASA/CXC/NGST

G29–38: a new class of X-ray source

Confirmed to 4.5 – 5.9 σ

Cunningham et al. (2022), Nature, 602, 219

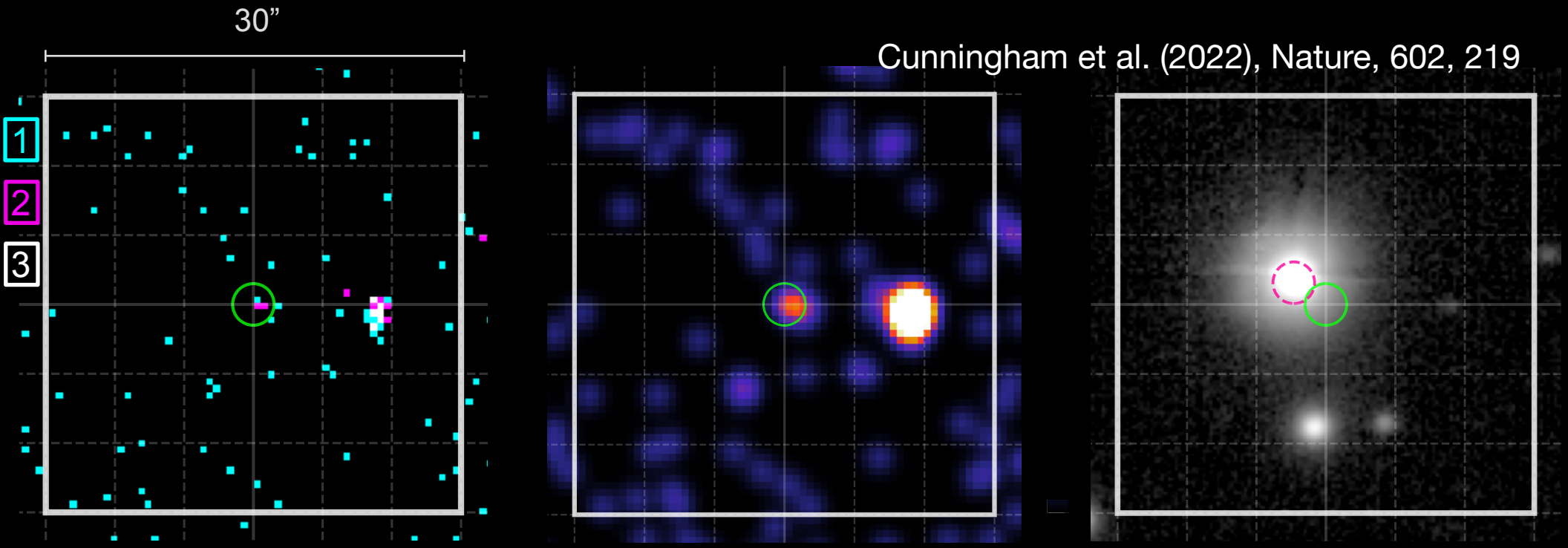

115 ksec (32 hr) *Chandra* observation of G29–38

G29–38: a new class of X-ray source

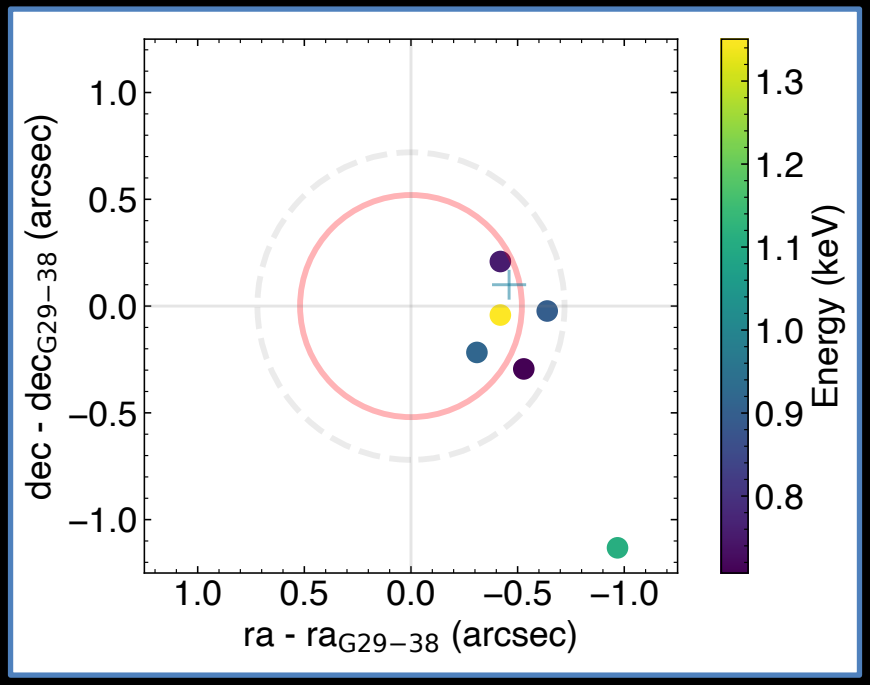

$$F_X = 1.97^{+1.55}_{-0.48} \cdot 10^{-15}\,\mathrm{erg\,s^{-1}\,cm^{-2}}$$

$$D = 17.53 \pm 0.01\,\mathrm{pc}$$

$$L_X = 7.24^{+5.66}_{-1.76} \cdot 10^{25}\,\mathrm{erg\,s^{-1}}$$

$$k_B T = 0.5 \pm 0.2\,\mathrm{keV}$$

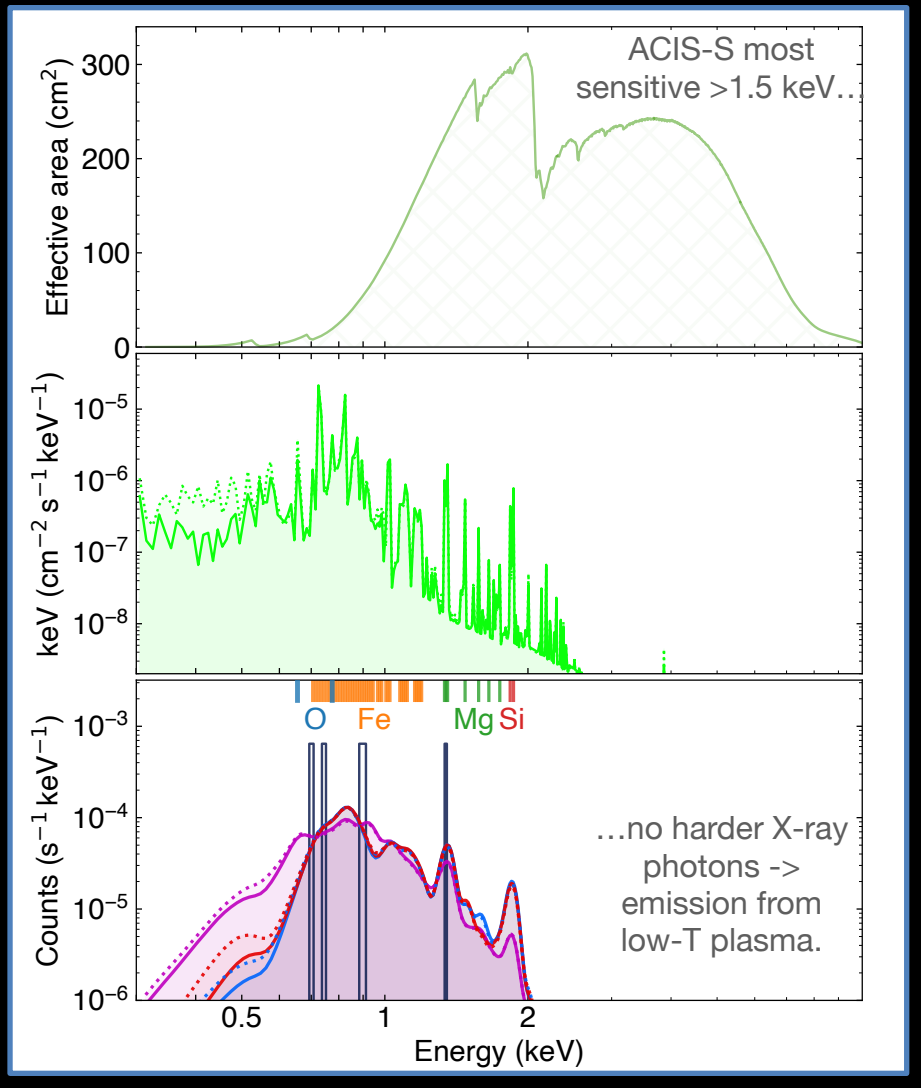

G29–38: an independent Mdot

Cunningham et al. (2022), Nature, 602, 219

Measured X-ray Mdot agrees with spectroscopic inferred Mdot

Lower limit appears favour models with enhanced mixing

More observations needed to rule out no overshoot

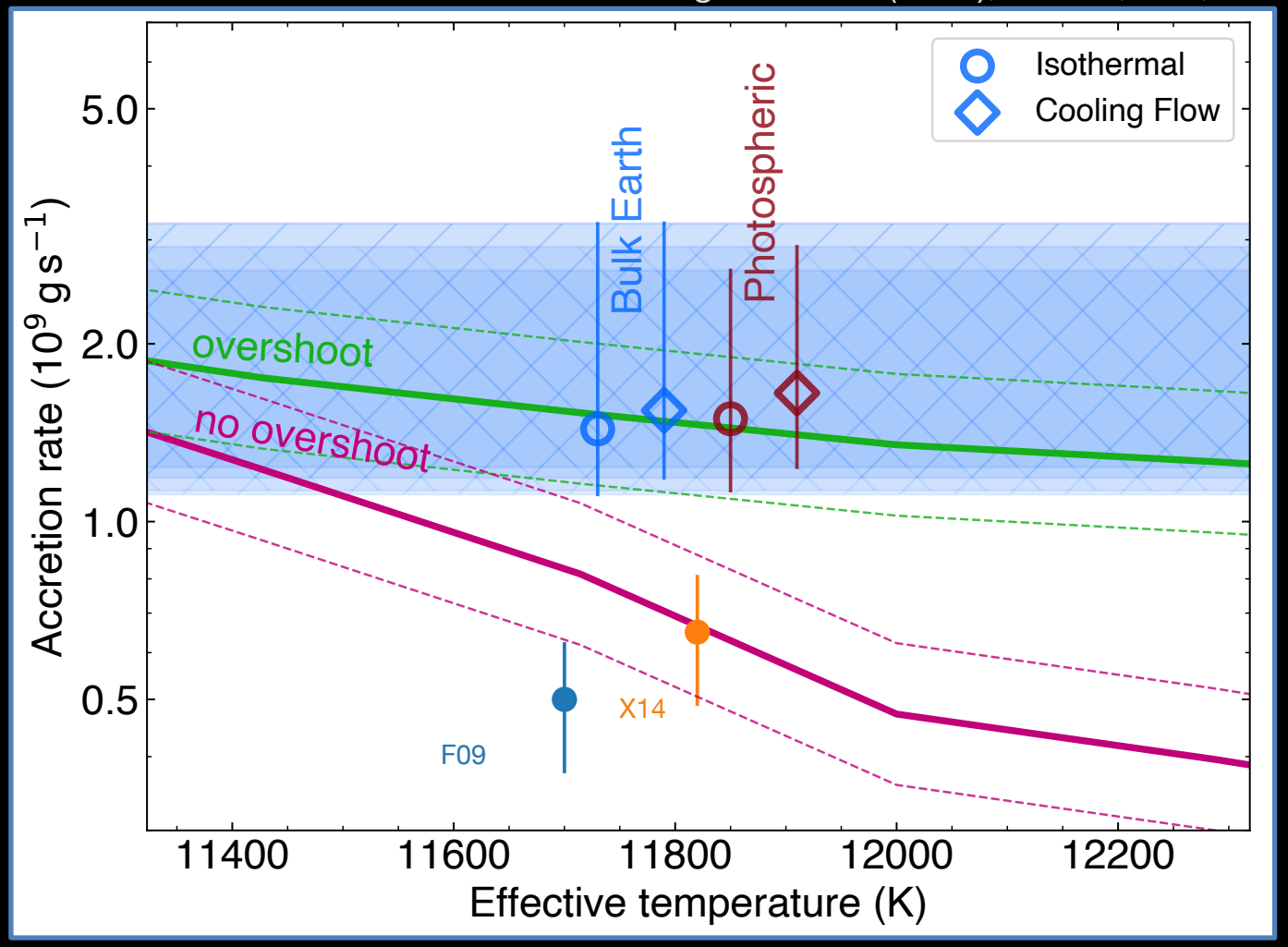

Accretion rate upper limit

- **Unobserved X-ray flux**
- ~~Cyclotron emission cooling~~ (B<1.5 kG)

Constraining the EUV flux → **Chandra+HST: XUV Differential Emission Measure**

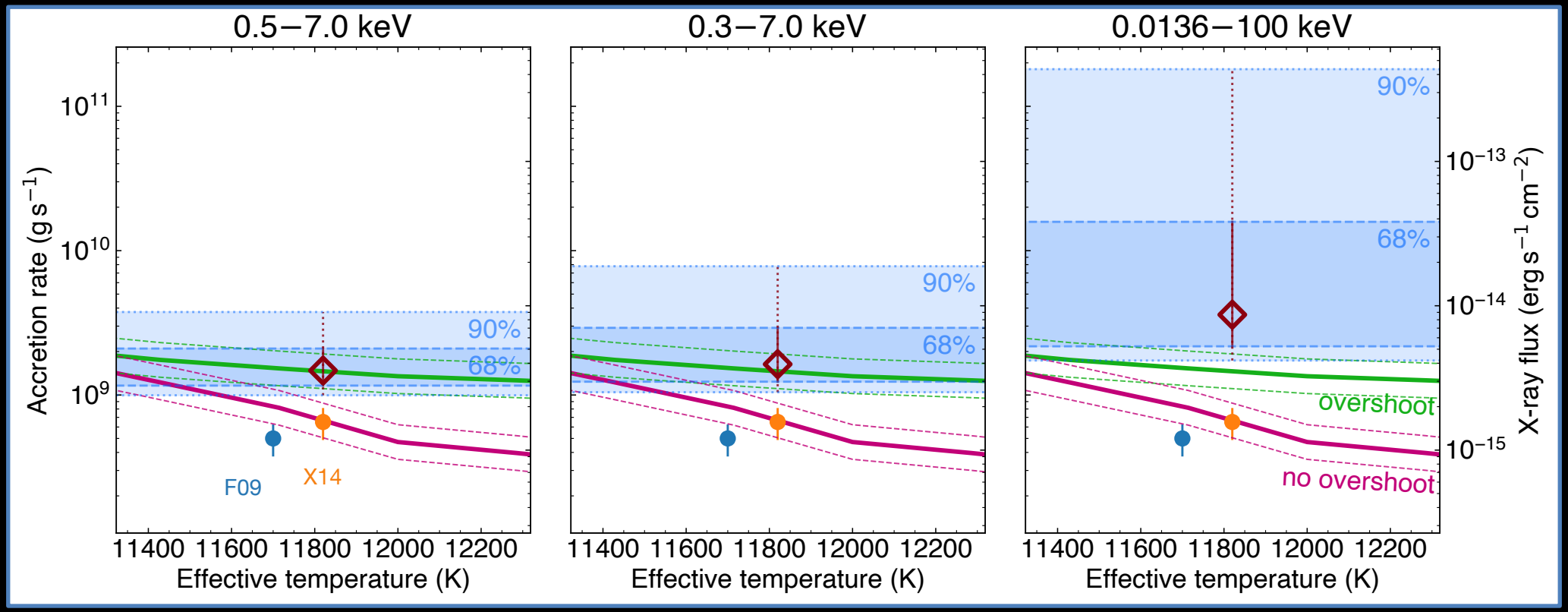

Chandra ACIS-S
2020

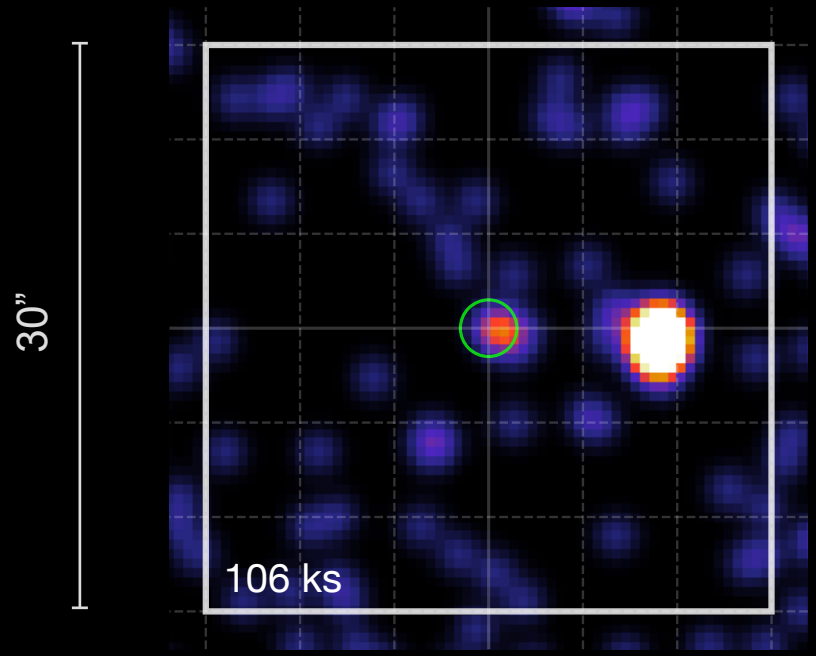

Cunningham et al. (2022)
Nature, 602, 219

XMM-Newton EPIC/MOS
2005 (PI: Muno)

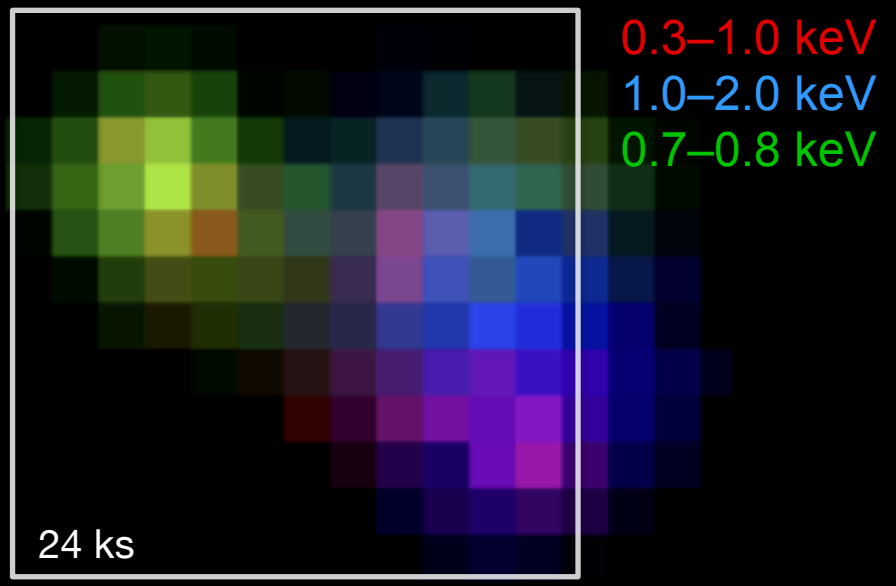

Estrada-Dorado et al. (2023)
ApJL, 994, 6

Jura et al. (2009)
Farihi, Fossati, Wheatley et al. (2018)

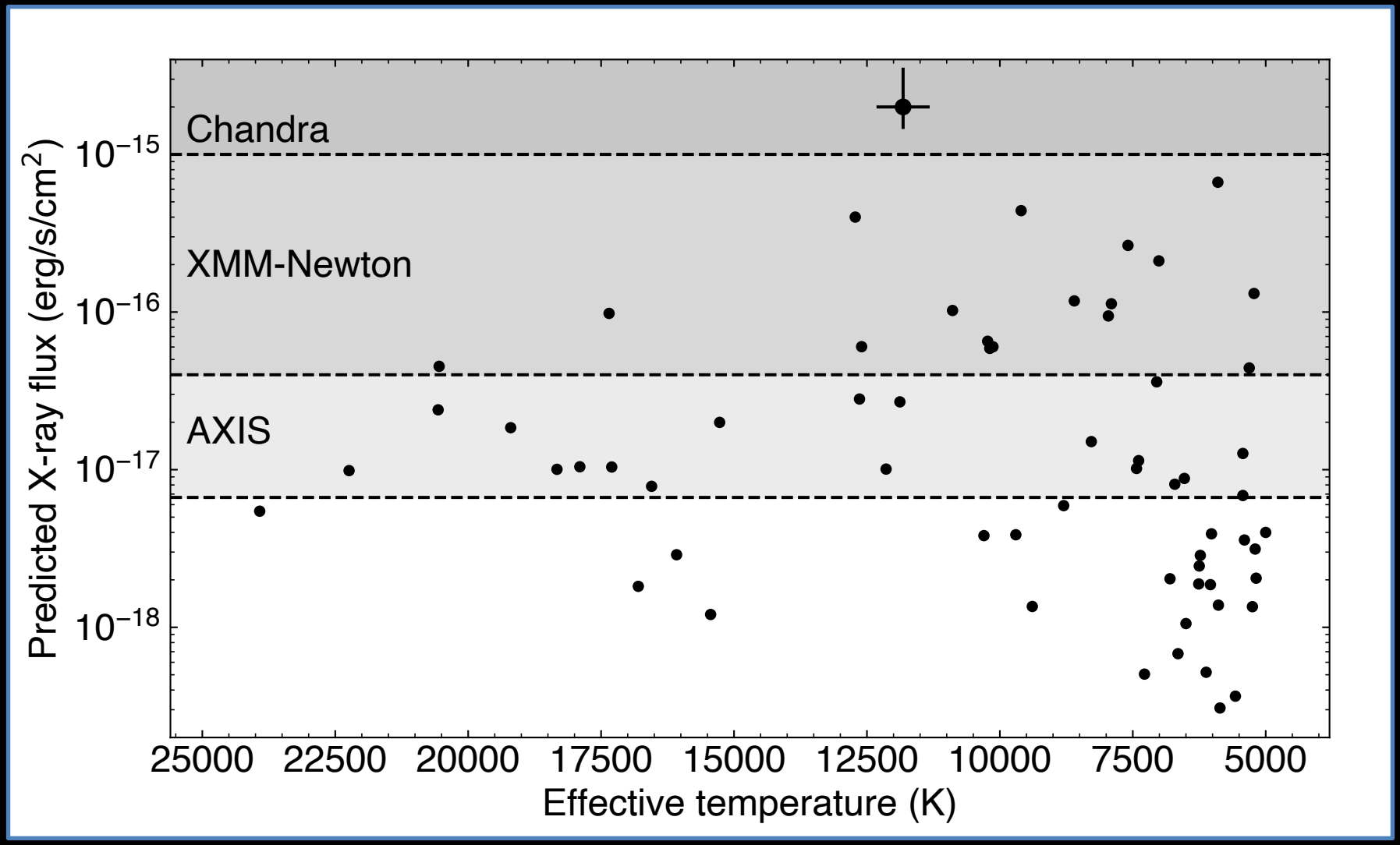

Corrales, Stassun, Cunningham et al. (2023)

Serendipitous discovery of a new metal-polluted white dwarf (4XMM-DR13)

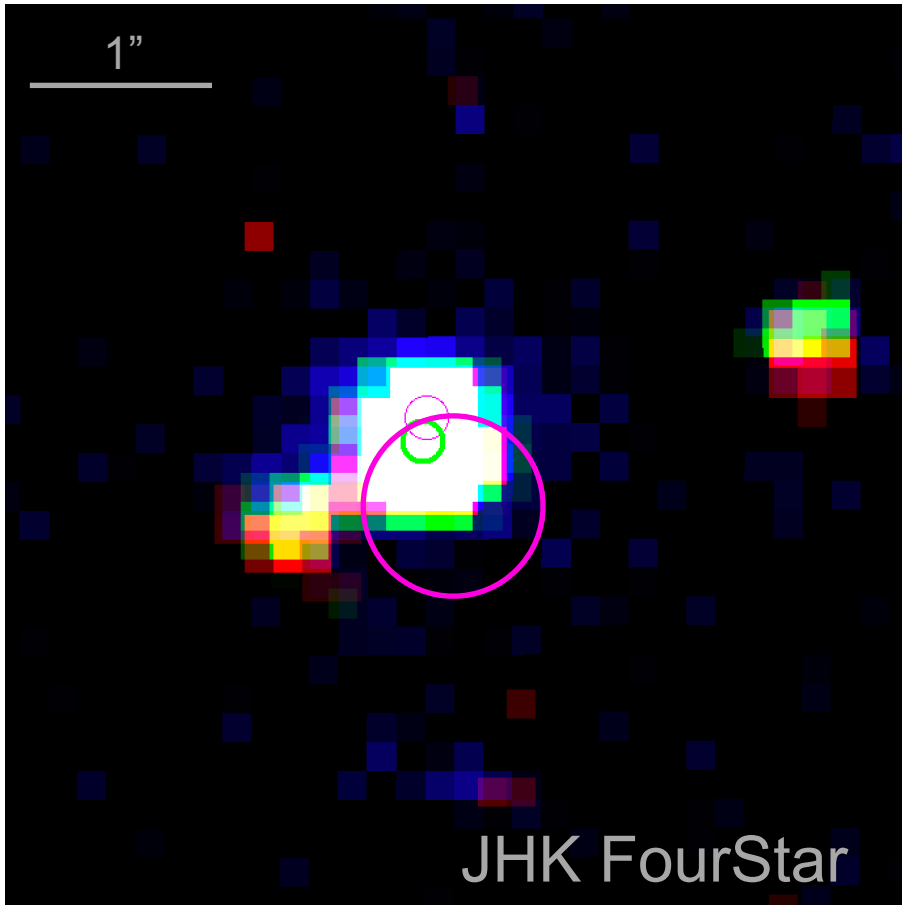

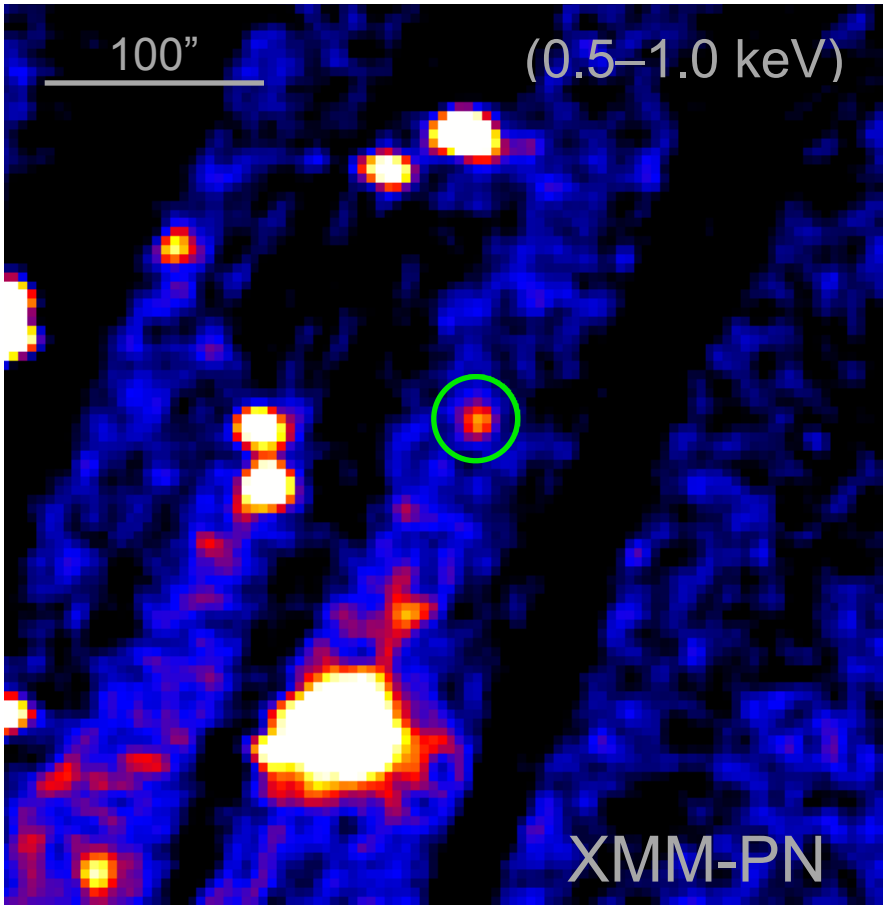

Cunningham+24, in prep.

Two-temperature, optically-thin APEC model

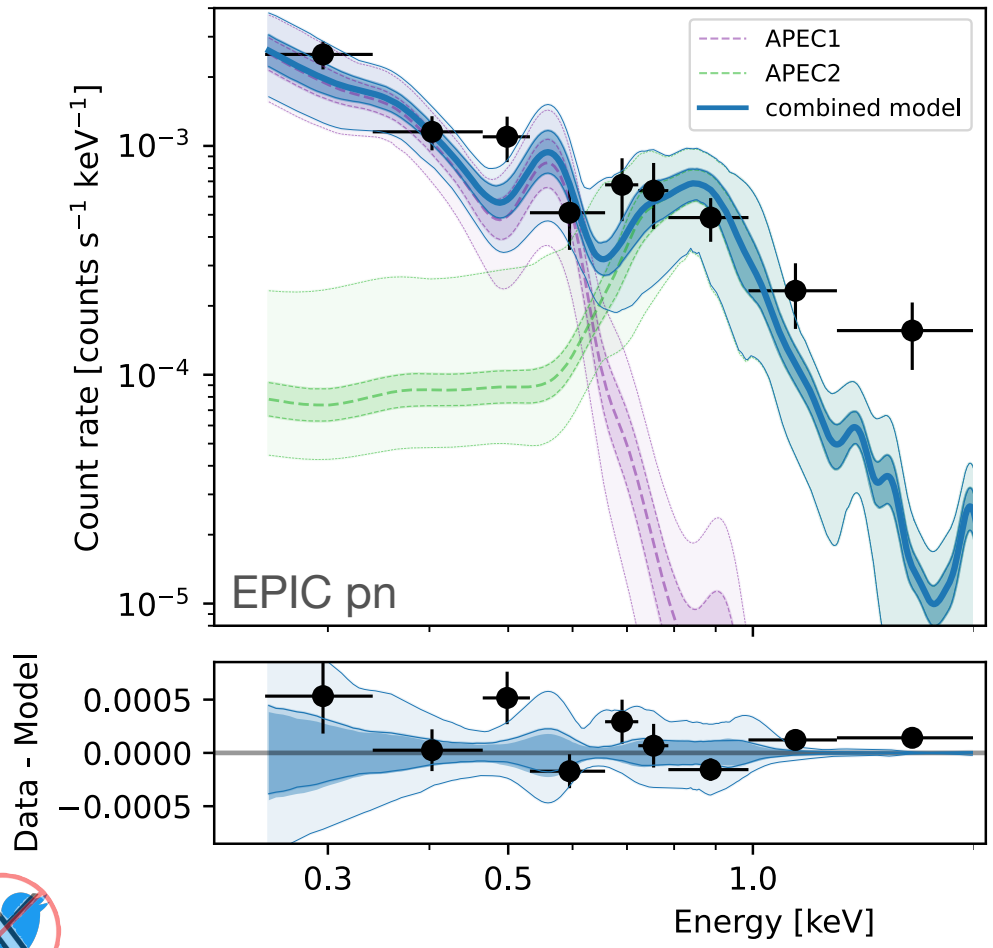

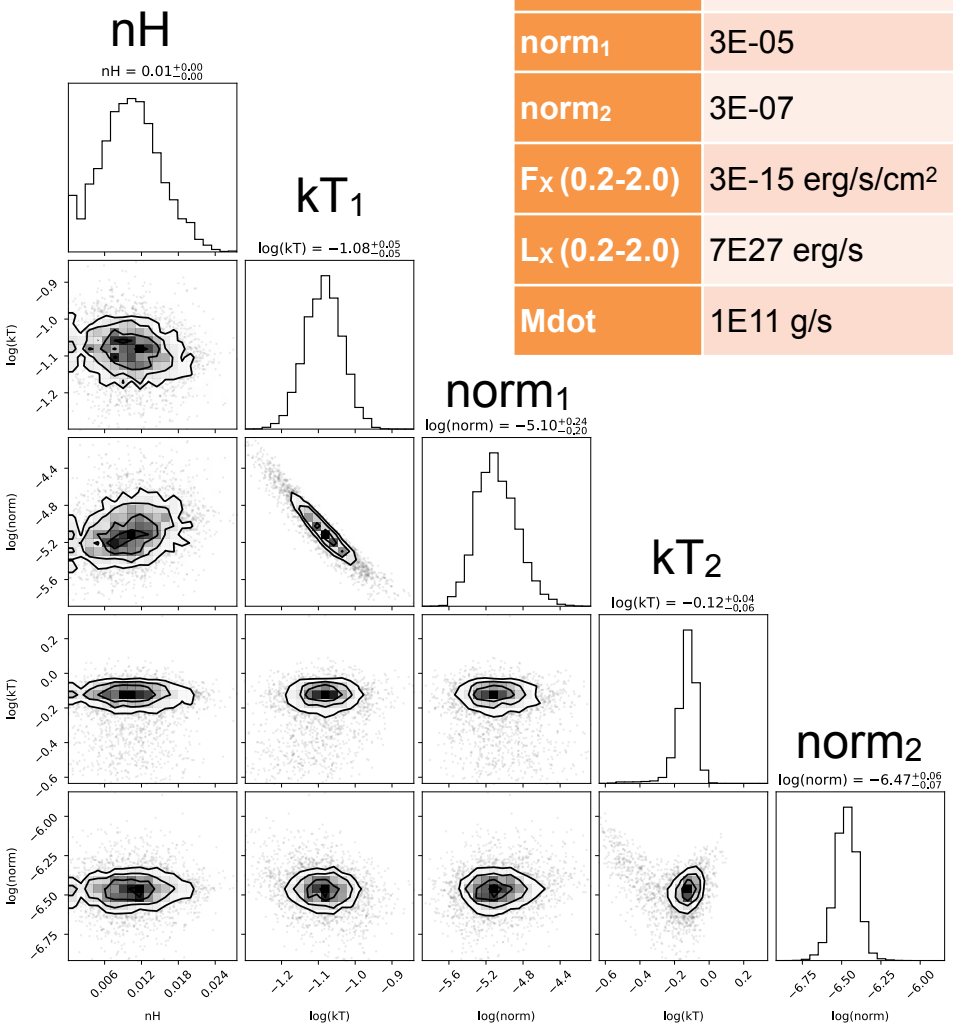

kT_1	0.07±0.01 keV
kT_2	0.7±0.1/0.2 keV
$norm_1$	3E-05
$norm_2$	3E-07
F_X (0.2-2.0)	3E-15 erg/s/cm^2
L_X (0.2-2.0)	7E27 erg/s
Mdot	1E11 g/s

Optical spectroscopy - confirms a new metal-polluted white dwarf

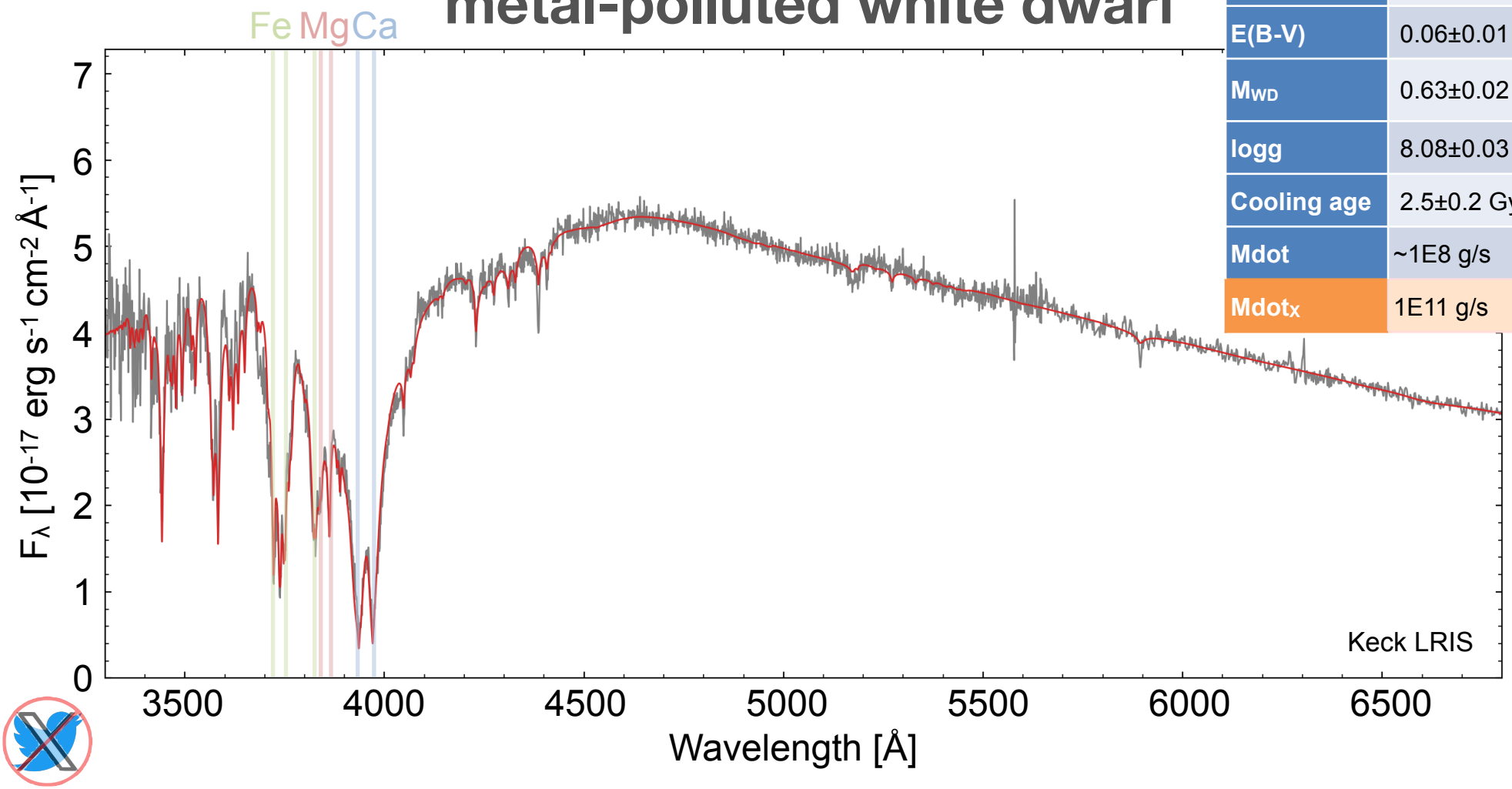

T_{eff}	6340±40 K
R_{WD}	0.0119±0.0002 $R_\odot$
E(B-V)	0.06±0.01 mag
M_{WD}	0.63±0.02 $M_\odot$
logg	8.08±0.03
Cooling age	2.5±0.2 Gyr
Mdot	~1E8 g/s
$Mdot_X$	1E11 g/s

Parent body composition

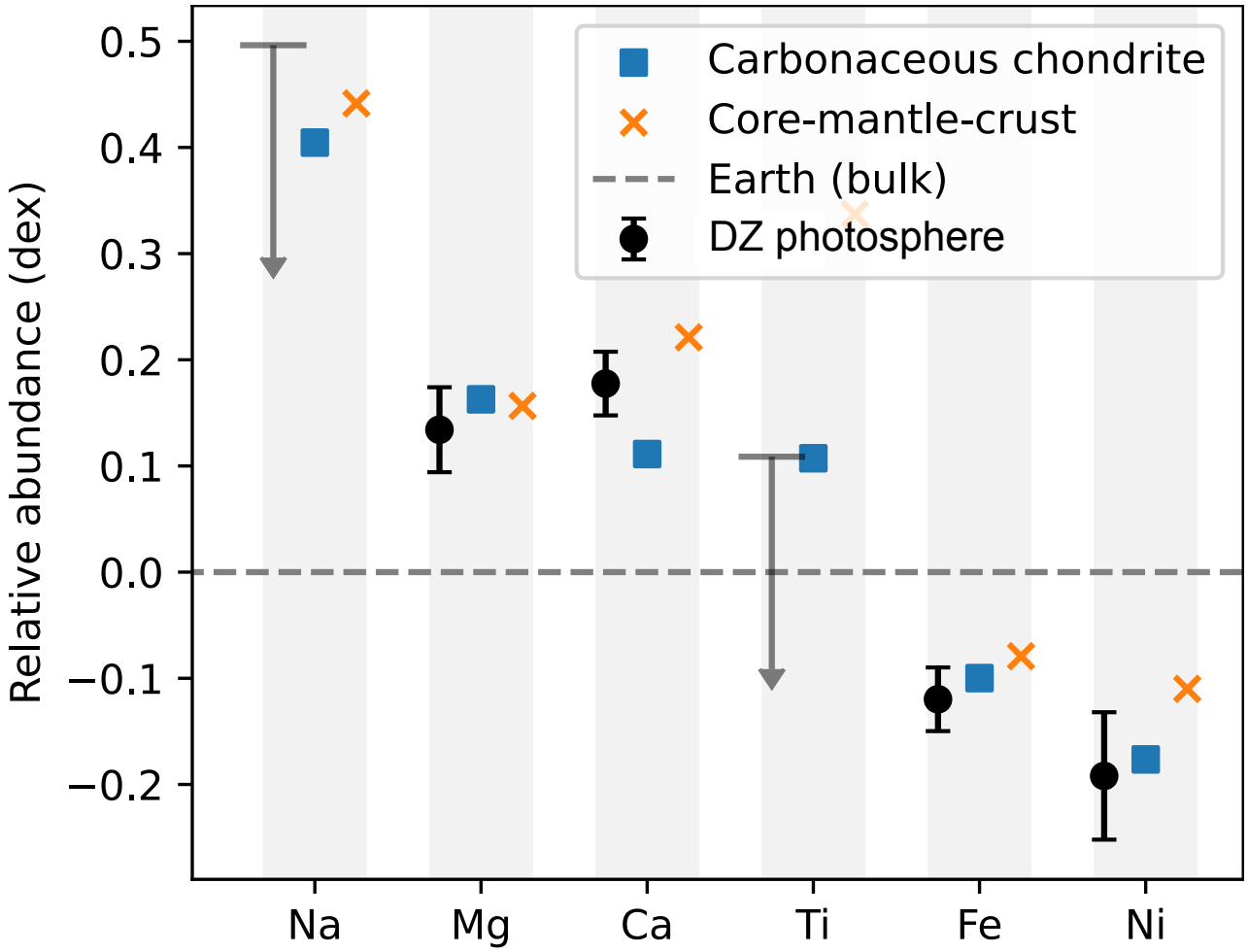

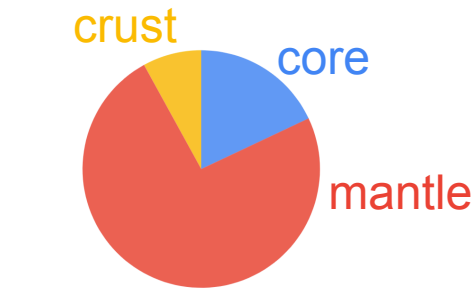

Core-mantle-crust

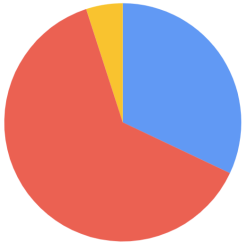

Bulk Earth

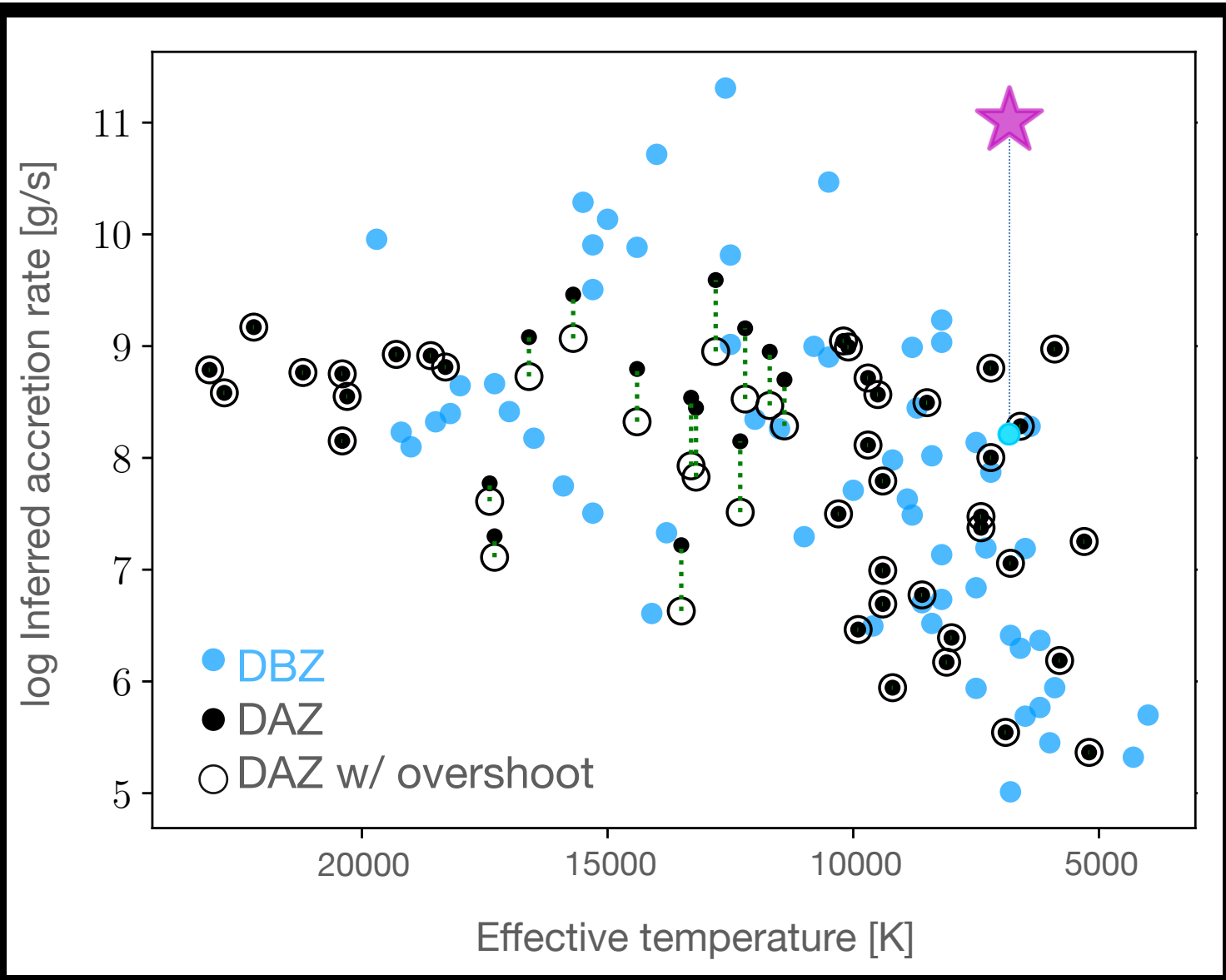
log Inferred accretion rate [g/s]
11
10
9
8
7
6
5
20000
15000
10000
5000
Effective temperature [K]
DBZ
DAZ
DAZ w/ overshoot

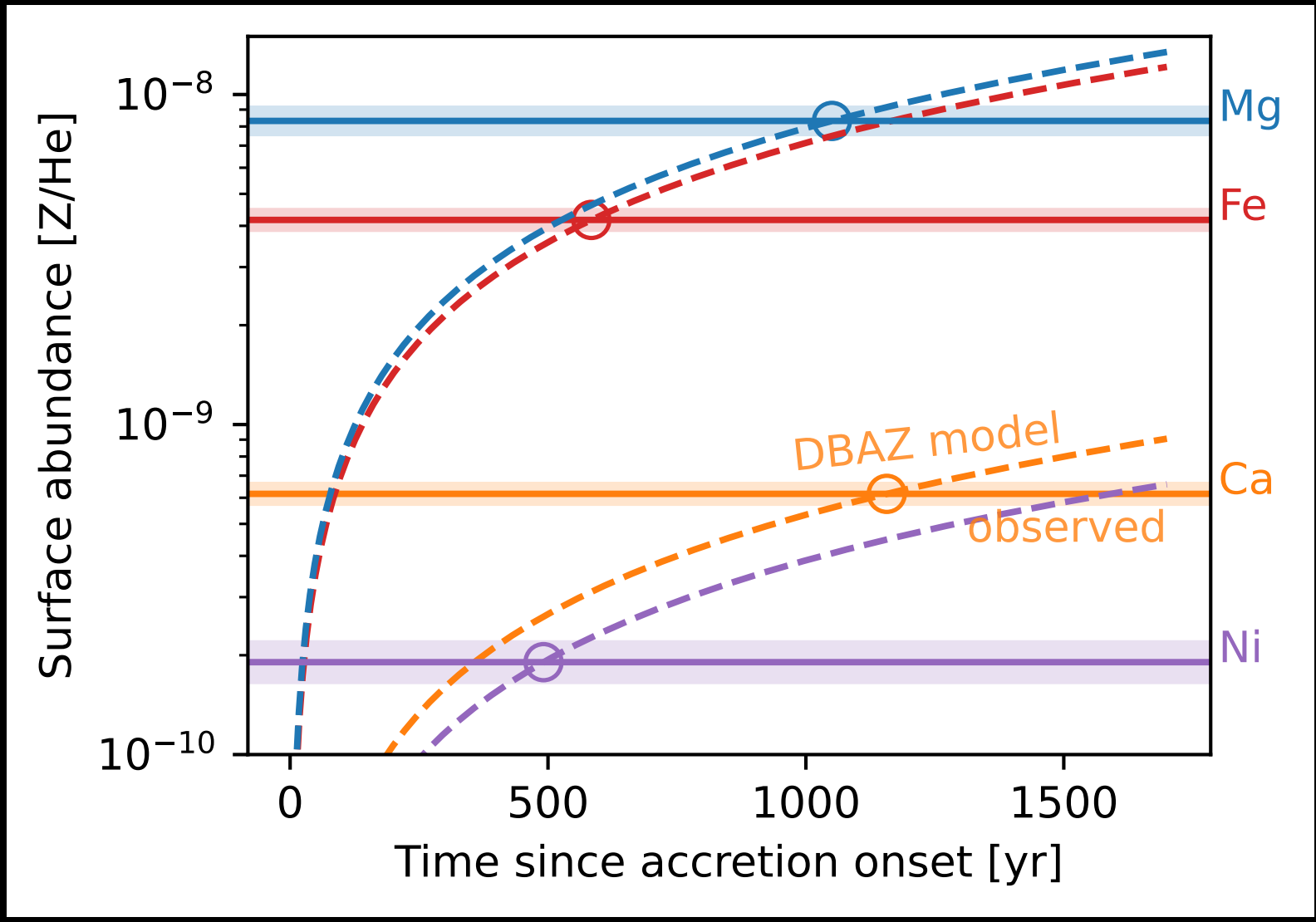
Surface abundance [Z/He]
10^{-8}
10^{-9}
10^{-10}
0
500
1000
1500
Time since accretion onset [yr]
Mg
Fe
Ca
Ni
DBAZ model
observed

Optical spectroscopy - confirms a new metal-polluted white dwarf

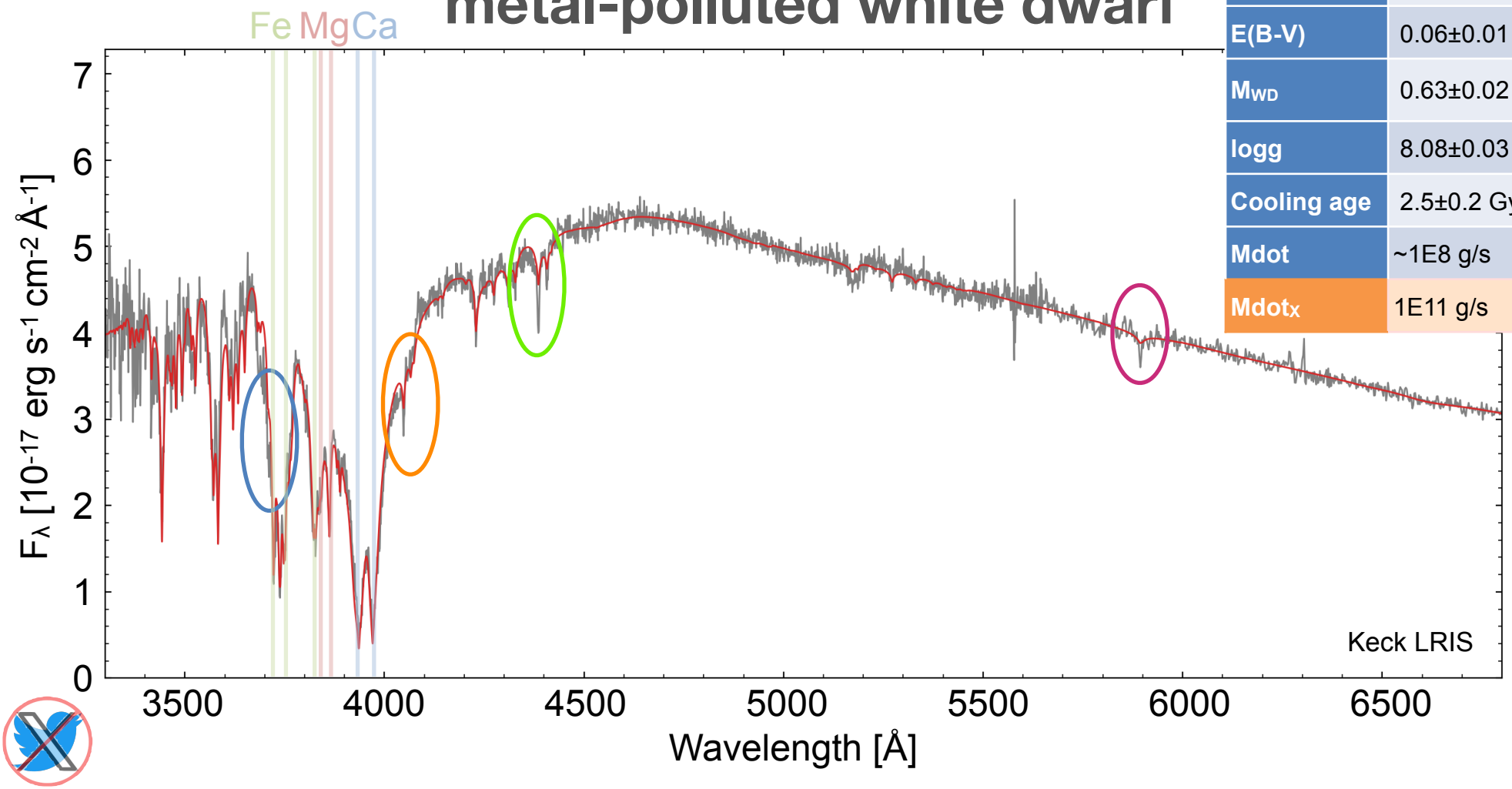

T_{eff}	6340±40 K
R_{WD}	0.0119±0.0002 $R_\odot$
E(B-V)	0.06±0.01 mag
M_{WD}	0.63±0.02 $M_\odot$
logg	8.08±0.03
Cooling age	2.5±0.2 Gyr
Mdot	~1E8 g/s
$Mdot_X$	1E11 g/s

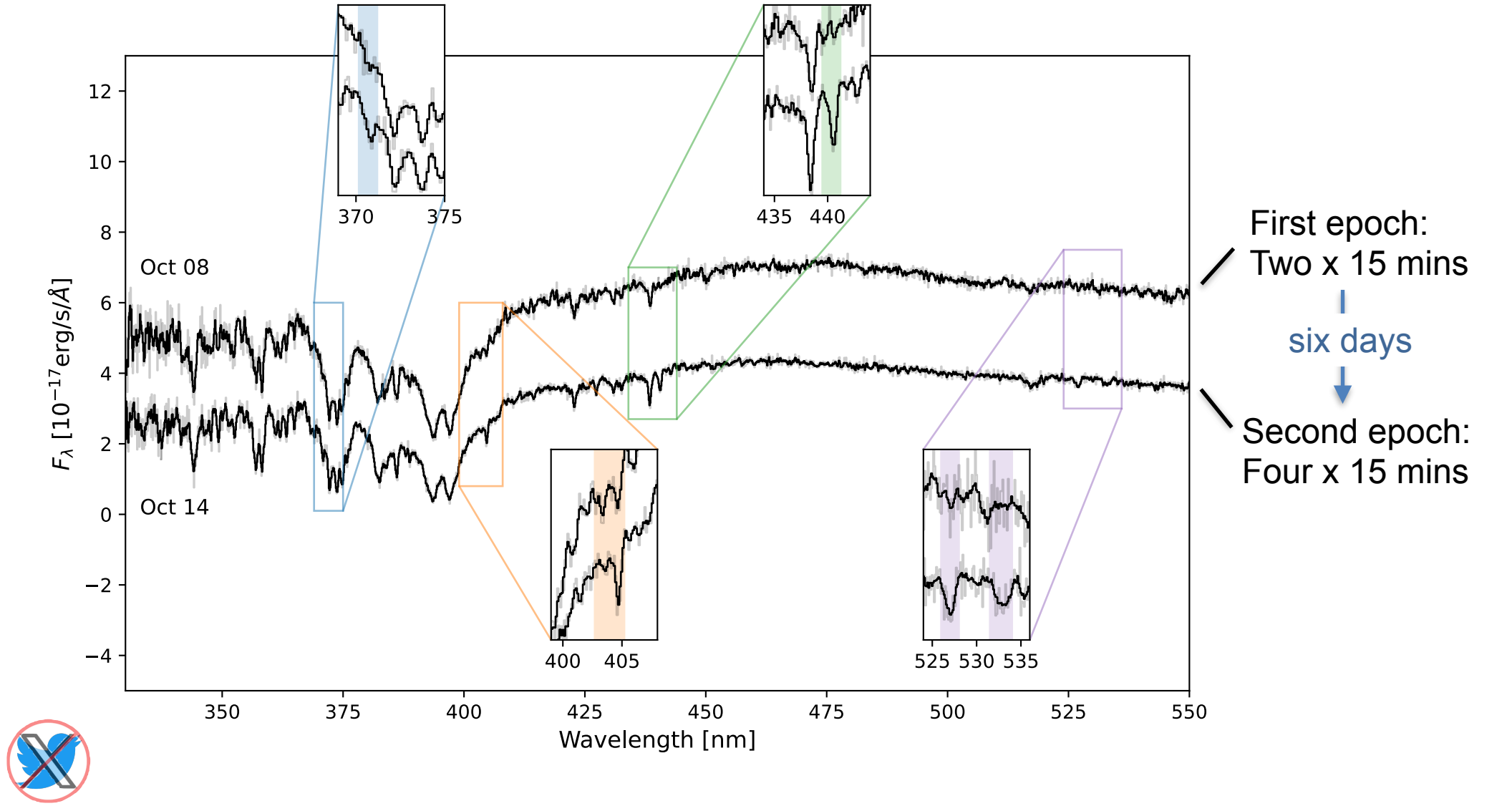
Oct 08
Oct 14
F_λ [10^{-17}erg/s/Å]
Wavelength [nm]
First epoch:
Two x 15 mins
six days
Second epoch:
Four x 15 mins

Serendipitous discovery of two new low-state polars (4XMM-DR13)

$B_{\rm WD} \approx 23\,{\rm MG}$

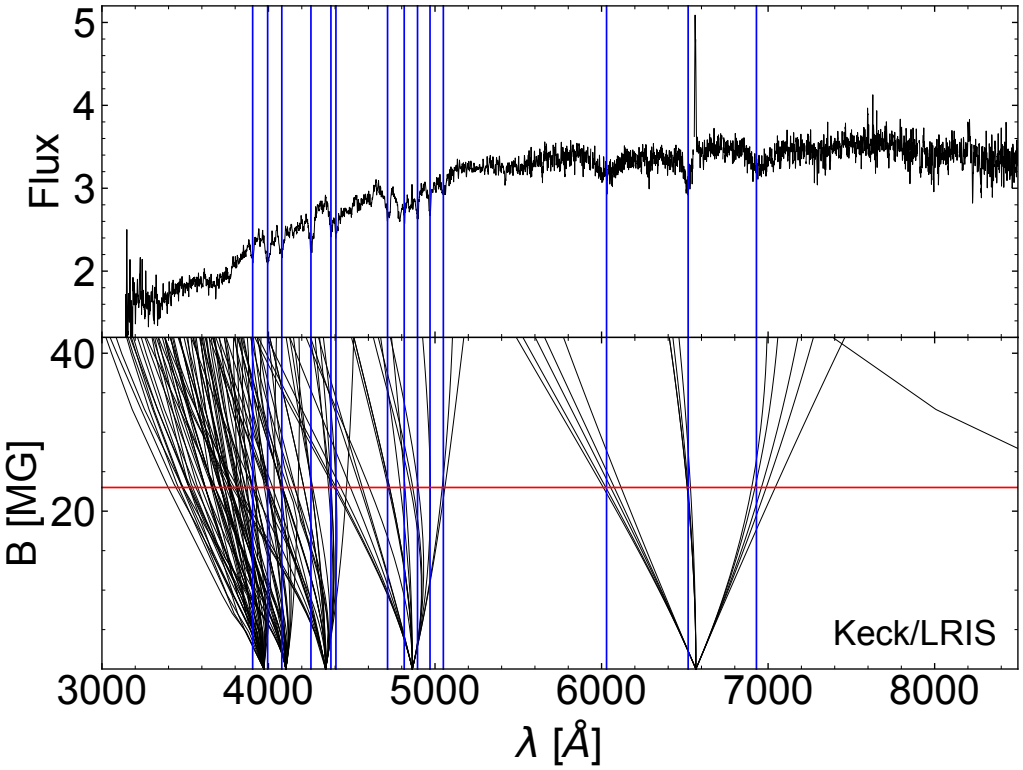

$B_{\rm WD} \approx 15\,{\rm MG}$

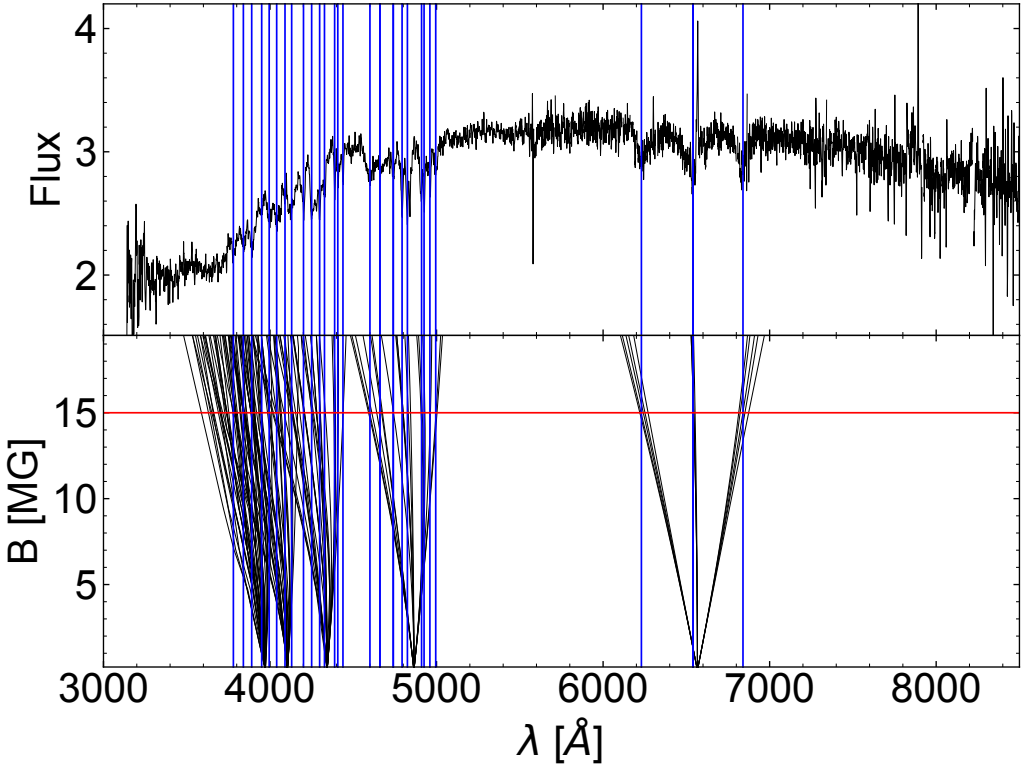

Cunningham et al. (2024), in prep.

Serendipitous discovery of two new low-state polars

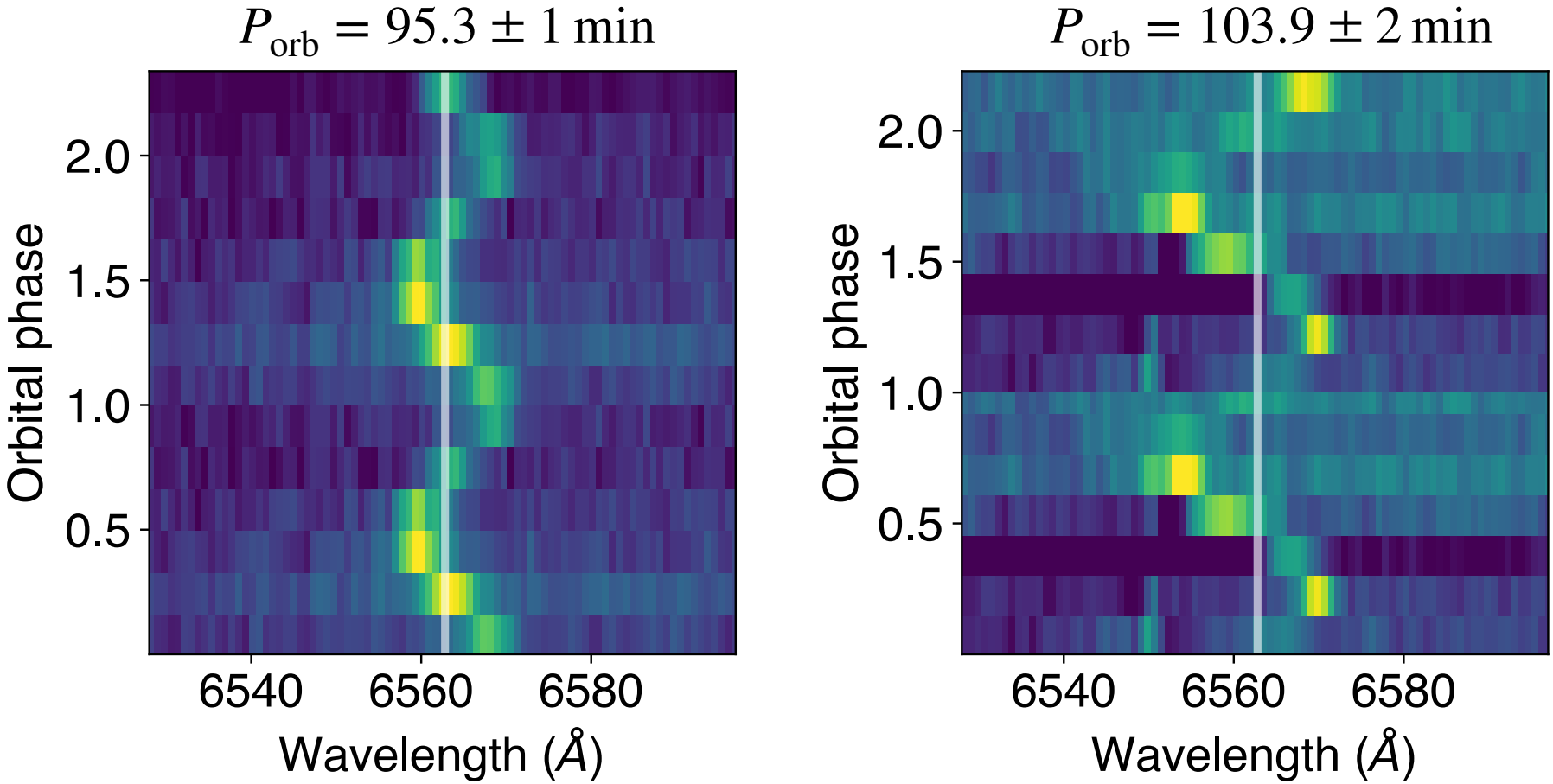

Cunningham et al. (2024), in prep.

Serendipitous discovery of two new low-state polars

$$F_{\rm X}^{(0.25-10.0\,{\rm keV})} = (1.4 \pm 0.4) \times 10^{-14}\,{\rm erg\,s^{-1}\,cm^{-2}}$$
$$L_{\rm X}^{(0.25-10.0\,{\rm keV})} = (7 \pm 2) \times 10^{28}\,{\rm erg\,s^{-1}}$$
$$\dot{M}_{\rm X} \approx 8 \times 10^{11}{\rm g\,s^{-1}}$$

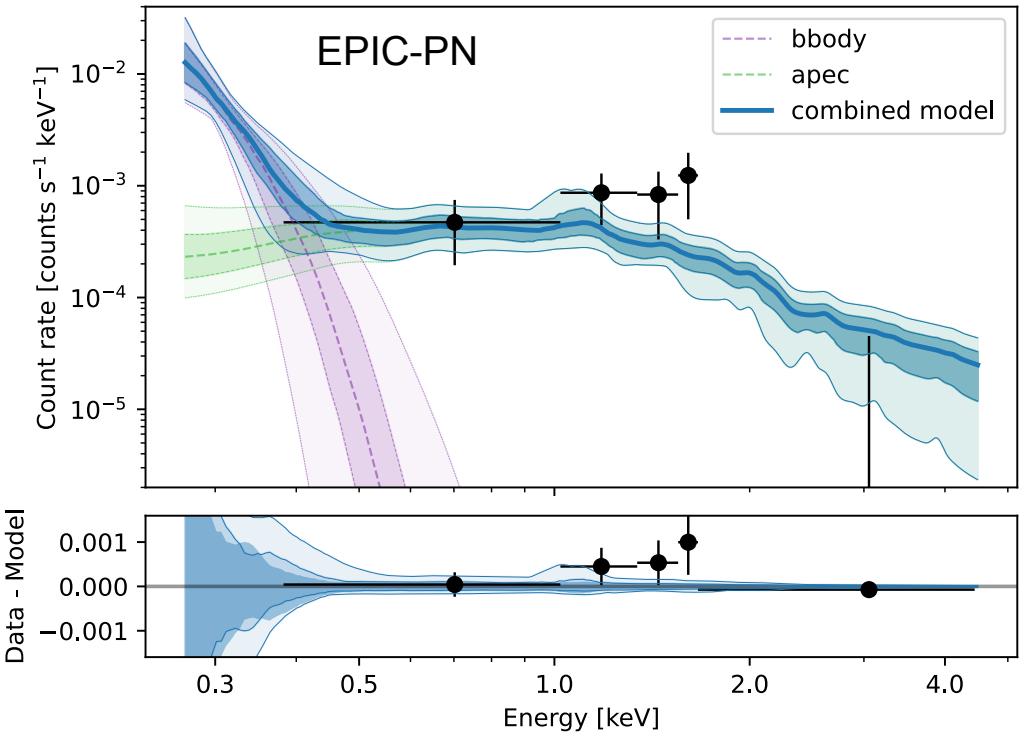

$$F_{\rm X}^{(0.25-10.0\,{\rm keV})} = (5 \pm 1) \times 10^{-14}\,{\rm erg\,s^{-1}\,cm^{-2}}$$
$$L_{\rm X}^{(0.25-10.0\,{\rm keV})} = (3.4 \pm 0.7) \times 10^{29}\,{\rm erg\,s^{-1}}$$
$$\dot{M}_{\rm X} \approx 2 \times 10^{12}{\rm g\,s^{-1}}$$

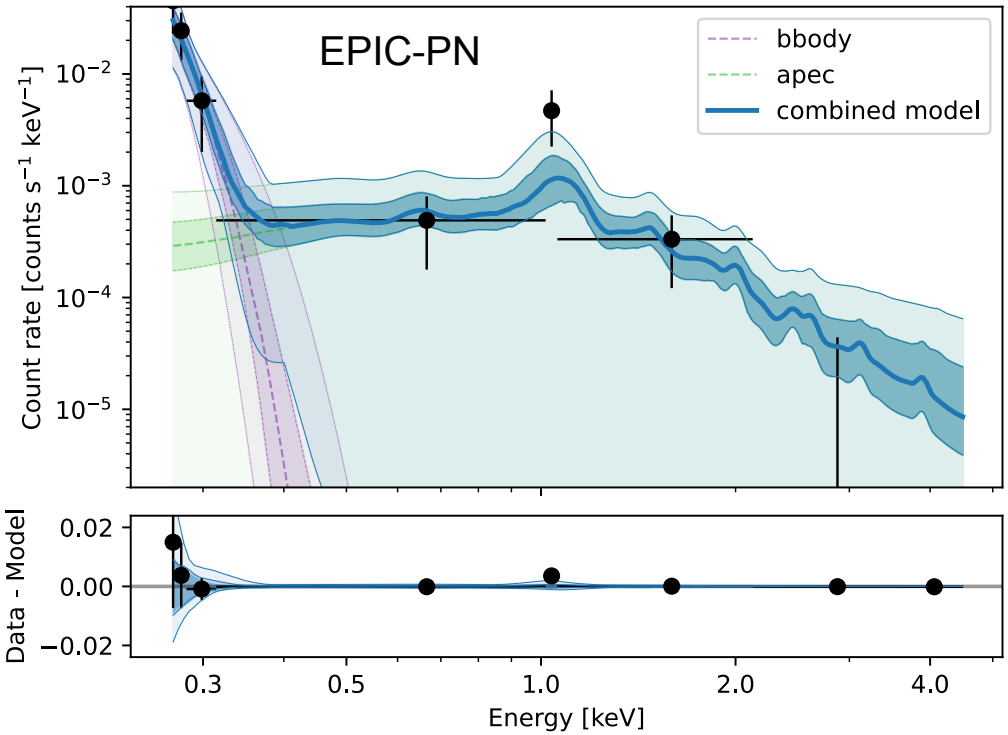

Cunningham et al. (2024), in prep.

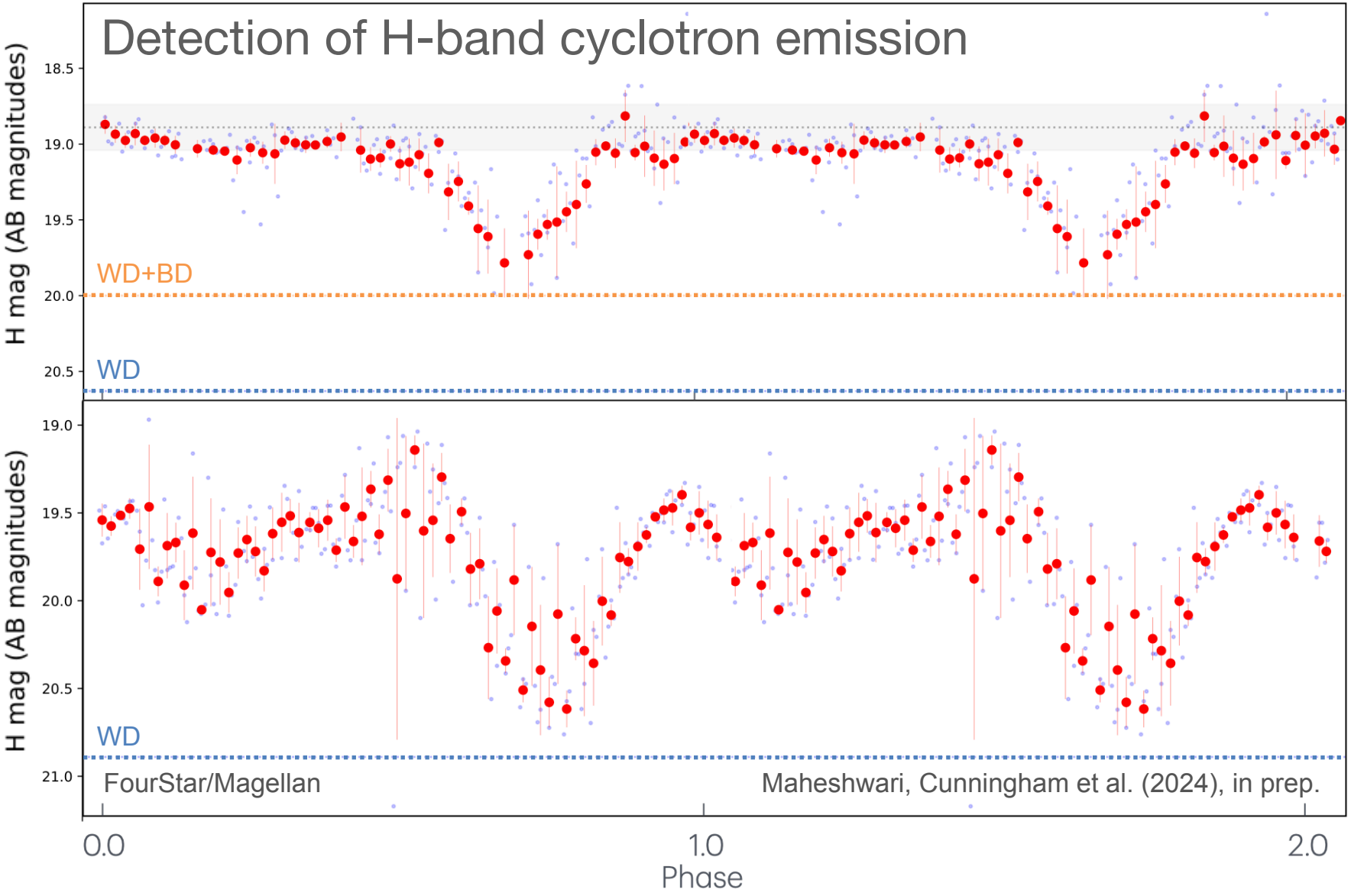
Detection of H-band cyclotron emission
H mag (AB magnitudes)
18.5
19.0
19.5
20.0
20.5
WD+BD
WD
H mag (AB magnitudes)
19.0
19.5
20.0
20.5
21.0
WD
FourStar/Magellan
Maheshwari, Cunningham et al. (2024), in prep.
0.0
1.0
2.0
Phase

Conclusions

- Recent Chandra observations confirm metal-polluted white dwarfs as a new class of soft X-ray source (4.5–5.9σ) - redetected with XMM
- Measured X-ray flux ($2 \cdot 10^{-15}\,\mathrm{erg/s/cm^2}$) provides first independent constraint on Mdot; consistent with spectroscopic inferred accretion rates
- Ongoing search for similar systems, using 4XMM-DR13 source catalogue, and targeted observations, revealing interesting low accretion rate systems

Thanks for listening

Tim Cunningham
tim.cunningham@cfa.harvard.edu
warwick.ac.uk/timcunningham

Serendipitous discovery of a new metal-polluted white dwarf

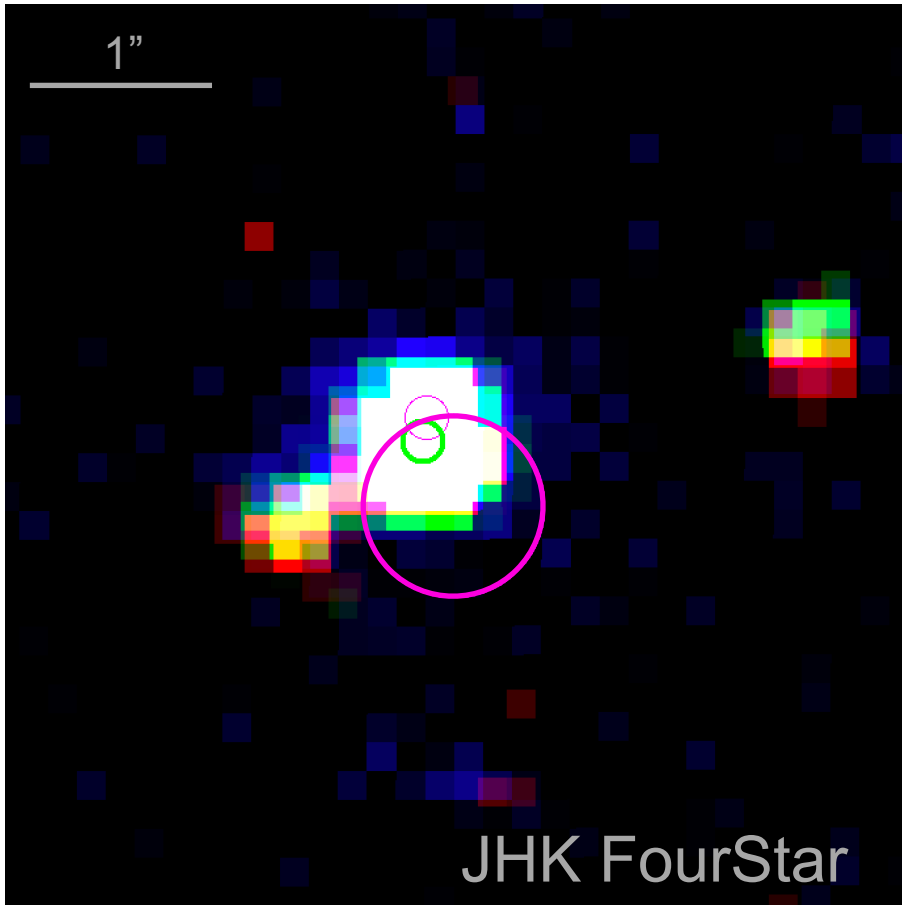

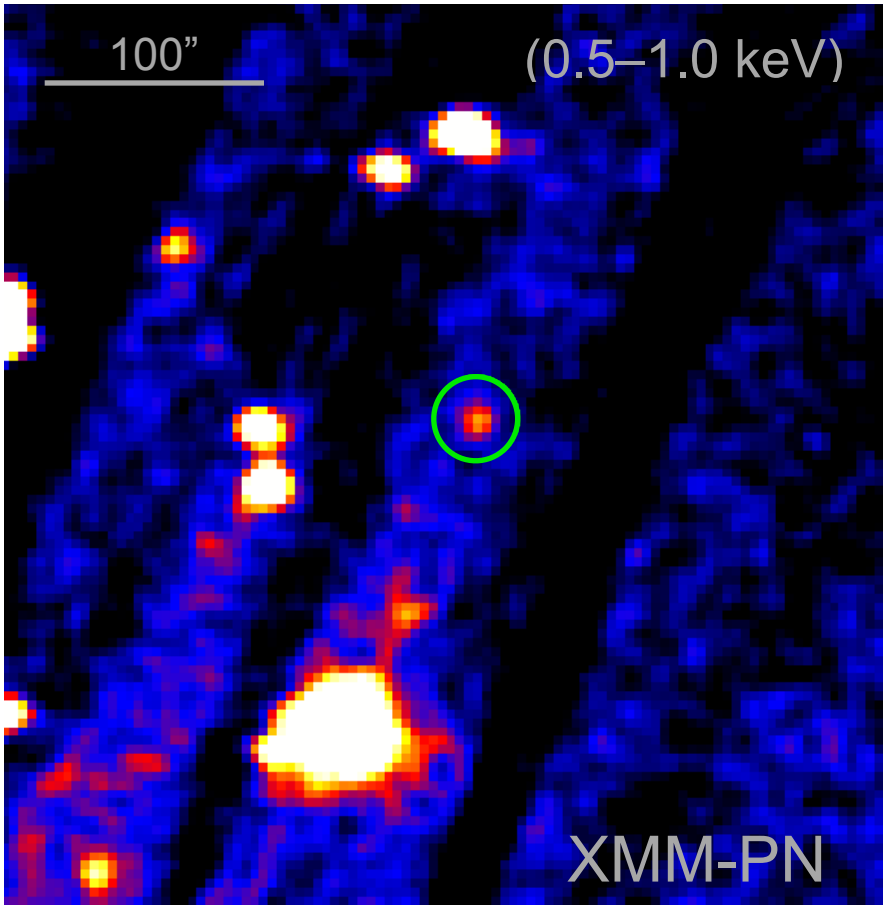

Cunningham+ in prep.

Serendipitous discovery of a new metal-polluted white dwarf

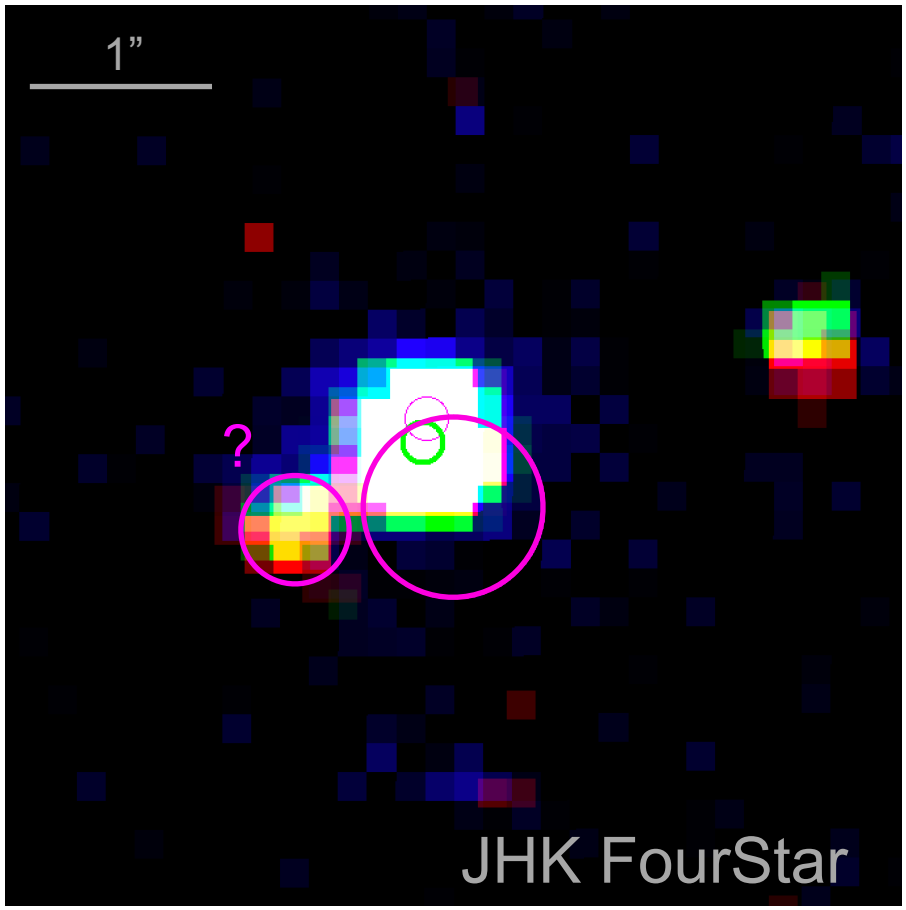

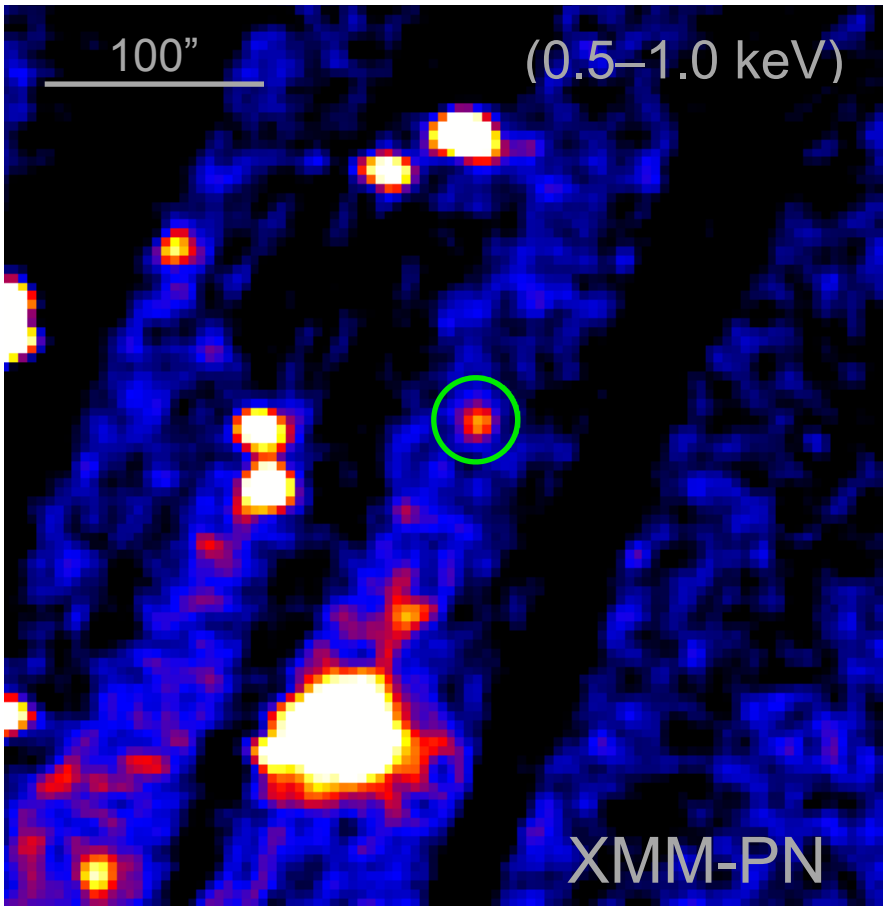

Cunningham+ in prep.

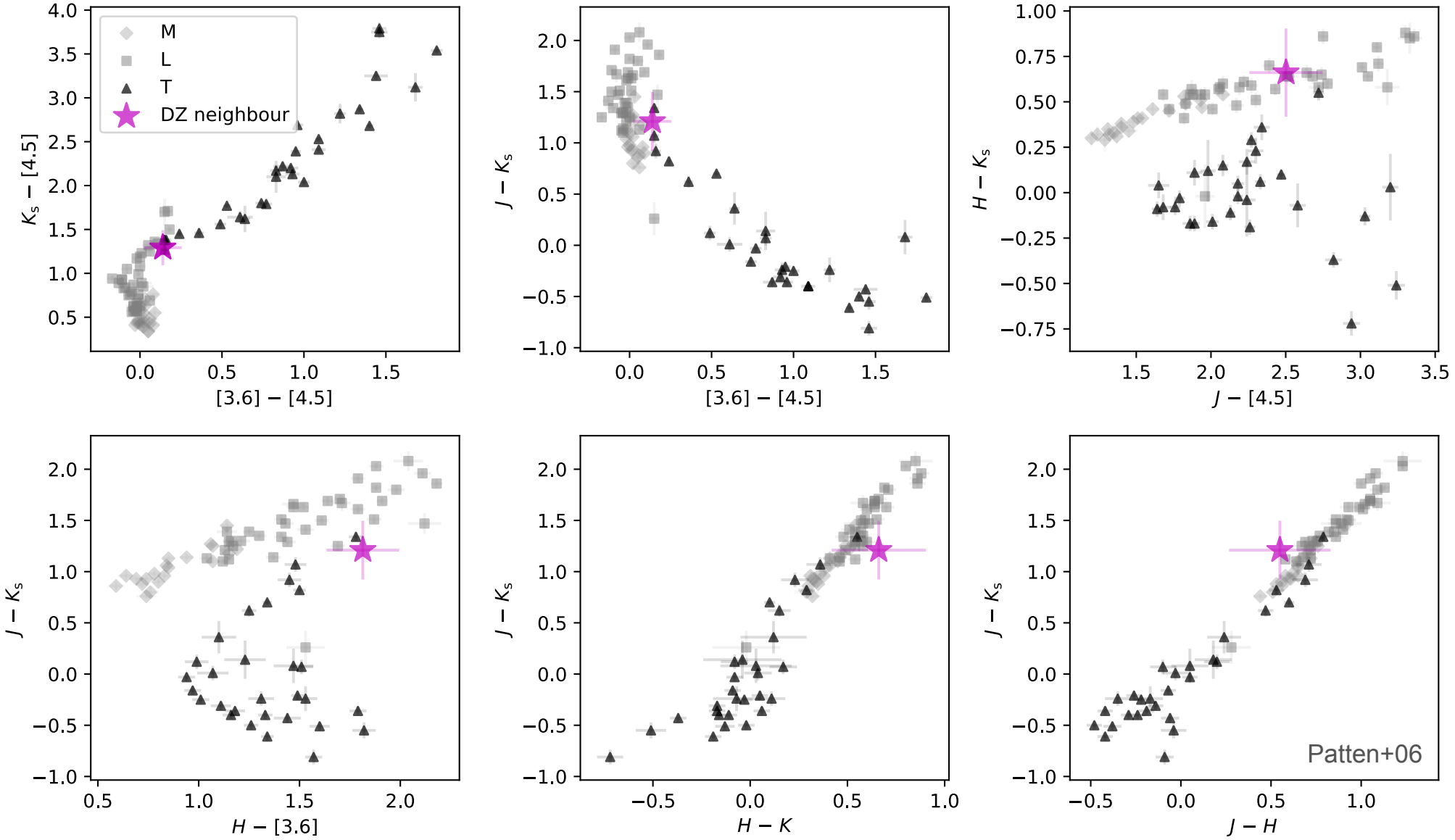
M
L
T
DZ neighbour
$K_s - [4.5]$
$[3.6] - [4.5]$
$J - K_s$
$[3.6] - [4.5]$
$H - K_s$
$J - [4.5]$
$J - K_s$
$H - [3.6]$
$J - K_s$
$H - K$
$J - K_s$
$J - H$
Patten+06

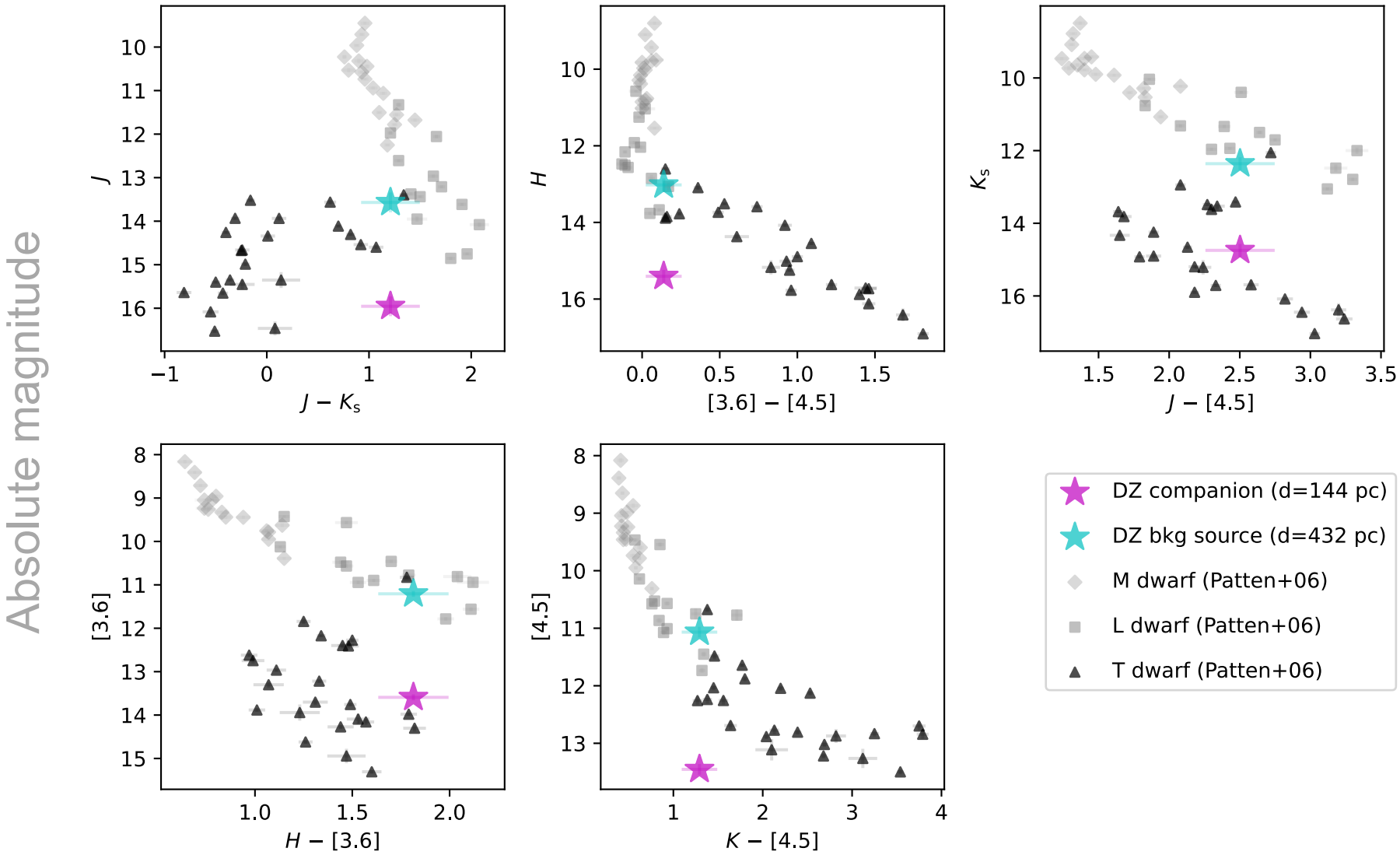
Absolute magnitude
J
J − Ks
H
[3.6] − [4.5]
Ks
J − [4.5]
[3.6]
H − [3.6]
[4.5]
K − [4.5]
DZ companion (d=144 pc)
DZ bkg source (d=432 pc)
M dwarf (Patten+06)
L dwarf (Patten+06)
T dwarf (Patten+06)

M-dwarf sample (CARMENES; Cifuentes et al. 2020) scaled by distance to JHK mag

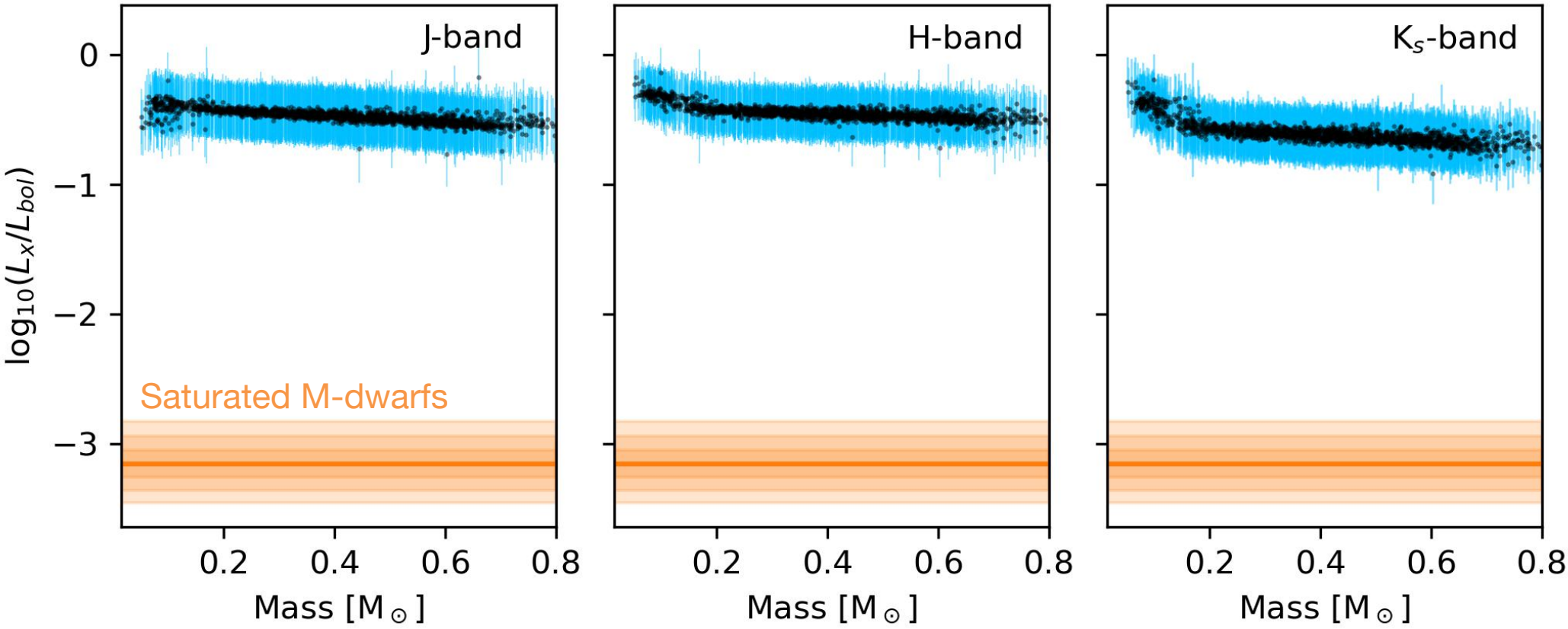

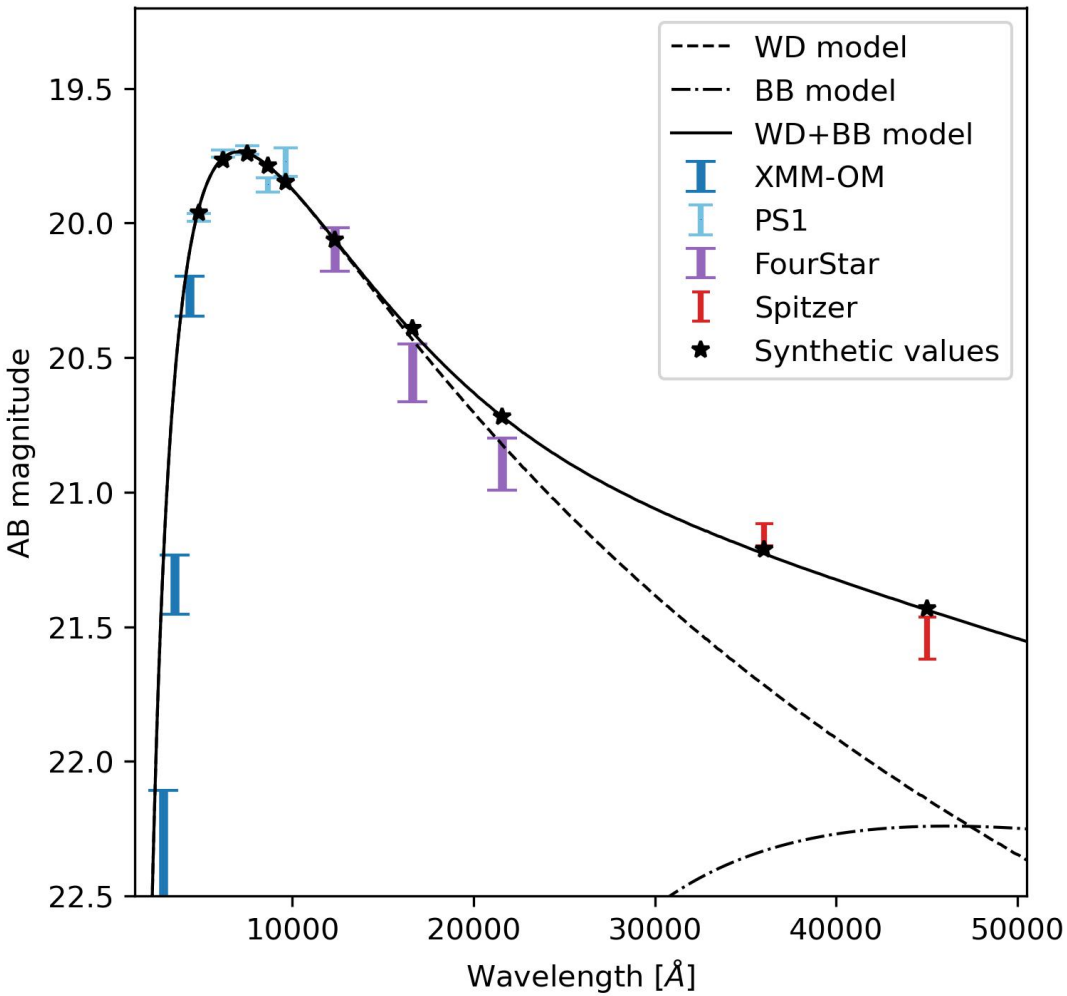
WD model
BB model
WD+BB model
XMM-OM
PS1
FourStar
Spitzer
Synthetic values
AB magnitude
Wavelength [Å]

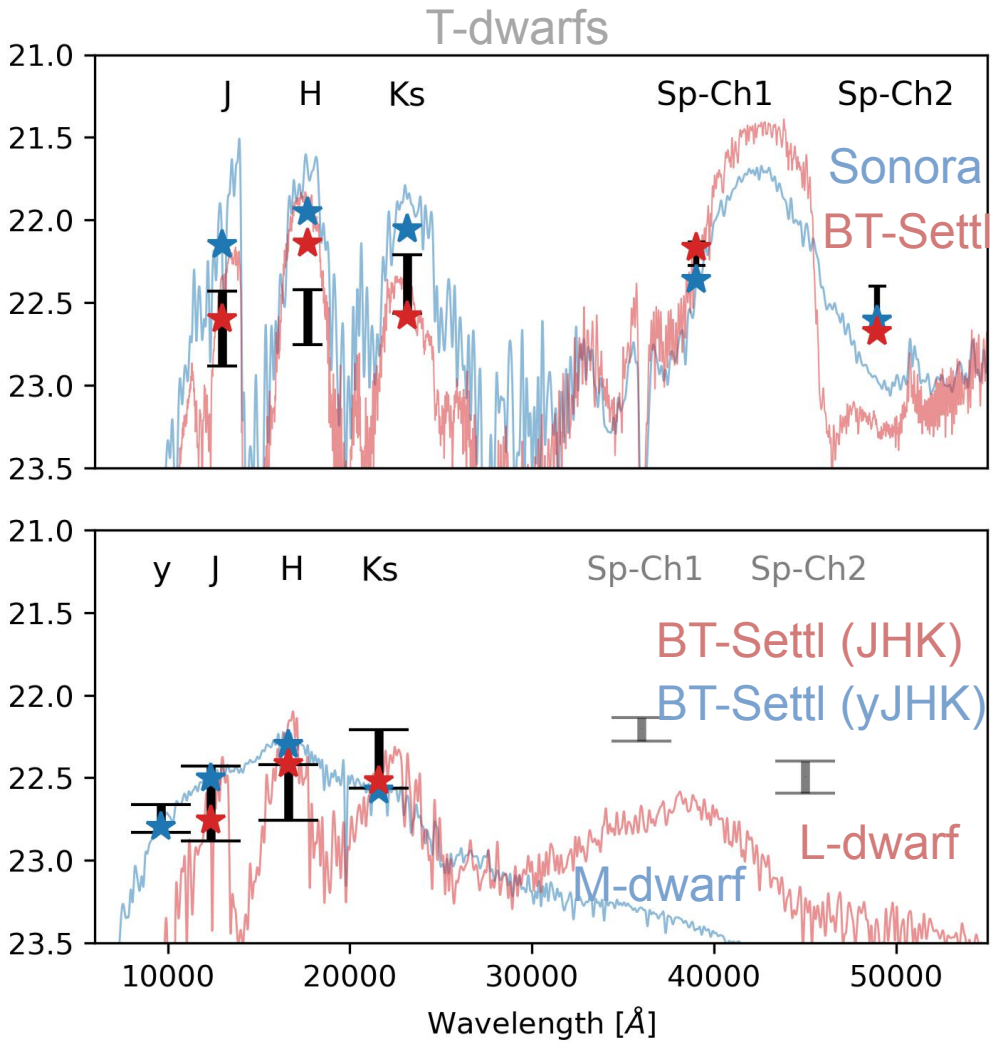
T-dwarfs
J
H
Ks
Sp-Ch1
Sp-Ch2
Sonora
BT-Settl
y
BT-Settl (JHK)
BT-Settl (yJHK)
L-dwarf
M-dwarf
Wavelength [Å]

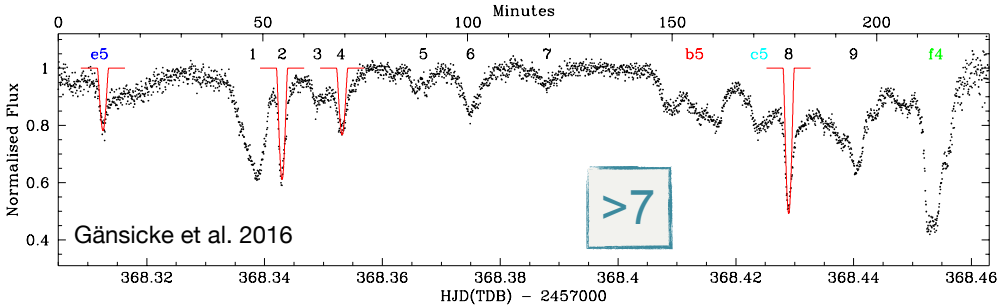

>7

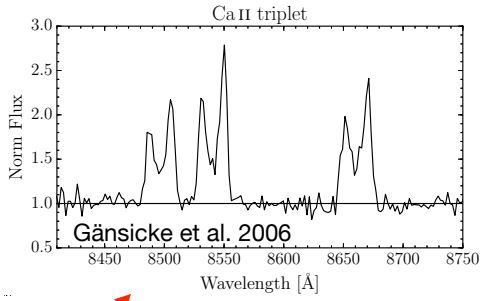

≈0.07%

Manser et al. 2020

Transits

Gas

White dwarf

Atmospheric pollution

Dust

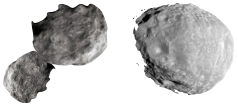

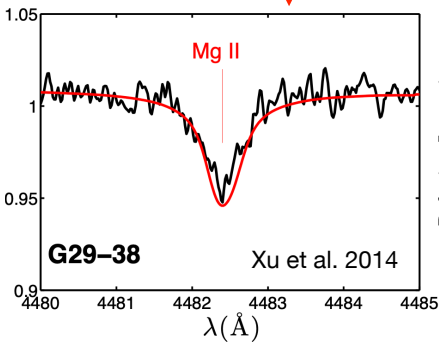

25—50%

Zuckerman et al. 2003
Zuckerman et al. 2010
Koester et. al. 2014

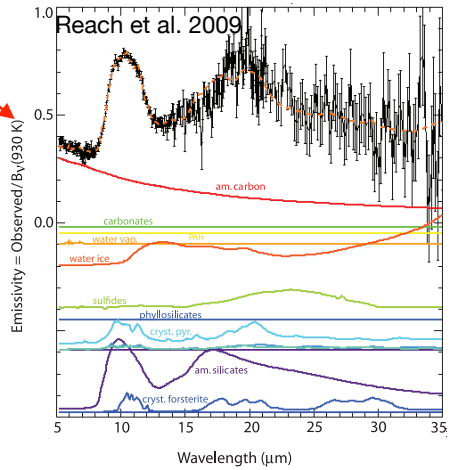

1—3%

Farihi et al. 2009
Rocchetto et al. 2015
Wilson et al. 2019

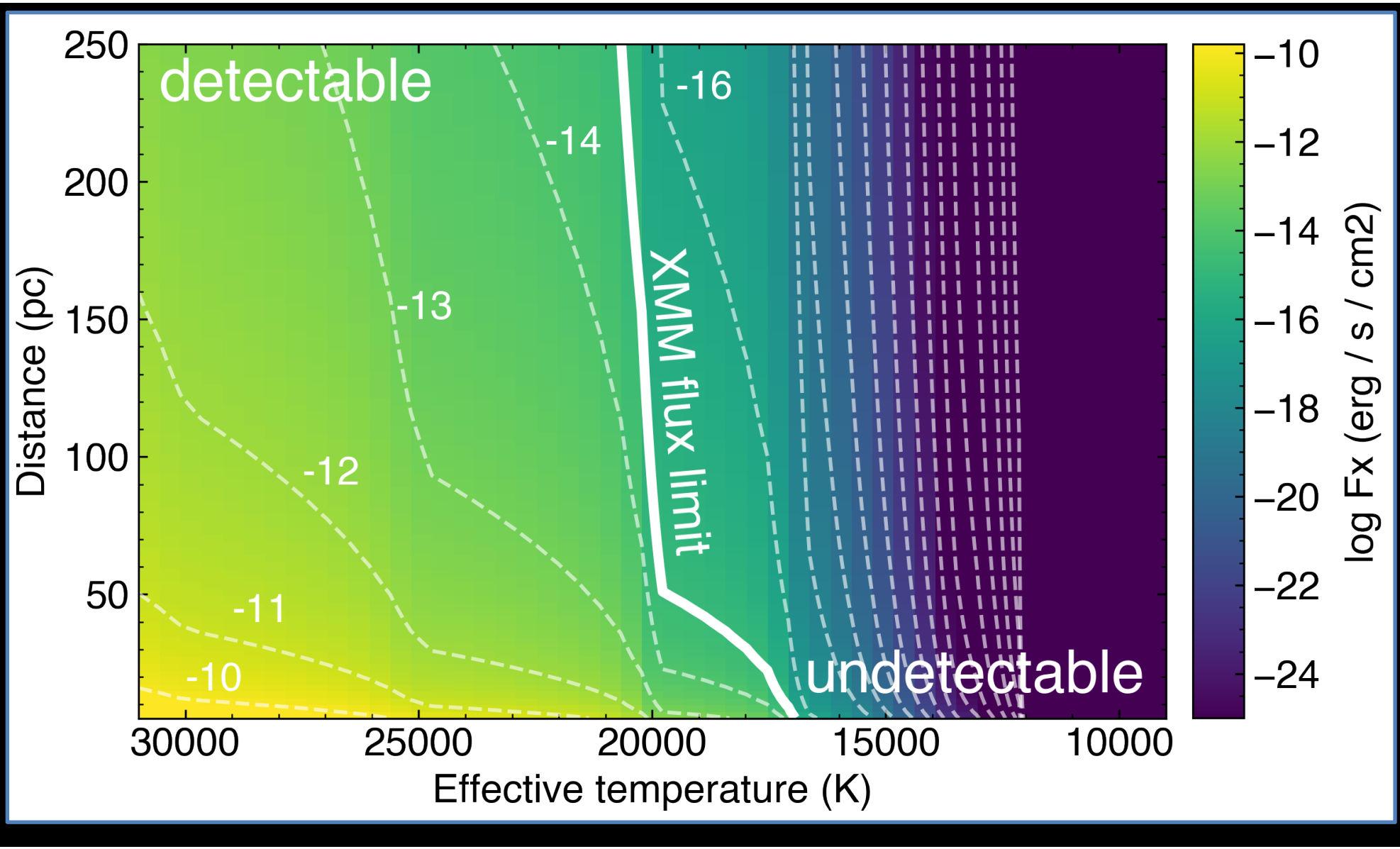
detectable
undetectable
XMM flux limit
-10
-11
-12
-13
-14
-16
250
200
150
100
50
Distance (pc)
30000
25000
20000
15000
10000
Effective temperature (K)
−10
−12
−14
−16
−18
−20
−22
−24
log Fx (erg / s / cm2)

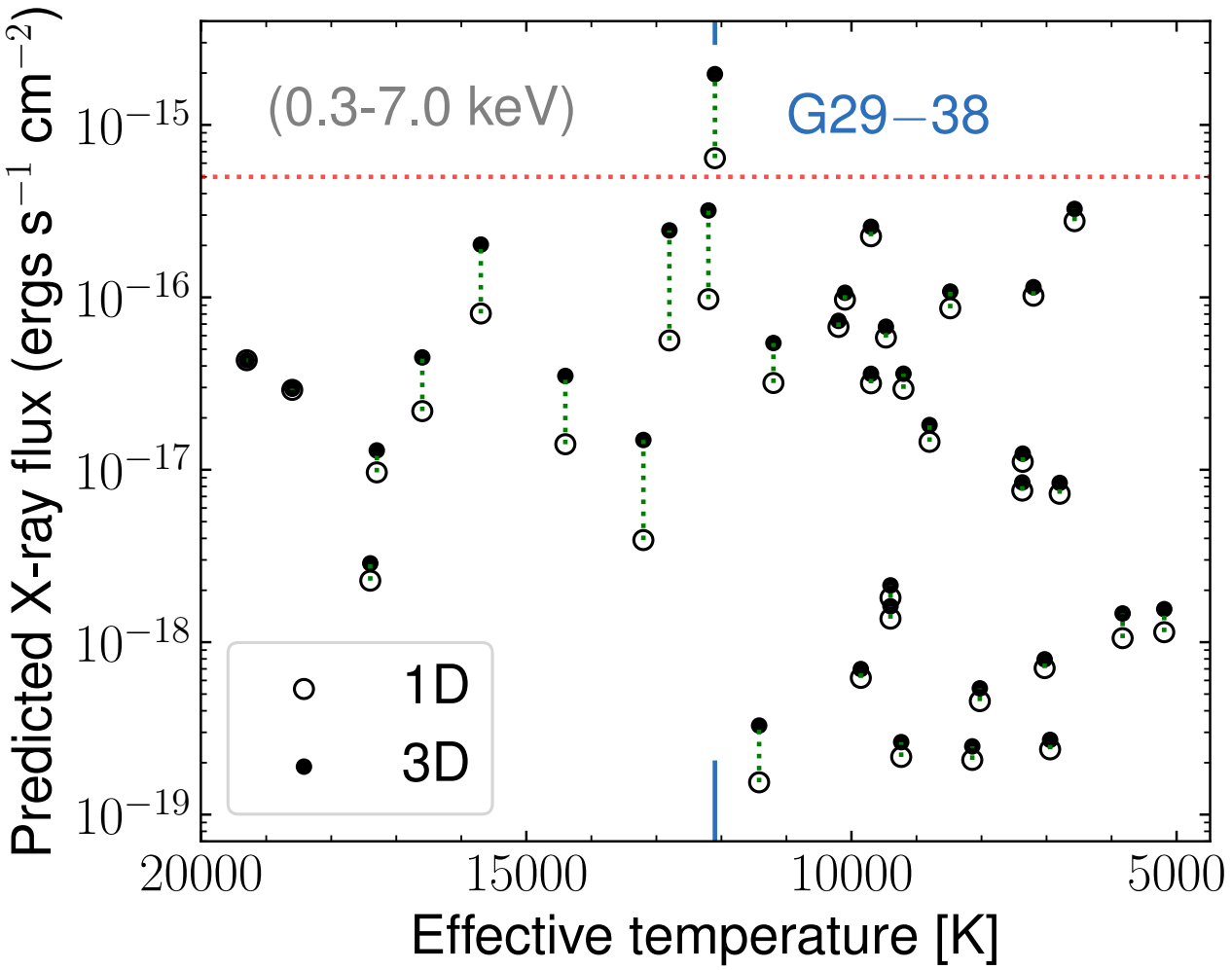
(0.3-7.0 keV)
G29−38
1D
3D
Predicted X-ray flux (ergs s^{-1} cm^{-2})
10^{-15}
10^{-16}
10^{-17}
10^{-18}
10^{-19}
20000
15000
10000
5000
Effective temperature [K]

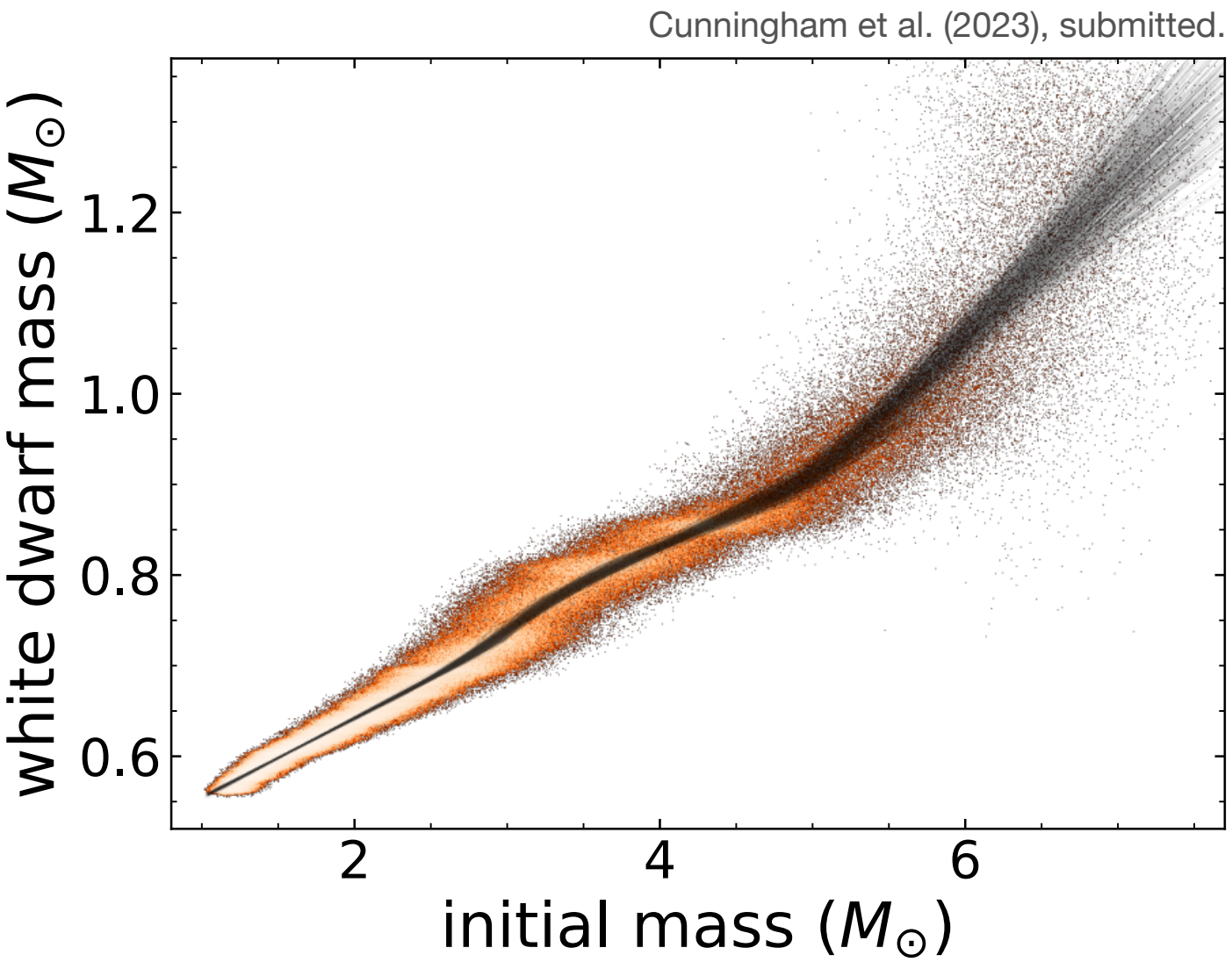
Cunningham et al. (2023), submitted.
white dwarf mass ($M_\odot$)
0.6
0.8
1.0
1.2
2
4
6
initial mass ($M_\odot$)

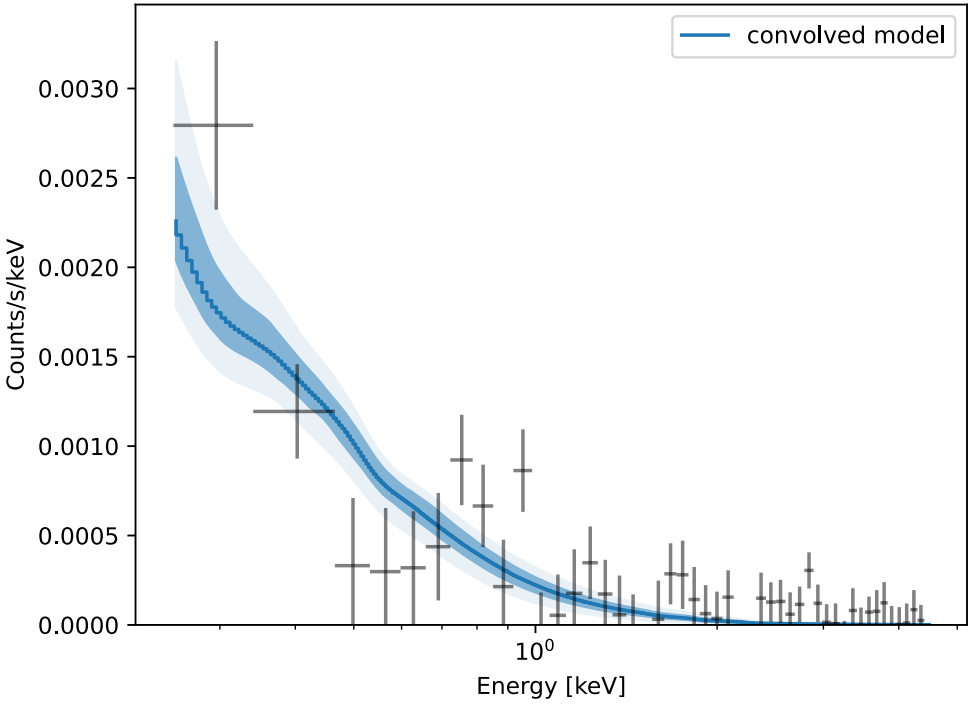
convolved model
0.0030
0.0025
0.0020
0.0015
0.0010
0.0005
0.0000
Counts/s/keV
10^0
Energy [keV]

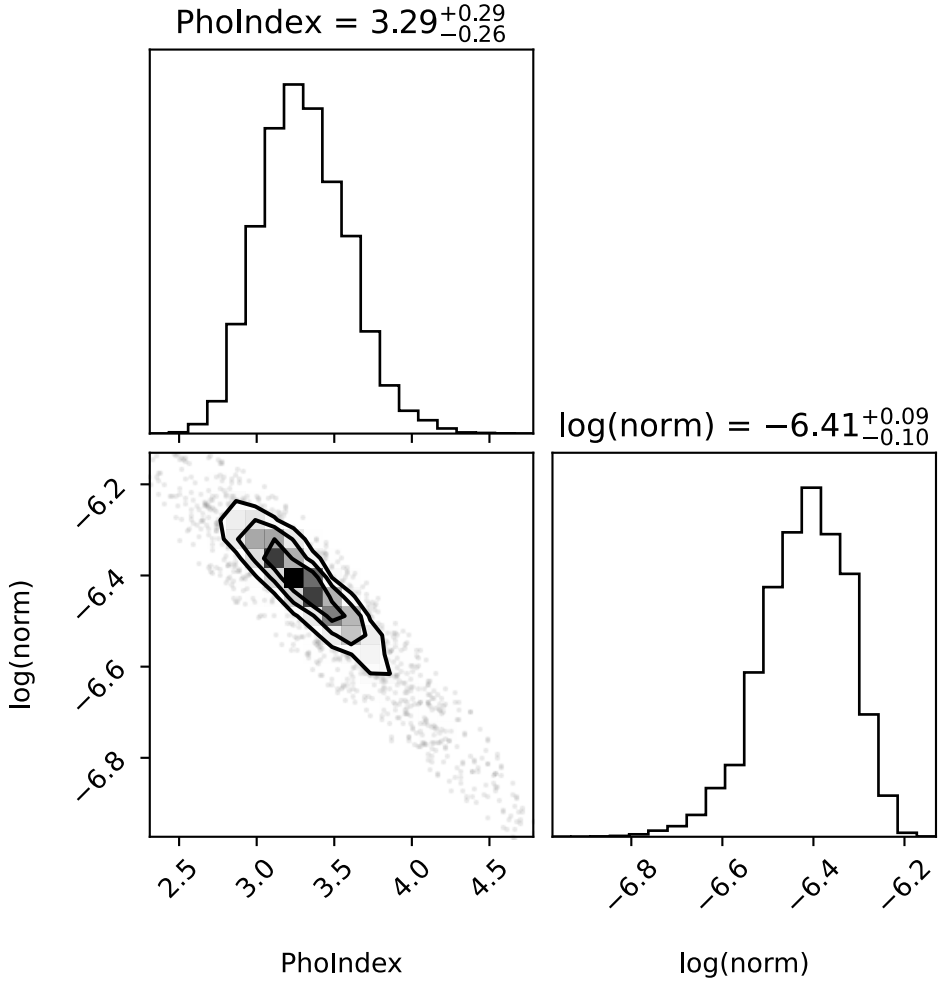
PhoIndex = $3.29^{+0.29}_{-0.26}$
log(norm) = $-6.41^{+0.09}_{-0.10}$
log(norm)
−6.2
−6.4
−6.6
−6.8
2.5
3.0
3.5
4.0
4.5
PhoIndex
−6.8
−6.6
−6.4
−6.2
log(norm)

T_{eff}	6340±40 K
R_{WD}	0.0119±0.0002 $R_\odot$
E(B-V)	0.06±0.01 mag
log(H/He)	-3.5±0.1
log(Na/He)	-9.5±0.1
log(Mg/He)	-8.1±0.4
log(Ca/He)	-9.2±0.3
log(Ti/He)	-10.7±0.2
log(Fe/He)	-8.4±0.3
log(Ni/He)	-9.7±0.6
M_{WD}	0.63±0.02 $M_\odot$
logg	8.08±0.03
Cooling age	2.5±0.2 Gyr

Ca/Fe = -9.2 + 8.4 = -0.8
Ti/Fe = -10.7 + 8.4 = -2.3
Mg/Fe = -8.1 + 8.4 = 0.3